Technische Universität München
Fakultät für Medizin

Development of a dendritic cell vaccine against HCC using the immunogenic oncolytic virus VSV-NDV

Julia Beate Gold

Vollständiger Abdruck der von der Fakultät für Medizin der Technischen Universität München zur Erlangung einer

Doktorin der Medizin (Dr.med.)

genehmigten Dissertation.

Vorsitz: Prof. Dr. Florian Eyer

Prüfer*innen der Dissertation:

1. Priv.-Doz. Dr. Jennifer Altomonte
2. Prof. Dr. Angela Krackhardt

Die Dissertation wurde am 12.10.2022 bei der Technischen Universität München eingereicht und durch die Fakultät für Medizin am 21.03.2023 angenommen.

Table of contents

1. Introduction

1.1 Hepatocellular Carcinoma

1.1.1 Epidemiology and Aetiology

Liver cancer is the sixth most frequently diagnosed cancer entity and the third most frequent reason for cancer-related death worldwide. There is an impressive geographic imbalance in its incidence (Figure 1); 85% of all cases occur in East Asia (mainly China) and Sub-Saharan Africa. In Germany the incidence is lower, liver cancer being the thirteenth most frequently diagnosed cancer and eighth most common cause for cancer related death (WHO, 2018). In the Western world the incidence is rising, mainly due to changing age structures, whereas it decreases in the countries with high incidence. Unfortunately, there is still an increase on a global scale. Of all primary liver cancers, the hepatocellular carcinoma (HCC) is by a wide margin the most common one.

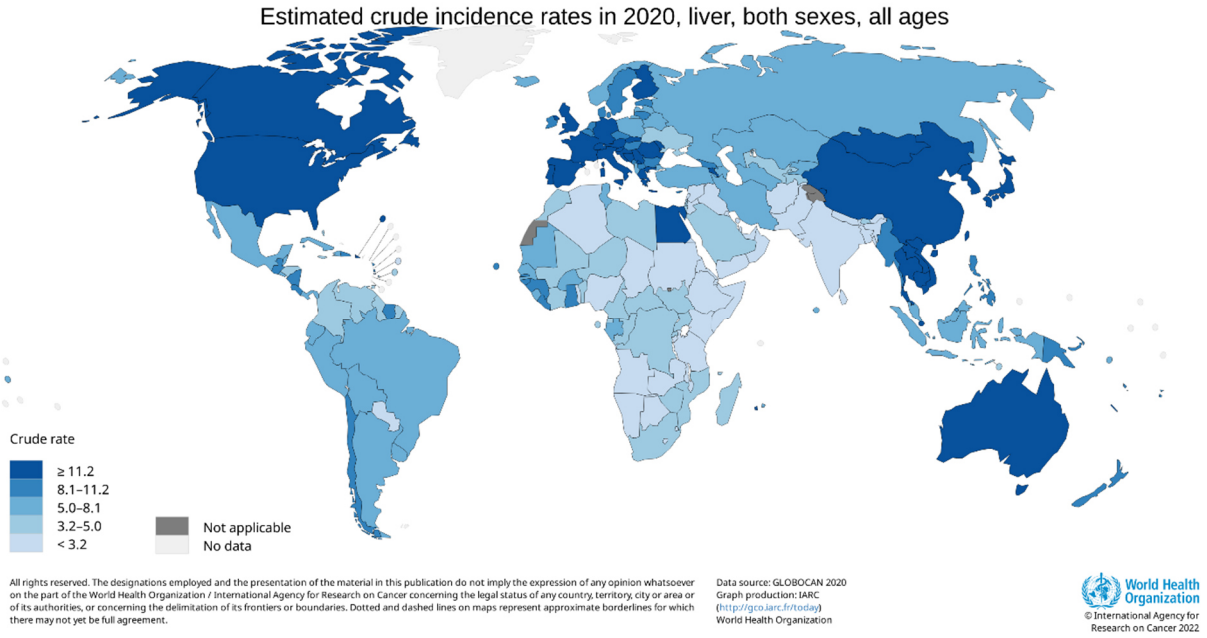

Figure 1: Incidence of liver cancer worldwide (2020)

Most cases of HCC occur in a cirrhotic liver, and one-third of all cirrhotic patients develops HCC (Sangiovanni et al., 2006). To give a broad overview, it can roughly be summarized that in third world countries cirrhosis is most frequently caused by infection with Hepatitis B virus (HBV), Hepatitis C virus (HCV) or the fungus Aflatoxin B1. There is a strong correlation between exposure to Aflatoxin B1, p53 mutations and HCC, even potentiated in individuals with HBV infection (Hsu et al., 1991). In countries of the Western world the main reason is steatohepatitis associated with alcohol abuse or metabolic syndrome.

1.1.2 Prognosis and standard treatment in Europe

In Europe, the HCC in a cirrhotic liver is treated according to the stage of the disease, defined by the Barcelona Clinic Liver Cancer (BCLC) staging system (Figure 2). This takes into consideration

- size (<2cm, <3cm or >3cm) and number (single, 2-3 or multinodular) of the tumor nodules,
- liver function and
- resectability/portal invasion/extrahepatic spread.

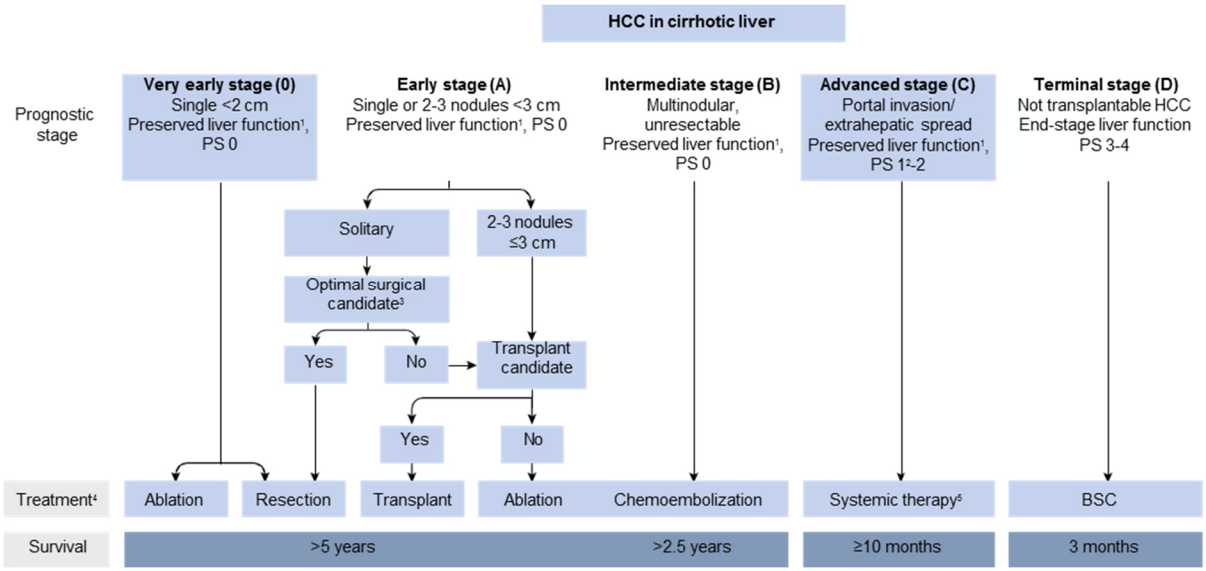

Figure 2: Treatment of HCC in a cirrhotic liver, depending on the BCLC staging (overview)

Ablation

Thermal ablation with radiofrequency (RFA) is the standard of care for early-stage HCC not suitable for resection. Fractional heat which is generated by high-frequency alternating current is applied into the tumor, usually percutaneously. It creates a coagulative necrosis within the tumor that extends into the peri-tumoral tissue to eliminate possible undetected satellites. RFA outcompetes other ablation methods like percutaneous ethanol injection, microwave, laser and cryoablation or external radiation (EASL, 2018).

Resection

Surgery leads to the best outcome of all treatment options in HCC but is only possible in early stages (BCLC 0 and A). It represents the treatment of choice in non-cirrhotic patients and – depending on additional parameters like portal hypertension, expected volume of functional liver remnant and the patient's performance status – is also recommended in a cirrhotic liver. Especially in anterolateral and superficial localisations, minimally invasive surgery is beneficial in properly trained centres.

Resections can also be performed in patients with initially later stages of disease, if down-staging was successful using other treatment options. After resection with curative intent, follow-up is highly recommended due to high rates of treatable recurrence.

Transplantation

Unresectable patients are assessed for cadaveric liver transplantation (LTx) applying the Milan criteria:

- one tumour nodule <5cm or three tumour nodules <3cm
- no extrahepatic manifestations (=no metastases)
- no vascular invasion (e.g., into the portal vein)

They are the precondition for registration on the waiting list for organ procurement, patients beyond these criteria need be downstaged first. Even though there is an intensive discussion about an expansion of the criteria concerning the tumor size (LTx with tumours up to 6.5cm), the inclusion of predictive biomarkers like alpha-fetoprotein (AFP) or the application of imaging with 18F-FDG-PET/CT, the current Milan criteria have been valid since 1996 (Gunsar, 2017). A challenging alternative is the living donor liver transplantation (LDLT), which represented 7.2% of all liver transplantations at Eurotransplant in 2018 (Eurotransplant, 2019). Probably due to a lack of comparative studies between cadaveric LTx and LDLT, surgical challenges and ethical aspects, it still remains a debated second-line treatment in Europe (Nadalin et al., 2016).

Embolization

Transarterial chemoembolization (TACE) takes into account that the tumour is dependent on arterial blood supply and that progressing HCC shows an intense arterial neo-angiogenic activity, whereas the liver tissue mainly receives venous inflow. In general, TACE includes the intraarterial infusion of a cytotoxic agent into the tumor (e.g., doxorubicin or cisplatin), and then a particle embolization of the tumor-feeding blood vessels is performed. This combination results in a stronger cytotoxic and ischaemic effect than either method alone, particle embolization not only preventing blood supply but furthermore improving the pharmacokinetics of the chemotherapy.

In selective internal radiation therapy (SIRT), also called radioembolization, radioactive substances (e.g., 131-Iodine-labelled Lipiodol, Yttrium-90-containing microspheres) are infused into the hepatic artery. It requires a preliminary angiography of the hepatic artery including protective coiling of extrahepatic branches and evaluation of potential extrahepatic blood distribution using 99Tc macroaggregated albumin. To date, only few small studies compared TACE and SIRT, but the trend shows less toxicity and prolonged progression-free intervals in SIRT. Unfortunately, SIRT is more demanding and requires much more expenditure than TACE.

Systemic therapy

HCC is one of the most chemotherapy-resistant tumour entities due to the coexistence of two hepatic diseases in most patients. Cirrhosis not only compromises the immune system and therefore deteriorates chemo-associated systemic infections but can furthermore change the metabolism of

chemotherapeutic drugs and enhance their toxicity. Different drugs and combined schemes like Doxorubicin or FOLFOX (folic acid, 5-Fluoruracil + Oxaliplatin) have been tested in clinical trials, but either didn't meet their primary endpoint or didn't show a benefit over standard treatment.

Sorafenib, an oral multi-tyrosine kinase inhibitor, is the first-line therapy for advanced stage HCC (BCLC C) since 2007. It is well-tolerated and showed an increase in median overall survival (OS) in the initial phase III study from 7.9 to 10.7 months (Llovet et al., 2008). Nevertheless, there is no recommendation for its use in an adjuvant setting. The first-line alternative multi-kinase inhibitor, Lenvatinib, targets the vascular endothelial growth factor (VEGF)-receptor, the fibroblast growth factor receptor and the platelet-derived growth factor receptor. In a comparative trial it showed longer progression-free survival than Sorafenib, but more grade 3 adverse events (Kudo et al., 2018). Furthermore, also the combination of the anti-PD-L1 antibody Atezolizumab with the anti-VEGF antibody Bevacizumab is a possible treatment option (Finn et al., 2020). Patients that progressed on first-line therapy can be treated second-line with the multi-kinase inhibitor Regorafenib. Showing a comparable safety profile to Sorafenib, Regorafenib improved the median OS from 7.8 months on placebo to 10.6 months (Bruix et al., 2017).

Best supportive care

The management of terminal HCC focuses on best supportive care, excluding tumour-directed treatment. Most patients suffer from pain due to liver capsule distension, immobility or metastases. In case of severe pain, opioids are the preferred treatment. Non-steroidal anti-inflammatory drugs should be avoided because they are associated with an increased risk of gastrointestinal bleeding, decompensation of ascites and nephrotoxicity. Palliative radiotherapy is indicated in well-identified bone metastases that cause pain or display a high risk of spontaneous fracture. In line with tumor burden and cirrhosis, absorption and metabolism of nutrients is altered, leading to weight loss and muscle wasting. Because the nutritional status has been found to independently correlate with OS of advanced HCC patients (Pinato, North, & Sharma, 2012), nutritional intervention can be highly beneficial. The level of psychological distress in HCC patients is higher than in most other cancer entities (Zabora, BrintzenhofeSzoc, Curbow, Hooker, & Piantadosi, 2001) and psycho-oncological care is highly recommended. Because an underlying cirrhosis alters the pharmacokinetics of several drugs, treatment with benzodiazepines and other psychoactive drugs increases the risk of falling and, in case of benzodiazepines, the precipitation of an altered mental status and should therefore be considered very carefully (Tapper, Risech-Neyman, & Sengupta, 2015).

Since HCC is a very frequent and complex disease occurring in all parts of the world, only certain aspects could be reviewed here. For further information the "Clinical Practice Guidelines: Management

of hepatocellular carcinoma" by the European Association for the Study of the Liver, which also underlie this introduction, are recommended (EASL, 2018).

1.1.3 Current focus of research

All in all, the only chance for cure in HCC currently is a diagnosis at an early stage. Since most patients are unfortunately diagnosed later, there is an urgent need for the development of new therapies. This is especially important when taking into consideration the growing incidence of HCC worldwide.

Recent FDA-approvals

Several therapeutic agents targeting immune checkpoints, tyrosine kinases or angiogenesis have recently been approved by the U.S. Food and Drug Administration (FDA) for late-stage HCC-patients that have previously been treated with Sorafenib. In line with the current hope in checkpoint blockade, a phase II clinical trial has been conducted to investigate the effect of the anti-PD-1 antibody Nivolumab in HCC patients that have progressed or were intolerant to Sorafenib. The overall response rate was 14.3%, with 3 complete and 19 partial responses, of which 91% lasted longer than 6 months. The adverse events were manageable and similar to those previously observed under Nivolumab in other cancer entities. It was granted conditional approval in September 2017 (El-Khoueiry et al., 2017). The tyrosine kinase inhibitor Cabozantinib – approved in March 2019 (FDA, 2019) – targets those kinases that are involved in HCC progression and in the development of resistance to Sorafenib. It increased the OS by 2 months compared to the placebo group in a phase III trial (Abou-Alfa et al., 2018). Ramucirumab, a monoclonal antibody targeting VEGF-receptor 2, is a convincing example for the potential benefit of biomarker-selected treatment. It significantly increased OS and progression-free survival (PFS) in patients with alpha-fetoprotein (AFP)-levels ≥400ng/ml and was therefore approved in May 2019 (Zhu et al., 2019).

Characteristics of the hepatic immune system and its impact on HCC immunotherapy

Due to its role as the body's major metabolizer the liver tissue is constantly physiologically exposed to nutritional, pathogenic and toxic antigens. In order to avoid autoimmune reactions including destruction of hepatic tissue, the liver is equipped with mechanisms for intrinsic tolerance and immune escape (Mahipal, Tella, Kommalapati, Lim, & Kim, 2019). The hepatic sinusoids are lined with liver sinusoidal endothelial cells (LSEC) and are populated with the liver-specific Kupffer cells (KC) and Hepatic stellate cells (HSC), that all contribute to antigen sequestration, in addition to common immune cells like dendritic cells (DC) and natural killer (NK) cells (Altomonte & Ebert, 2014). For example, LSECs – antigen-sequestrating endothelial cells with the full capacity for antigen presentation lining the liver sinusoids – clearly reduce their capacity of antigen processing and presentation (low MHC) as well as co-stimulation (low CD80/86) upon the influence of endotoxin, while maintaining their sequestration function. This leads to decreased T-cell activation and most probably serves the

physiological need to clear gut-derived antigens without eliciting an immune response (P. A. Knolle et al., 1999). In response to lipopolysaccharides (LPS), KCs – the liver resident macrophages – secrete the anti-inflammatory cytokine IL-10, which subsequently leads to downregulation of the secretion of pro-inflammatory IL-6 and TNFα (P. Knolle et al., 1995). Activated HSCs – vitamin A storing, profibrotic pericytes – are capable of transforming mature peripheral blood monocytes into myeloid derived suppressor cells (MDSC) that dampen immune responses (Hochst et al., 2013).

In chronically inflamed livers, the milieu is even more immunosuppressive. E.g., in chronic HBV infection, circulating and hepatic plasmacytoid DCs (pDCs) are defective in their NK cell activating properties due reduced expression of the NK cell ligand OX40L (Martinet et al., 2012). Furthermore, biopsies from patients with HBV or HCV infection or autoimmune hepatitis contain higher numbers of PD-1 expressing lymphocytes than those from healthy patients, the level of expression of PD-1 family members even correlates with the degree of necroinflammation (Kassel et al., 2009).

All these phenomena hamper immune reactions against HCC-derived antigens, therefore promoting cancer development. Additionally, compared to a normal liver pool, the cytokine profile in noncancerous hepatic tissue of metastatic HCC shows a unique signature with an increase in anti-inflammatory IL-4, IL-5, IL-8, and IL-10 and a concomitant decrease in pro-inflammatory IL-1α, IL1-β, IL-2, IFN-γ, and TNF (Budhu et al., 2006).

It has already been shown that the degree of immunosuppression in the liver is connected with worse disease outcome, e.g., higher PD-1 expression correlates with higher post-surgical tumor recurrences, and increased regulatory T cell (Treg) and MDSC numbers are associated with aggressive tumors (Mahipal et al., 2019). This implies that the availability of an immune response does make a difference in the development of HCC. Due to the non-immunogenic milieu (low costimulatory molecules, secretion of anti-inflammatory cytokines, expression of checkpoint inhibitors, high numbers of suppressive immune cells) there is a great chance that counteracting these features will induce an anticancer immune response that patients will profit from.

1.2 Oncolytic Virotherapy

1.2.1 Overview

In recent years oncolytic virotherapy has gained more and more importance in the field of cancer therapy reflected by many clinical and preclinical studies going on (Macedo, Miller, Haq, & Kaufman, 2020). In 2015, the first oncolytic virotherapy has been approved by the FDA as well as the European Medicines Agency (EMA): talimogene laherparepvec (also known as T-VEC, OncoVEX$^{GM\text{-}CSF}$ or Imlygic©) can be used for the treatment of late-stage Melanoma (Pol, Kroemer, & Galluzzi, 2016).

The history of oncolytic virotherapy started in the beginning of last century with a reported case of a patient with late stage-cervical carcinoma who – after rabies-vaccination – experienced a significant regression in tumor burden (de Pace, 1912). After the first demonstration of viral oncolysis under laboratory conditions in 1922, several clinical trials in humans aiming to cure cancer with different potentially "oncolytic" viruses were conducted, but "clinical application as attempted to date offers little hope for significant therapeutic response" (Southam, 1960). In the 1970s and 80s there have been several cases of regression in Burkitt's and Hodgkin's lymphoma after measles infection (Bluming & Ziegler, 1971; Taqi, Abdurrahman, Yakubu, & Fleming, 1981), and due to the enormous progress in genetic engineering as a potential strategy to alter oncolytic viruses (OV) in their antitumor specificity they have since then again been a field of interest as a potential cancer therapeutic.

OVs are characterized by an inherent or engineered specificity to preferentially infect, replicate in and kill tumor cells. Interestingly, the cellular changes induced by virus infections resemble those acquired during carcinogenesis, for example the inactivation of p53, inhibition of apoptosis and the induction of mitosis. This results in facilitated replication of some viruses in malignant cells (Everts & van der Poel, 2005). First, malignant cells often have attenuated innate immune defence mechanisms due to their necessity to escape detection and destruction by the immune system. Very important is the defective IFN-signalling in cancer cells (Stojdl et al., 2000), which makes tumors especially susceptible for Vesicular Stomatitis Virus (VSV) (Everts & van der Poel, 2005), whereas healthy cells protect themselves from virus infections via IFN-release that induces an anti-viral immune response. Moreover, tumor cells tend to be immortal including resistance to apoptosis which is favourable for virus replication (Russell, Peng, & Bell, 2012). At last, some types of cancer cells overexpress different virus receptors that facilitate the uptake of specific OVs (Chaurasiya, Chen, & Warner, 2018).

To date there are many different types of oncolytic viruses. Some of them have a natural preference for malignant cells, such as autonomous parvovirus H1, reovirus, mumps virus as well as VSV and Newcastle Disease Virus (NDV), whereas measles, polio, influenza, vaccinia, adeno-, and herpes simplex virus (HSV) in contrast have to be genetically modified to be cancer specific (Everts & van der Poel, 2005; Russell et al., 2012).

1.2.2 Direct and indirect mechanisms of antitumor activity

Direct infection and cell lysis

Oncolytic viruses – like every virus infection – kill their target cells by direct infection. Within the replication cycle of a virus, a single viral particle can infect a host cell and hijack its replication machinery to produce viral progeny. This results in progressive exhaustion of the host cell followed by cell lysis with a release of abundant viral particles.

Furthermore, target cell death is triggered by cytotoxic viral proteins produced within the infected cell (Marchini, Scott, & Rommelaere, 2016). E.g., late in the life cycle of adenoviruses they produce the E3 11.6kD death protein and E4ORF4 protein that are directly cytotoxic to cells (Mullen & Tanabe, 2002).

Antiangiogenic properties

Some oncolytic viruses – like VSV (Breitbach et al., 2011) or Vaccinia Virus (Breitbach et al., 2013) – do have the inherent ability to target the blood vessels of a tumor and to induce vascular destruction. As a result of upcoming knowledge on the aberrant morphology of tumor vasculature, other OVs now have engineered features to specifically stop the tumor's blood supply, not only by disruption of the vessels or clotting but also via downregulation of angiogenetic factors or by production of antiangiogenic factors (Toro Bejarano & Merchan, 2015).

Stimulation of the host's immune system against the tumor

Maybe even more important than the direct lysis of tumor cells by OV-infection is the stimulation of the host's immune system against the tumor induced by viral oncolysis. First, infection of the host with an oncolytic virus – like every virus infection – leads to an activation of the immune system. Extra- and intracellular pattern recognition receptors (PRR) sense the virus' pathogen-associated molecular patterns (PAMP). In the early antiviral innate immune response, this leads to cellular responses like the activation of DCs including uptake and presentation of viral antigens and especially to the activation of NK cells. Furthermore, the production of cytokines and other mediators during the innate response is crucial for the induction of an inflammation, whereas the secretion of IFN type I leads to an "antiviral state" which is inter alia characterized by the synthesis of endonucleotidases that degrade viral RNA. The powerful adaptive immune response, which is initiated by the innate immunity, reacts to a virus infection via the destruction of infected cells by CD8+ cytotoxic T-lymphocytes (CTL) and with the secretion of virus-neutralizing antibodies by B-cells that were stimulated by CD4+ helper-T-cells type 1 (T_H1-cells).

On the one hand this anti-viral immune response is problematic in that it leads to a rapid clearance of the virus, but on the other hand it's a great chance to overcome the immunosuppressive effects of the tumor microenvironment (TME). Since the tumor cells provide a niche for virus replication, the inflammatory and immune-activating processes will take place exactly where the mechanisms of defence are needed and enable anti-cancer immune responses. E.g., it has been shown that OV treatment not only increases the levels of immunostimulatory cytokines (Koske et al., 2019), but furthermore enhances DC activation including antigen-uptake (Y. Kim et al., 2015).

Moreover, the destruction of malignant cells by OVs leads to the liberation of the tumor's damage-associated molecular patterns (DAMPs) and PAMPs. This enables the immune system to direct its

response against exactly these cancer molecules, mainly via their engulfment by DCs with the following stimulation of CTLs or NK cells.

OVs that induce an ICD, which are mainly fusogenic OVs such as measles virus or NDV, but also mumps and Sendai virus, are particularly immune-stimulatory (Krabbe & Altomonte, 2018). The mechanisms and characteristics of the ICD are explained later.

1.2.3 Hurdles in the development of oncolytic virus-based therapies

Route of application

A crucial question in the treatment with OVs is the application route. While intratumoral injection on the one hand provides high viral titers at the site of interest and was successful in several clinical trials, it will be less helpful in the treatment of unknown distant metastases and in tumors that are not easily accessible. Therapeutic approaches applying the virus into the bloodstream on the other hand have to face the problems of sequestration of the virus in liver and spleen, lack of extravasation of the viral particles and neutralisation of the virus by antibodies (Russell et al., 2012). In the future, possible solutions might be the encapsulation of OV in extracellular vesicles (Garofalo et al., 2018), engineering OVs to specifically replicate in tumor endothelial cells (Toro Bejarano & Merchan, 2015) or the use of carrier cells like T cells (Melzer et al., 2019).

Intratumoral spread

Even though OV's inherent tumor specificity is often due to defective viral defense mechanisms in malignant cells, the tumor's immune response is not abrogated completely, attenuating intratumoral virus spread. The application of small molecules (Otsuki et al., 2008) or other chemical compounds (Diallo et al., 2010) as suppressors of the residual IFN responsiveness or drugs increasing the tumor's connective tissue permeability (Russell et al., 2012) are interesting approaches, but the use of fusogenic viruses providing intratumoral spread by cell-cell-fusion is especially promising due to its additional benefit of stimulating the immune system (Krabbe & Altomonte, 2018). The use of immunosuppressive drugs in order to facilitate intracorporal as well as intratumoral virus spread has been an interesting strategy in the past decades (Ikeda et al., 1999), but apart from safety concerns it has become evident that the induction of an anti-tumoral immune response by the OV is an important part of its therapeutic effect (Koks, De Vleeschouwer, Graf, & Van Gool, 2015) that would be abrogated by an immunosuppressant.

Safety

As already implied above, safety concerns are a considerable hurdle in oncolytic virotherapy. Theoretically there is the possibility that a virus applied to a patient might mutate, regain its pathogenic potential, and spread, especially since it has been documented in some cases that treated patients

excrete virus in the urine and also exhale it. However, there are to date no reports about oncolytic virus transmission to contact persons (Russell et al., 2012). Furthermore, the application of viral vectors engineered for improved safety substantially lowers the likelihood of re-mutation to a pathogenic, especially in the case of hybrid vectors like VSV-NDV (Abdullahi et al., 2018).

1.3 The newly engineered oncolytic virus VSV-NDV

1.3.1 The original parental viruses

Vesicular stomatitis virus

Vesicular stomatitis virus is an oncolytic virus with an inherent tumor specificity that is generally non-pathogenic for humans. Its infection naturally causes disease in cattle, horses and swine, characterized by vesicular lesions and ulcerations around the mouth, hoofs and teats and a substantial decline in productivity (Letchworth, Rodriguez, & Del C. Barrera, 1999). Infection in humans can cause debility and mild flu-like symptoms but has only been reported in some rare cases in the agricultural, veterinary or laboratory context (Wongthida et al., 2016). In 1988 there was a reported case of a 3-year-old boy suffering from severe encephalitis caused by the Indiana strain of VSV (Quiroz, Moreno, Peralta, & Tesh, 1988), suggesting the possibility of severe side effects in oncolytic virotherapy with VSV. In the past few years, the further development of wild type VSV as a therapeutic agent for humans has been hampered by studies showing a severe neuro- and hepatotoxicity in rodents and non-human primates treated with wild type VSV (Abdullahi et al., 2018).

Structure of VSV

VSV belongs to the family of Rhabdoviridae and is an enveloped, bullet-shaped, negative-stranded RNA virus whose genome of approximately 11,000 nucleotides encodes for five viral proteins. Attachment to the host cell is mediated by VSV's glycoprotein (G protein) that interacts with the ubiquitously expressed low density lipoprotein (LDL)-receptor, inducing receptor-mediated endocytosis of the VSV-particle into an endosome. At a decreased pH upon fusion with a lysosome, the conformation of the G protein changes, mediating the release of the VSV genome into the cytosol (Melzer, Lopez-Martinez, & Altomonte, 2017). Now the viral replication process, completely taking place in the cytoplasm, starts. The matrix (M) protein plays a crucial role for the cytotoxicity of VSV. In addition to being a structurally relevant protein for the viral particle, it prevents host gene expression by inhibition of all three host RNA-polymerases (Lyles, 2000). Therefore VSV-induced tumor cell death is a result of the general shutdown of host RNA and protein synthesis. The remaining proteins are the large polymerase (L) protein as well as the phosphoprotein (P) that are necessary for replication of the viral genome and furthermore the nucleocapsid (N) protein, enveloping the entire RNA genome.

Benefits of VSV as an oncolytic virus

The inherent tumor specificity of VSV is due to its susceptibility to the antiviral mechanisms induced by type I interferons (mainly IFNα and IFNβ). After pre-treatment with IFN and upon infection with VSV, healthy cells induce anti-viral defence mechanisms and inhibit synthesis of viral mRNA, whereas tumor cells continue the production of viral particles (Belkowski & Sen, 1986; Stojdl et al., 2000). This suggests that tumor cells have impaired IFN-signalling mechanisms, probably to avoid recognition by the immune system, which gives VSV the chance to replicate in malignant cells without being cleared. Apart from its inherent tumor specificity, VSV represents a beneficial platform for virus-based immunotherapies due to its ability to infect a wide range of host cells and its rapid replication and cell killing kinetics that allow the therapy to work before the virus is neutralised by antibodies. Fortunately, there is no pre-existing immunity against VSV in most humans. More practical advantages of working with VSV are the existence of an established genetic system for generating recombinant vectors and the possibility to produce high titer stocks (Abdullahi et al., 2018; Melzer et al., 2017).

Newcastle disease virus

Alike VSV, Newcastle disease virus is inherently specific for malignant cells and in general not pathogenic for humans. NDV is a highly contagious avian pathogen and relatively stable towards temperature and on different materials outside its natural host, being a risk for birds including pets but also for poultry industry. The last big outbreak in the south of the United States in 2002/2003 resulted in the culling of 3.16 million birds which cost 121 million dollars, whereas another outbreak in 2018/2019 made it necessary to euthanize many pets ("Avian Health: Virulent Newcastle Disease," 2019). On average, 2-15 days post-exposure, infected animals show a haemorrhagic intestinal infection or respiratory and neurological symptoms such as tremors, ataxia or paralysis. The exact symptoms and severity of the disease depend on the virulence of the respective strain (Brown & Bevins, 2017).

Structure of NDV

Belonging to the *Avulavirus* genus in the family of *Paramyxoviridae*, NDV is a spherical, enveloped virus. Its genome consisting of negative-sense single-stranded RNA with approximately 15,000 nucleotides encodes for six structural proteins (Cuadrado-Castano, Sanchez-Aparicio, Garcia-Sastre, & Villar, 2015). Enveloping the genome, the matrix (M) protein does not only define the shape of the viral membrane but is furthermore essential for the budding of membrane vesicles (Shnyrova et al., 2007) and potentially new viral particles. Three additional proteins – the nucleoprotein (NP), the phosphoprotein (P) and the large polymerase protein (L) – form the ribonucleoprotein (RNP) complex, which acts as the nucleocapsid but is also the replication unit of the virus.

Most interesting are the hemagglutinin-neuraminidase (HN) and fusion (F) glycoproteins on the outer viral membrane. The binding of the HN to its receptor on the host cell surface marks the beginning of

the infection and triggers F-protein mediated fusion of virus and cell membrane. This enables the RNP proteins to enter the cytoplasm where replication takes place (Cuadrado-Castano et al., 2015).

Benefits of NDV as an oncolytic virus

Animal-experiments showed that NDV is clearly not neurotropic and tested in clinical trials it was very well tolerated. Wild type strains only caused mild conjunctivitis and laryngitis. This was not even the case in attenuated strains whose only side effect was low-grade fever (Lorence et al., 1994). Taking into consideration these low-grade off-target effects, NDV seems to be quite specific for malignant cells, but in the last decades there were different ideas about the mechanism.

First, sensitivity of tumor cells to NDV is substantially elevated by the expression of *ras*-oncogenes within the cells (Lorence et al., 1994), but defective interferon pathways might also contribute to its tumor-specificity (Everts & van der Poel, 2005). In 2011 it was shown that NDV specifically selects apoptosis-resistant cells while the induction of a type I IFN-response didn't attenuate virus spread (Mansour, Palese, & Zamarin, 2011).

NDV is a fusogenic virus. This implies that tumor cells infected with NDV fuse – mediated by their fusogenic surface glycoproteins – with neighbouring cells and form large multinucleated syncytia, substantially facilitating intratumoral spread. Syncytia formation is highly beneficial because first it enables one single virion to potentially infect the whole tumor with a minimal release of virus into the surrounding tissue or systemic circulation, which minimizes the therapeutic dose. Second, these syncytia die by an immunogenic cell death. This not only eliminates the malignant cells but even stimulates the immune system against the tumor by various mechanisms (Krabbe & Altomonte, 2018).

1.3.2 The hybrid vector VSV-NDV

The hybrid vector VSV-NDV consists of the backbone of VSV, but its cell surface glycoprotein (G) has been replaced by the surface HN- and fusion F-protein of NDV. Furthermore, the F-protein has been previously modified to form syncytia even in the absence of exogenous proteases and to be hyperfusogenic [F3aa(L289A)] (Figure 3).

This hybrid complementarily combines the benefits while abrogating the disadvantages of each virus. VSV contains various favourable characteristics such as the ability to infect many different host cells and to replicate very quickly, moreover it doesn't integrate into the host's genome because it completes its replication cycle in the cytoplasm and finally it is possible to produce high titer stocks. Nevertheless, the clinical translation of VSV has been strongly hampered by its hepato- and neurotoxicity, which is at least partly mediated by the G-protein. The major benefit of NDV is its fusogenicity, mediated by the HN- and F-protein, but the clinical translation of this virus has been substantially dampened since the FDA classified it as a "select agent" in 2008. The virulence of NDV is

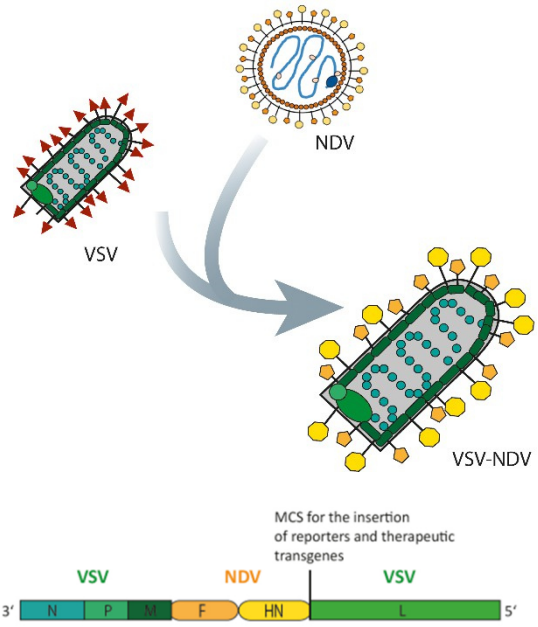

Figure 3: Illustration of the composure of VSV-NDV. VSV-G protein has been replaced by NDV-HN & -F, increasing safety and efficacy of OV therapy.

caused by the V-protein, which results from an edited sequence of the phosphoprotein (P)-gene by frame-shift and possesses the ability to block IFN-signalling via induction of STAT1-degradation (Huang, Krishnamurthy, Panda, & Samal, 2003).

Since neither the VSV G-protein nor the NDV P-gene are included in VSV-NDV, this hybrid provides enhanced safety with regards to hepato- and neurotoxicity and environmental risks for birds, respectively. Furthermore, syncytia formation – including all its benefits as the ICD – can be successfully observed upon infection with VSV-NDV, whilst the replication and cell killing kinetics are not as quickly as upon VSV-infection, but still quicker than with wild type-NDV (Abdullahi et al., 2018).

1.4 Dendritic Cells

Dendritic cells are a crucial mediator of the immune system, initiating innate as well as adaptive immune responses: they patrol all tissues and, upon recognition of an antigen, secrete cytokines and interact with several other immune cells. For his discovery of DCs as an independent cell type (Steinman & Cohn, 1973, 1974), Ralph Steinman was awarded the Nobel Prize in Physiology or Medicine in 2011 posthumously ("The Nobel Prize in Physiology or Medicine 2011," 2019).

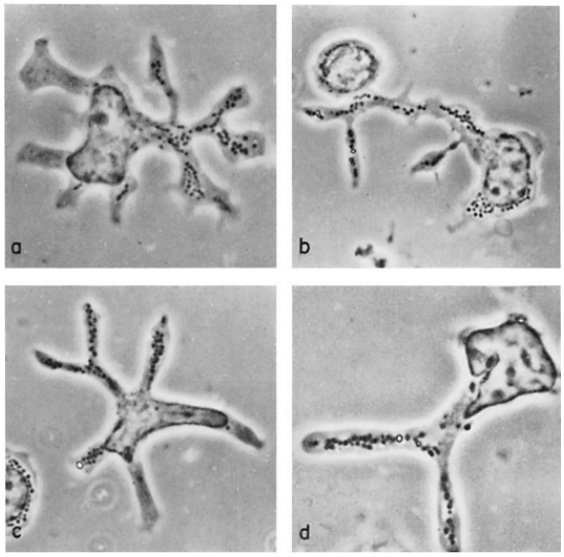

Figure 4: Phase-contrast micrographs of DCs isolated from mouse spleen by R. Steinman 1973

The name “dendritic cells” derives from the ancient Greek word “δένδρον” (“dendron” = tree) because in an inactive state dendritic cells consist of many branched processes that vary in length and width like the branches of a tree (Figure 4).

Dendritic cells are a highly diverse cell type consisting of many different subsets. Therefore, this chapter will first give a broad overview of the functions of DCs in general, hereafter a closer look will be taken at the different subsets.

1.4.1 Activation and mechanisms of action

Activation of dendritic cells

Immature dendritic cells are present in all "barriers" of the human body – e.g., skin, mucosa and intestine – but also in solid organs like heart or kidney in order to capture antigens such as bacterial and viral peptides, apoptotic/necrotic and tumor material, immune complexes and lipids via phago-/pinocytosis and receptor-mediated endocytosis. Whereas phagocytosis (solid particles >1µm) and pinocytosis (extracellular fluids and soluble antigens) are unspecific and actin-mediated, constitutive membrane processes, receptor-mediated endocytosis into clathrin-coated vesicles is very specific and nearly every existing PRR (like the C-type lektin receptor or Toll-like receptor (TLR), but also the complement receptor) is expressed on the surface of DCs for this purpose. This allows the DCs to capture nearly every antigen – the ones that can be recognized by a PRR as well as those that have escaped recognition by a phagocytic receptor.

Inflammatory cytokines, tissue damage, but also the binding of antigens to phagocytic receptors lead to DC activation. E.g., TLR-signalling stimulates the expression of the chemokine receptor CCR7 on the DC surface, which is a binding site for the chemokine CCL21 produced by lymphatic tissue. CCL21 leads to several changes in DC function, that are summarized as "licensing" of a dendritic cell. First, CCL21 attracts DCs and therefore leads to migration towards spleen and lymph nodes via lymphatic vessels. Second, it promotes the presentation of the antigens on many MHC-I and II while the engulfment of new antigens is stopped. Third, the expression of costimulatory molecules (crucial for T-cell interaction: CD80, CD86) is supported.

The activation of dendritic cells is furthermore supported by autocrine mechanisms. After lysosomal degradation of an ingested pathogen, the particles (e.g., unmethylated DNA) are released into the cytoplasm. Via signalling of the intracellular TLR-9, pro-inflammatory cytokines such as Interleukin (IL)-6, IL-12, IL-18 or IFNs are produced and act back onto the DC, promoting the expression of costimulatory molecules.

The presentation of antigens on the DC surface works as follows: An antigen which has been engulfed into a vesicle is degraded in a lysosome and loaded onto an MHC-II molecule (endocytic pathway for extracellular antigens), whereas proteins of the cytosol and endoplasmic reticulum (ER) are degraded in the proteasome (cytoplasm) and transported via the TAP[1] transporter into the ER, where they are loaded onto MHC-I (ER pathway for intracellular antigens)[2]. This would implicate, that antigens

[1] Some viruses (e.g. herpesviruses or adenoviruses) interfere with the TAP transporter and inhibit the transport of proteins into the ER to avoid presentation of virus antigens on MHC-I and a subsequent immune response (Verweij et al., 2015).

[2] When antigens directly enter the cytosol, e.g. upon virus infection, they also enter this pathway. Since DCs are susceptible to infection by some viruses, this can occur, and virus particles will be presented on MHC-I.

endocytosed by DCs could only be loaded onto MHC-II and could therefore activate CD4+ T-cells only. However, in a process called “cross presentation”, peptides of extracellular origin can also be loaded onto MHC-I molecules and subsequently be presented on the cell surface. This process, details of which are still a topic of research, does not occur in all antigen-presenting cells (APC) but seems to be most efficient in a subset of DCs that expresses the transcription factor BATF3 and the chemokine receptor XCR1.

Interaction with T-cells

Antigen-presenting DCs travel to the T cell zone of a lymphatic organ and secrete the chemokine CCL19, which specifically attracts naïve T cells. To induce a T cell response, the DC forms an immunological synapse (Figure 5) with a T cell whose T-cell-receptor (TCR) is specific for the antigen presented on the DC’s MHC molecule. The three major components of this immunological synapse are the following:

1) The MHC-molecule presenting the antigen interacts with the TCR-complex (specific TCR + invariant CD3 and ζ chains + CD4 for interaction with MHC-II or CD8 for interaction with MHC-I), confirming the specificity of this T-cell for the presented antigen.
2) Costimulatory molecules on the DC (CD80, CD86) interact with their ligand on the T cell (CD28).
3) The DC secretes cytokines for activation of the T cell and polarization towards the subset whose ability is needed most in context of this antigen.

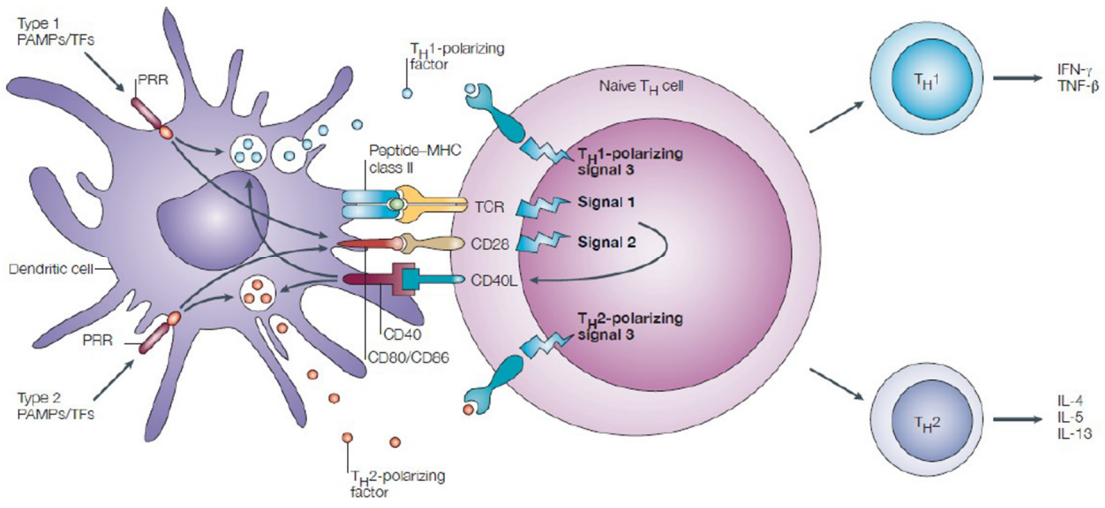

Figure 5: A dendritic cell activating a T cell, forming an immunological synapse

In principle, a DC can induce antigen-specific immunity or antigen-specific tolerance, depending on the DC’s state of activation. Immature DCs don’t express enough MHC and costimulatory molecules, which in contact with an antigen-specific T-cell leads to T-cell anergy, apoptosis or differentiation into Tregs. This seems to be important for the prevention of autoimmunity (Filley & Dey, 2017). But when the DC is mature and these three signals are given, the T-cell is activated and can carry out its various tasks. In the context of antitumor immunity, the cytotoxic activity of CTLs seems to be most important.

In general, there is no T cell response without the presentation of antigens by APCs in the context of costimulatory molecules. DCs are the most potent APCs for the initial activation of T cells because they can engulf a vast repertoire of different antigens and efficiently cross-present them. Macrophages and B cells mainly process soluble and intracellular antigens and present them to T-cells that have already been activated by DCs to receive T-cell help (via cytokines and surface molecules), whereas the only aim of antigen presentation by DCs is to activate T cells.

NK-cell stimulation

Among the vast amounts of cytokines secreted by activated DCs, there are also IL-15, that stimulates the proliferation of NK cells, and IL-12, that activates NK cell killing and secretion of IFN-γ.

NK cells are an early line of defence in the destruction of especially abnormal (potentially malignant) and virus-infected cells. They express neither TCRs nor immunoglobulins, but their activity is regulated by an accurate balance between signals from inhibitory and activating receptors. NKG2D receptors recognize stress-induced surface molecules and tilt the balance towards activation, whereas the recognition of MHC-I (present on all healthy cells) suppresses activation. If DCs now secrete IL-12 and IL-15, the balance will be tilted towards activation and NK cells act out their "natural killing" activity, mainly by secreting perforin and granzymes, but also via TNFα, Fas-ligand or TRAIL.

A high natural cytotoxic activity of peripheral-blood lymphocytes is associated with reduced risk of cancer in humans (Imai, Matsuyama, Miyake, Suga, & Nakachi, 2000), most likely due to their ability to kill in an MHC-independent manner, since tumors often evade the immune system by downregulating MHC on their surface (Karre, Ljunggren, Piontek, & Kiessling, 1986). Representing 30-50% of all hepatic lymphocytes, the percentage of NK cells in the liver is 6-10 times higher than in the blood, suggesting a high potential for an anti-tumor effect of these liver NK cells once they are activated by DCs.

By the production of large amounts of various cytokines and cell-cell contacts, DCs interact with several other immune cells as well. How much these interactions, like for example the one with mast cells (A. Dudeck, Suender, Kostka, von Stebut, & Maurer, 2011; J. Dudeck et al., 2017), contribute to a strong immune response remains to be discovered, but it once more underlines the DC's central mediator role in the development of an immune response.

1.4.2 Subsets of human dendritic cells and their function

Human dendritic cells consist of three major subpopulations: classical DCs type 1 and 2 (cDC1 & 2, also known as myeloid DCs type 1 and 2) and plasmacytoid DCs (pDC). They share a similar origin (Figure 6) – which is distinct from monocyte development – but show slight differences in their life cycle and function (Merad, Sathe, Helft, Miller, & Mortha, 2013). Additionally, there are the special subsets of

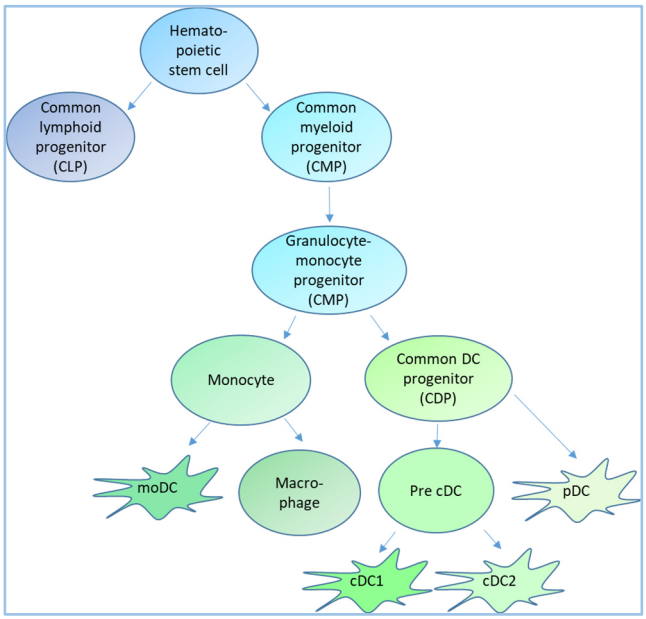

Figure 6: Human dendritic cell lineage

The three major DC-subsets share the same origin – the common DC progenitor (CDP) –, while moDCs develop from the monocytic lineage.

monocyte-derived DCs (moDC) and Langerhans cells (LC), the DCs of the skin. Today DC-subsets are defined by their lineage, differences in expression of key transcription factors (e.g., levels of IRF4 & 8) and gene expression, whereas the traditional definition as "lymph node resident DC" or "migratory tissue DC" is rather anatomically relevant and describes their current mechanism of action. In general, all DC subsets can act out most functions of the other subsets but to another extent. DCs arise from progenitor cells in the bone marrow, don't proliferate in the periphery, and having a lifespan of days to weeks they have to be replaced continuously (Collin & Bigley, 2018).

Plasmacytoid dendritic cells

After already being described in the 1950s (Lennert & Remmele, 1958), plasmacytoid dendritic cells were found to anatomically resemble plasma cells with their prominent ER and golgi. They sense foreign nucleic acids from virus infections, bacteria or malignancies via TLR 7 and 9 (Bao & Liu, 2013), respond with the production of abundant amounts of type I IFNs (Cella et al., 1999; Siegal et al., 1999) and upon cytokine response increase their capacities in antigen-presentation. They take up smaller amounts of antigen than cDCs but preserve the engulfed antigens for longer periods of time. Upregulating both MHC-I and II, pDCs induce CD4+ and CD8+ T cell responses and – upon uptake of soluble and cell-associated tumor antigens – are especially potent activators of CTL antitumor immune responses (Tel et al., 2013). Apart from IFN I they also release other pro-inflammatory cytokines like IL-6 and 12, CXCL 8 and 10 or CCL 3 and 4 (Swiecki & Colonna, 2015).

Furthermore, pDCs have been discussed to play a role in the pathogenesis of chronic infections as well as autoimmune diseases. In chronic Hepatitis B, the virus hampers pDC function; upon infection, there is no IFN-α production and the expression of co-stimulatory molecules or the interaction with NK cells or monocytes is diminished (Woltman, Op den Brouw, Biesta, Shi, & Janssen, 2011). In psoriasis and systemic lupus erythematosus the recognition of self-RNA complexed with a peptide leads to IFN-α production by pDCs (Ganguly et al., 2009; Lande et al., 2011). Plasmacytoid DCs accumulate mainly in the blood and lymphoid tissues (Merad et al., 2013).

Classical dendritic cells

Human classical DCs type 1 are discussed to accumulate rather in different lymphoid and non-lymphoid tissues than in the blood. They have been characterized to show high capacities in cross-presenting antigens to CD8+ CTLs via MHC-I (Bachem et al., 2010), furthermore they support T_H1-responses and NK cell-activation via secretion of IL-12 (Collin & Bigley, 2018). Interestingly, cDC1 are – in contrast to cDC2 – resistant to productive virus infection, making sure that their function is not impaired by virus replication (Silvin et al., 2017). Upon many other PRRs, cDC1 express TLR3 for the recognition of dsDNA, leading to the production of IFN I via IRF3. Furthermore, they play an important role in the clearance of HCV due to their function as major producers of IFN III (Yoshio et al., 2013).

Indeed most functions are not restricted to cDC1 but furthermore shared with classical DCs type 2, which are the most abundant cDCs in the blood as well as in tissues (up to ten times more than cDC1) (Collin & Bigley, 2018). They synthesize even larger amounts of IL-12 (Nizzoli et al., 2013), and possessing many different PRRs like TLRs, lectin-, RIG-like and NOD-like receptors they response to a broad range of antigens via secretion of immune-stimulatory (TNF-α, IL-6, IL-23) as well as inhibitory cytokines (IL-10), but in contrast to cDC1 they are constantly low in IFN III-production. CDC2 possess the ability to activate T_H1-, T_H2-, T_H17- and CD8+ cytotoxic T cells (Collin & Bigley, 2018).

Monocyte-derived dendritic cells

Monocyte-derived DCs (moDC), also known as “inflammatory DCs”, share the granulocyte-monocyte-progenitor with the “common” DC-lineage but directly derive from monocytes (Figure 6). There are resident populations of moDCs in healthy skin, lung or intestine tissue that expand in an inflammatory setting. They secrete IL-1, -12 and -23, as well as TNF-α, express CCR7 and are potent stimulators of CD4+ and CD8+ T cells. In contrast, other literature suggests that moDCs function mainly at the site of inflammation instead of migrating to the lymph node (Guilliams & van de Laar, 2015). MoDCs share many markers with and are not easily distinguishable from cDC2 (Collin & Bigley, 2018).

Langerhans cells

Langerhans cells are the DCs of the basal epidermis and, in brief, maintain the epidermal health concerning tolerance to commensals as well as defence from pathogens (Collin & Bigley, 2018). The salient aspect which makes them a distinct subset is their ability of self-renewal: once established by primitive and foetal liver haematopoiesis, they maintain their number by mitosis under steady-state conditions and are only dependent on replacement from the bone marrow after massive depletion, e.g. caused by UV-radiation (Kanitakis, Morelon, Petruzzo, Badet, & Dubernard, 2011). When the LCs recognize a foreign pathogen, the TNF-α and IL-1β present in the inflamed skin loosens their connection to the surrounding epithelium. They are known to migrate to their skin-draining lymph nodes (LN) where they prime naïve CTLs (Banchereau et al., 2012; Collin & Bigley, 2018). Moreover,

they are not only dependent on but also stimulate skin inflammation via presentation of lipid antigens to T_H17-cells that react with the secretion of IL-17 and IL-22 (J. H. Kim et al., 2016).

1.5 Dendritic cell-based cancer immunotherapies

Already in the 1990s, only 20 years after the discovery of the DCs, human clinical trials showed the benefits of dendritic cell vaccines in the treatment of different cancer entities. The idea underlying the approach is to activate DCs and to load them with tumor-specific antigens so that they mediate innate and adaptive immune responses against these tumor-specific antigens. By now there are two established routes for the introduction of the antigens: direct targeting of antigens to DCs *in vivo* and antigen-loading of generated DCs *ex vivo.* The antigens are exposed to the DCs in many different forms like peptides, whole cell lysates or nucleic acids (Filley & Dey, 2017). Many clinical and preclinical studies were already able to show the immune activation as a response to different approaches of DC-vaccination, whereas an improvement of the clinical outcome often didn't change significantly.

1.5.1 *In vivo*-targeting of dendritic cells

There are various approaches to target DCs *in vivo*. In the beginning, the idea was to couple an antigen to an antibody which is specific for a DC-surface molecule, e.g. OVA was coupled to an antibody against DEC-205, a DC-surface molecule (Bonifaz et al., 2002), but currently, researchers are mainly working on nanoparticles for the delivery of nucleic acid-based vaccines. For example mRNA-containing liposomes are designed with specific linkers for an optimal DC-targeting and mRNA-uptake (Wang et al., 2018), whereas other nanoparticles consist of immune-active polymers (Rajput et al., 2018). An increase in OS in Melanoma-bearing mice was also shown in a similar approach using gold nanoparticles for DNA-delivery to DCs (Gulla et al., 2019). Interestingly, also an adenoviral vector expressing a human glioma-specific antigen was successfully investigated for the targeting of DEC-205, resulting in prolonged survival of mice with Glioma (J. W. Kim et al., 2018). In these approaches, the risk of inducing tolerogenic responses has to be considered, especially in patients with dysfunctional immune responses due to pre-treatment, highlighting the possible importance of DC maturation activators (Filley & Dey, 2017).

1.5.2 Antigen-loading *in vitro*

Peptide- and protein-pulsed DCs

Peptides are widely used in various approaches to pulse DCs. A phase I clinical trial showed the safety and immunogenicity of a DC vaccine against pancreatic cancer consisting of DCs pulsed with a WT-1 peptide (Yanagisawa et al., 2018). In a phase II study in newly diagnosed GBM-patients, the DCs were pulsed with six different synthetic peptide epitopes targeting GBM tumor/stem cell-associated antigens. The treatment was well tolerated and significantly improved the PFS by 2.2 months (Wen et

al., 2019). The major limitation in the use of peptides is their restriction to a specific HLA-type. This either implies that patients with other human leucocyte antigen (HLA)-types can't be treated or that peptides specific for different HLA-types have to be synthesized. The above-mentioned study in GBM-patients used peptides for different HLA-types and interestingly showed that the immunogenicity of the approach is highest in HLA-A2-positive patients. Apart from peptides, also larger proteins can be engulfed and processed by DCs, making the selection of HLA-compatible sequences during processing possible, but the selected ones might not be as immunogenic as necessary (Filley & Dey, 2017).

RNA-based approaches

An efficient strategy of antigen-loading is the introduction of TAA-encoding, *in vitro*-transcribed mRNAs into mature DCs by electroporation, that are then expressed by the DCs. This approach is independent of the patient's HLA-type and the availability of patient material and it is feasible to produce enough mRNA. Interestingly, the capacity of CTL activation is higher in DCs pulsed with only one type of mRNA compared to DCs pulsed with mRNAs encoding for different TAAs. It is therefore favourable to pulse separate aliquots of DCs with different mRNAs to elicit a broad immune response against various tumor antigens. This avoids the selection of antigen-loss variants and even optimizes CTL activation (Subklewe et al., 2014). The CTL-stimulating capacity can be further enhanced by checkpoint blockade, e.g. using antibodies against PD-1 or LAG-3 (Lichtenegger et al., 2018).

The transduction of dendritic cells with an adenoviral vector encoding for TAAs is another way to introduce genetic information into the DCs. In a phase II trial, DCs were infected with an adenovirus encoding the full-length gene for p53. The vaccine was shown to be safe and to induce an immune response but unfortunately failed to significantly improve OS (Chiappori et al., 2019).

The use of whole-cell lysates

The use of whole cell lysates to pulse DCs resembles most the situation during an immune response in the body. A phase II clinical trial in late-stage HCC patients investigated the safety and efficacy of repeated intravenous application of mature DCs stimulated with lysed HepG2 cells, a human hepatoblastoma-cell line. The therapeutic was tolerated with evidence of antitumor efficacy, in some cases it even induced measurable antitumor immune responses, but since there was no complete response and only one patient showed a radiologically assessed partial response, further improvement is necessary (Palmer et al., 2009). The use of whole tumor cell lysates is also tested in preclinical studies in other cancer entities like pancreatic or breast cancer, demonstrating promising immune activating properties of the pulsed DCs (Pan et al., 2019; Tomasicchio et al., 2019).

Combination with oncolytic virotherapy

A few promising investigations have already been made on the combination of oncolytic virotherapy and DC vaccines. E.g., DCs stimulated with NDV-lysed lung cancer cells *in vitro* have been shown to stimulate T-cells more effectively than freeze-thaw-lysed lung cancer cells, taking into consideration T cell-proliferation as well as IL-2 and IFN- γ secretion (Zhao et al., 2018). Moreover, DCs stimulated with NDV-lysed breast cancer cells increased the expression of costimulatory molecules and the secretion of IFN- γ by memory T-cells (Schirrmacher, Lorenzen, Van Gool, & Stuecker, 2017).

Route of DC-application

The different possible routes for DC-injection that have been investigated so far are intradermal (i.d.), intranodal (i.n.), intralesional (i.l.) and intravenous (i.v.)) application. To date it is still difficult to define the best route of application, but none has yet been identified to be constantly superior to the others.

I.d. application is probably the least complicated route. In a phase II clinical trial performing four i.d. vaccinations each one was applied into a different site, injecting into the proximal upper and lower extremities bilaterally close to the axillary and inguinal nodal basins (Chiappori et al., 2019). Interestingly, a clinical study showed that pre-treatment of the vaccination site with a potent recall antigen (such as tetanus/diphtheria toxoid) significantly increased trafficking of the injected DCs to the regional LNs and efficacy of tumor-specific DCs, improving the clinical outcome (Mitchell et al., 2015).

The difficulty in i.n. injection is the accuracy of the application, leading to a big variation in DC numbers that reach the lymph node (Huber, Dammeijer, Aerts, & Vroman, 2018). A clinical study using HER2 peptide-pulsed DCs underpins that the importance of DC numbers at the LNs is uncertain, showing no significant difference in clinical outcome and immune activation comparing i.n. to i.l. injection, even though fewer DCs arrived at the tdLN in case of i.l. injection (Lowenfeld et al., 2017).

In a mouse experiment, peptide-pulsed bone-marrow derived DCs were injected i.d., i.p. or i.v. prior to tumor challenge. Only the animals pre-treated with DC-injection into the skin didn't show any tumor growth (Edele et al., 2014).

The only FDA-approved DC vaccine administers the DCs i.v. (Small et al., 2000), alike other clinical trials (Palmer et al., 2009).

1.5.3 The role of DC-subsets for an anticancer vaccine approach

Clinical trials directly comparing different DC subsets for anticancer vaccine approaches are urgently needed, especially since knowledge about the contribution of the subsets to antitumor immunity is lacking as well. Many approaches focus on moDCs because they are available in larger amounts whereas cDCs and pDCs are less than 1% of human peripheral blood mononuclear cells.

Experiments in mice demonstrated that different tumor-associated DCs with distinct functions are present within the lesion and that their proportions evolve during tumor growth. They especially showed that moDCs outperformed cDCs for antigen uptake and processing but didn't migrate to the tumor-draining LNs due to their lack in inducing CCR7-expression. Subsequently they inefficiently stimulated proliferation of $CD4^+$ and $CD8^+$ T cells and even suppressed T cell proliferation via production of immunosuppressive NO and secretion of IL-10, contributing to the immunosuppressive TME. Proliferation of specific $CD4^+$ and $CD8^+$ T-cells in the tumor-draining LNs was successfully promoted by cDC1, in line with their ability to induce CCR7, whereas cDC2s stimulated Th17-cells (Laoui et al., 2016).

Furthermore it might be favourable to take into account that the TME differs between tumor entities and patients, therefore an analysis of the immune cells present in a specific tumor might help in choosing the right DC subset (Huber et al., 2018).

State of DC-activation

For a successful anticancer vaccine, fully activated DCs are needed. Due to their important role in the prevention of autoimmune reactions, DCs are not only able to induce immune activation but also to generate antigen-specific tolerance. Only fully matured DCs possess enough costimulatory molecules and MHC on their cell surface to activate naïve T cells, whereas incompletely matured DCs induce T cell anergy, apoptosis or differentiation into regulatory T-cells (Treg) and therefore antigen-specific tolerance (Dhodapkar, Steinman, Krasovsky, Munz, & Bhardwaj, 2001).

In line with this consideration, the activation of DCs *in vitro* is an important aspect for a successful vaccine approach. A potent DC stimulator is the small molecule R848 (Resiquimod), a TLR7/8 ligand, as well as the synthetic RNA Poly I:C, a TLR3 ligand, both mimicking viral pathogen-derived products and enhancing IL-12 secretion by DCs (Subklewe et al., 2014). LPS are part of the outer membrane of gram-negative bacteria and, commonly used as a DC-stimulator (Lowenfeld et al., 2017), imitate a bacterial infection. Additionally, cytokines like TNFα, IL1β, IFNγ, and PGE_2 are often added to the DC culture as activating stimuli.

1.5.4 The successful example sipuleucel-T: DC-vaccination against prostate cancer

Being the first FDA-approved immunotherapy made from a patient's own cells, sipuleucel-T – PROVENGE by Dendreon Pharmaceuticals LLC. – is a dendritic cell-vaccine against castration-resistant metastatic prostate cancer ("Dendreon - About us: Our history," 2018). To date it is the only DC-vaccine approved by the FDA.

For the preparation of sipuleucel-T, autologous peripheral blood mononuclear cells (PBMCs) are isolated from the patient's own blood via leukapheresis, followed by several density gradients to

deplete erythrocytes, platelets, lymphocytes and low-density monocytes. The isolated cells are then incubated for 40 hours at 37°C in 5% CO_2-atmosphere with the fusion protein PA2024. This fusion protein contains the full-length human prostatic acid phosphatase, whose expression isn't limited to prostatic tissue but much higher in the prostate than in other human tissues (Graddis, McMahan, Tamman, Page, & Trager, 2011), and the full-length human granulocyte-macrophage colony-stimulating factor (GM-CSF). After washing steps, a minimum of 50 million PA2024-pulsed CD54+ cells are formulated in 250ml lactated Ringer's solution and infused intravenously into the patient (Small et al., 2000). CD54, a cell surface molecule also known as ICAM-1, is an activation marker of APCs and its increased expression serves to determine the potency of PROVENGE. The final product also contains T-, B- and NK cells.

Prior to the infusion, the patient is premedicated orally with paracetamol and an antihistamine to prevent acute infusion reactions. It is recommended to administer three complete doses of sipuleucel-T at two-week intervals, each infusion lasting 8 hours.

The "Immunotherapy for Prostate Adenocarcinoma Treatment" (IMPACT) phase-III clinical trial was conducted from 2003 to 2009 to test the OS after treatment with sipuleucel-T, including 512 men with metastatic castration-resistant prostate cancer. Compared to the placebo group it showed 22% relative reduction in the risk of death, complementing an improvement of 4.1 months in median OS (Figure 7), but didn't significantly affect the time to disease progression (Kantoff et al., 2010).

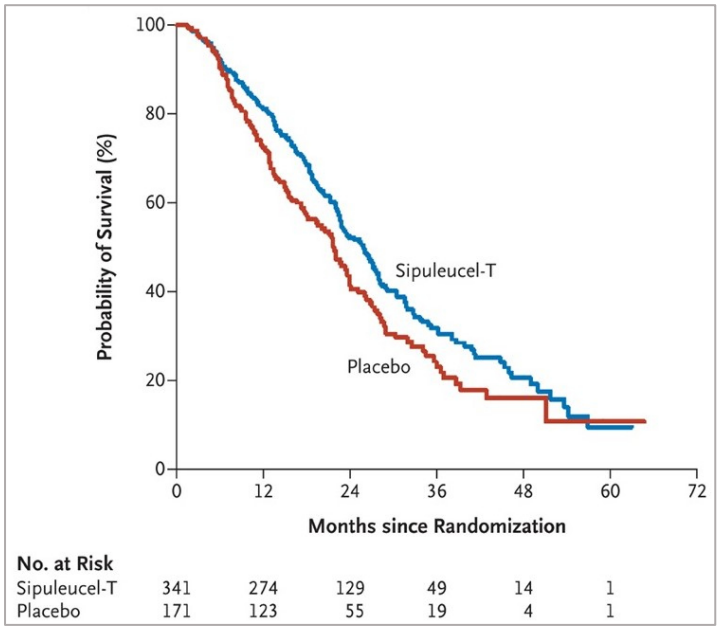

Figure 7: Kaplan-Meier-estimates of OS in the IMPACT trial

In general, PROVENGE was well tolerated. Apart from acute infusion reactions and the mild side effects of the standardized leukapheresis procedure, the most common side effects (reported by ≥ 15% of the study population) were chills and fever, fatigue and nausea, back pain, joint and headache, which in ~70% of the cases were mild or moderate in severity. Serious adverse events were mainly cerebrovascular events ("PROVENGE (sipuleucel-T)," 2019).

PROVENGE had also been approved by the EMA for "men with asymptomatic or minimally symptomatic metastatic (non-visceral) castrate-resistant prostate cancer in whom chemotherapy is

not yet clinically indicated" in the European Union in 2013. In 2015, the marketing authorization has been withdrawn because the holder – Dendreon UK Ltd. – decided to "permanently discontinue the marketing of the product for commercial reasons" ("Provenge - Withdrawal of the marketing authorisation in the European Union ", 2015).

1.6 Development of a VSV-NDV stimulated DC vaccine: Aim of my project

The aim of this project was a first proof of concept experiment to investigate the potential of a personalized dendritic cell vaccine against HCC, stimulated by the immunogenic oncolytic virus VSV-NDV, using a human *in vitro* cell culture model system and primary immune cells from healthy volunteers.

For a better understanding of the experimental steps of this project, the long-term concept of the potential therapeutic (Figure 8) and the rationale behind it will now be described here: A blood sample is taken from the HCC patient for the *in vitro* generation of monocyte-derived dendritic cells. In parallel, a sample of the tumor tissue is taken and infected *in vitro* with VSV-NDV to create a tumor cell lysate. Now this tumor cell lysate including the viral particles is incubated with the newly generated moDCs; during this incubation time the moDCs are not only activated but furthermore pulsed with tumor associated antigens (TAA). Now the moDCs are purified and administered to the patient.

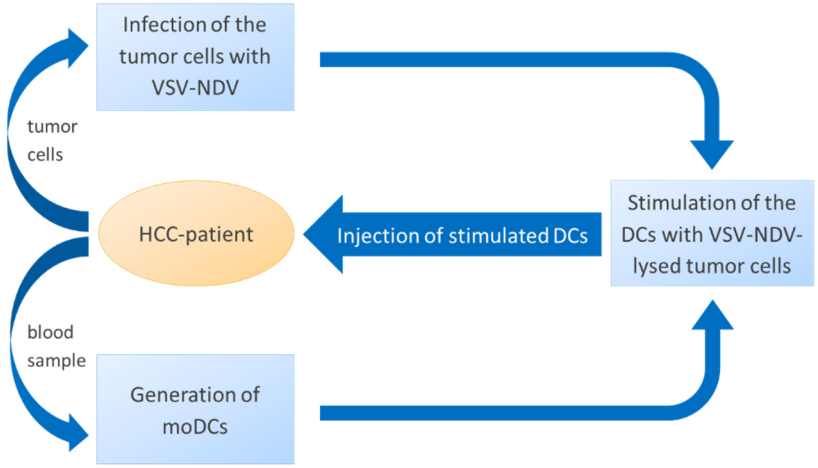

Figure 8: Overview of the concept of the VSV-NDV-stimulated DC vaccine

1.6.1 Dendritic cells elicit a broad and long-lasting immune response

Dendritic cells are the immune system's all-rounder. They are the most important APCs, patrol all tissues and furthermore take up and present all kinds of antigens. Subsequently they act as an initiator of innate as well as adaptive immune responses via the secretion of cytokines and interaction with $CD4^+$ and $CD8^+$ T cells; in addition, they are even able to induce memory T cells. The idea of our approach is that a DC – once it has engulfed a TAA – orchestrates a broad immune response (see 1.4) against the tumor and even creates T cell memory to prevent recurrence of the disease.

1.6.2 The patient's own tumor cells provide a broad range of tumor associated antigens

Using a whole cell lysate for pulsing the DCs, the DC-induced immune response will not only be directed against a single TAA but against many different ones, amplifying its potency. It furthermore prevents the risk of selection for antigen loss variants, which is a hurdle in other immunotherapeutic approaches like CAR-T-cell therapy (Simon & Uslu, 2018). Furthermore, tumors of the same entity differ a lot among individual patients, especially concerning the expression of TAAs (Subklewe et al., 2014). The benefit of using the patient's own tumor material is that the immune response will be directed exactly against the patient's own TAAs, providing a personalized therapy. This is particularly important in HCC, since it is characterized by considerable phenotypic and molecular heterogeneity (EASL, 2018).

1.6.3 VSV-NDV causes immunogenic cell death

Immunogenic cell death is a coordinated type of cell death that includes changes on the cell surface and the release of soluble mediators in a defined temporal sequence with the aim to stimulate an immune response against antigens of the dying cell.

On the one hand this contrasts with apoptosis, which is also a programmed type of cell death but doesn't induce an immune response, on the other hand with necrosis, which induces an inflammation but isn't regulated by any cellular program. The signals released by ICD operate on different receptors of DCs to stimulate the engulfment, processing and presentation of dead-cell-antigens by DCs (Figure 9). A few examples are explained in the following section.

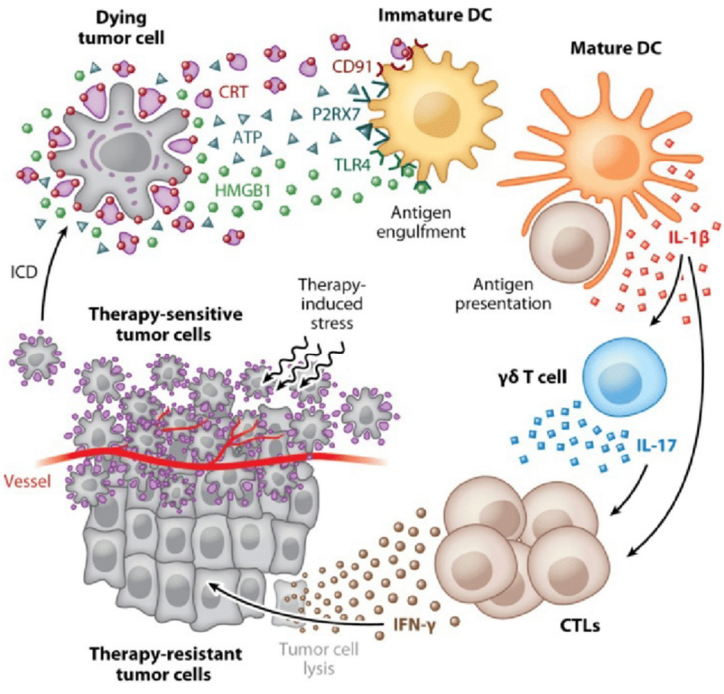

Figure 9: ICD leads to the release of various DC-activating mediators

Calreticulin (CRT) is a protein in the lumen of the ER. In the beginning of an ICD it is relocated to the outer surface of the cell membrane together with other ER-proteins due to ER-stress, binds to CD91 on DCs and acts as a potent engulfment signal for the uptake of antigens by the DCs (Panaretakis et al., 2009).

During the ICD, autophagy promotes the secretion of adenosine triphosphate (ATP) by the dying cancer cells. ATP acts as a chemoattractant for DCs and later T cells via predominantly binding to its P2Y2-receptors.

Moreover, ATP also binds to the P2RX7-receptors, initiating the inflammasome-dependent release of IL-1β, which is necessary for the priming of IFNγ-producing CD8+ T cells (Ghiringhelli et al., 2009). Altogether, ATP-release is of critical importance for the recruitment of immune cells.

Later during cell death, as the membrane becomes permeabilized, the dying cell releases the high mobility group box 1-protein (HMGB1), which is the most abundant non-histone chromatin protein. It binds different receptors on the surface of immune as well as nonimmune cells and promotes the release of proinflammatory cytokines, the recruitment of mononuclear cells and a humoral immune response (Kroemer, Galluzzi, Kepp, & Zitvogel, 2013). Especially important is the binding of HBGB1 to the TLR-4 on DCs, which is necessary for the cross-presentation of antigens by DCs (Apetoh et al., 2007).

In line with these findings, we hypothesize that the tumor cells dying via ICD – which is induced by infection with VSV-NDV – potently activate dendritic cells.

1.6.4 Every vaccine needs an adjuvant

An adjuvant is a substance that enhances the immunogenicity of the substances mixed with it. Every stimulation of the immune system needs an adjuvant so that the target antigen really elicits an immune response. In fact, many foreign proteins fail to induce an immune response when injected alone, but in combination with a pathogen they become immunogenic via induction of costimulatory molecules (Murphy & Weaver, 2017). In an infection, the “adjuvant” is usually the antigen itself, like a microbial particle (a PAMP like LPS or viral RNA). In preventive vaccination alum is often used for this purpose because it activates various immune pathways, but especially Th-2 responses and antibody formation and is therefore not the optimal adjuvant for an anticancer vaccine.

Synthetic TLR ligands are currently tested in clinical trials as adjuvants for anticancer vaccination, since TLR signalling initiates a strong APC activation including upregulation of MHC and costimulatory molecules, cytokine release and migration to the lymph nodes (Gouttefangeas & Rammensee, 2018).

Because VSV-NDV is a pathogen and can therefore serve as a source for PAMPs for TLR binding, we hypothesize that it acts as a strong adjuvant for DC activation. Since human DCs are difficult to activate *in vitro*, this might be necessary to potentiate the immune stimulatory effect already achieved by the foreign TAAs and the ICD.

2. Materials and Methods

2.1 Materials

2.1.1 Cytokines, antibodies and kits

Table 1: Cytokines and stimulation antibodies

Purified NA/LE Mouse Anti-Human CD3	BD Pharmingen
Purified NA/LE Mouse Anti-Human CD28	BD Pharmingen
Recombinant Human GM-CSF	PeproTech
Recombinant Human IFN-γ	PeproTech
Recombinant Human IL-1β	PeproTech
Recombinant Human IL-2	PeproTech
Recombinant Human IL-4	PeproTech
Recombinant Human TNF-α	PeproTech
Prostaglandin E2	biogems
R848 (Resiquimod)	InvivoGen

Table 2: Antibodies for flow cytometry

Antigen	**Clone**	**Host**	**Conjugated flurophore**	**Supplier**
CD3	OKT3	Mouse IgG2a	APC/Fire™750	BioLegend
CD4	SK3	Mouse IgG1	PacBlue	BioLegend
CD8	HIT8a	Mouse	PE	BD Pharmingen
CD14	61D3	Mouse	FITC	eBioscience
CD44	BJ18	Mouse IgG1	PerCP/Cy5.5	BioLegend
CD69	FN50	Mouse IgG1	APC	BioLegend
CD83	HB15e	Mouse IgG1	PerCP/Cy5.5	BioLegend
CD86	IT2.2	Mouse IgG2b	PE	BioLegend
CD274 (PD-L1)	MIH1	Mouse	APC	invitrogen
HLA-ABC (MHC-I)	G46-2.6	Mouse	BV421	BD Biosciences
HLA-DR (MHC-II)	L243	Mouse IgG2a	BV605	BioLegend
TCR β-chain (anti-mouse)	H57-597	Hamster	PE	BD Biosciences

Table 3: Kits

Product	**Supplier**
CytoTox 96® Non-Radioactive Cytotoxicity Assay	Promega
Human IFN-γ ELISA MAX™ Standard Set	BioLegend
LEGENDplex™ Multi-Analyte Flow Assay Kit	BioLegend
MojoSort™ Human Pan Monocyte Isolation Kit	BioLegend

2.1.2 Media and reagents

Table 4: Cell culture media and supplements

DMEM (1X) + GlutaMAX™-I	Thermo Fisher Scientific
DMEM F12 (1X) + GlutaMAX™-I	Thermo Fisher Scientific
RPMI 1640 Medium + GlutaMAX™-I	Thermo Fisher Scientific

Fetal Bovine Serum	Biochrom
Human Serum	Sigma-Aldrich
L-Glutamine 200mM	PAA cell culture company
Non-essential amino acids (100X)	GE healthcare
Penicillin/Streptomycin (10,000 U Pen + 10mg/ml Strep)	Sigma-Aldrich
Sodium pyruvate 100mM	Sigma-Aldrich
HEPES Buffer Solution	Thermo Fisher Scientific
Collagen Type I Rat Tail	Corning

Table 5: Chemicals and biological reagents

Bovine Serum Albumin	Sigma-Aldrich
Dimethylsulfoxide (DMSO)	Carl Roth GmbH & Co. KG
Dulbecco's phosphate buffered saline (1X)	PAN Biotech
Dulbecco's phosphate buffered saline with Ca^{2+} and Mg^{2+} (1X)	PAN Biotech
Dulbecco's phosphate buffered saline (5X)	PAN Biotech
EDTA	Sigma-Aldrich
Ethanol 80% (V/V)	Otto Fischar GmbH & Co. KG
Human TruStain FcX™	BioLegend
Heparin-Natrium 25.000	Ratiopharm
Isopropylalkohol	Otto Fischar GmbH & Co. KG
Lymphosep Lymphocyte Separation Media	biowest
Paraformaldehyde (PFA)	Sigma-Aldrich
Red Blood Cell Lysis Buffer (10X)	BioLegend
RetroNectin	TaKaRa
Trypan Blue Stain (0.4%)	Sigma-Aldrich
Trypsin-EDTA	PAN Biotech
Tween 20 Solution (10%)	Bio-Rad Laboratories
UltraComp eBeads compensation beads	invitrogen
UltraPure Water	Thermo Fisher Scientific
VioBlue viability dye	Miltenyi Biotec

2.1.3 Equipment and consumables

Table 6: Equipment

Product	**Supplier**
LUNA-FL™ Dual Fluorescence Cell Counter	logos biosystems
HERAeus Horizontal Laminar Flow Cabinet KS18	Thermo Fisher Scientific
Centrifuge 5415D + R	Eppendorf
Centrifuge 5702R	Eppendorf
Centrifuge 5910R	Eppendorf
CytoFLEX S Flow Cytometer	Beckman Coulter
Cryo 1 °C Freezing Container	Nalgene
Fridge + Freezer (-20°C)	Siemens
HERAfreeze HFU T Serie -86 freezer	Thermo Fisher Scientific
Ice machine	Ziegra
HERAcell 240 CO_2 Incubator	Thermo Fisher Scientific

Microscope 3/4 240023	Exacta & Optech GmbH
Axiovert 40 CFL Fluorescence microscope	Zeiss
MidiMACS™ Separator	Miltenyi Biotec
MACS® MultiStand	Miltenyi Biotec
Sunrise Absorbance Microplate Reader	Tecan
Stripettor™ Ultra Pipetboy	Corning
10, 20, 200, 1000 Pipettes	Eppendorf
300 Pipette multichannel	Eppendorf
Varioklav Dampfsterilisator EP-Z	HP Medizintechnik GmbH
Multipette® M4	Eppendorf
IKA Vibrax VX7	Janke & Künkel
Sonorex RK100	Bandelin
REAX top Vortex	Heidolph

Table 7: Consumables

Cryo.S™ PP cryo vials	Greiner Bio-One
Conical Tubes (15, 50 ml)	BD Falcon
Reagent Tubes (1.5, 2ml)	Eppendorf
Combitips® advanced	Eppendorf
Pipette Filter Tips (1000, 200, 20, 10µl)	StarLab
Pipette Tips (200µl)	StarLab
Serological Pipettes (5, 10, 25, 50ml)	Greiner Bio-One
LS Columns	Miltenyi Biotec
Tissue Culture Flasks (T25, T75)	TPP
Multiwell Tissue Culture Plates Flat Bottom (adherent, 96-, 6-well)	TPP
Multiwell Plates NUNC A/S Flat Bottom (non-adherent, 96-, 24-, 6-well)	Thermo Fisher Scientific
96-well Round Bottom Plates	Thermo Fisher Scientific
96-well NUNC-Immuno ELISA Plates	Thermo Fisher Scientific
96-well V-Bottom Plates	Thermo Fisher Scientific
SAFETY MULTIFLY Kanüle 21 G, mit Multiadapter	Sarstedt
Syringe Injekt® Solo (20ml)	Braun
Syringe Luer-Lok (10 ml)	Braun
Filtropur S Syringe Filter (0.2, 0.45 µm)	Sarstedt
Cell Strainer (70, 100 µm)	Greiner Bio-One
Adhesive Film for Microplates	VWR
Parafilm™ M	Bemis

2.1.4 Software

- Adobe Acrobat Reader DC (Dublin, Ireland)
- CytExpert (Avantor; Radnor, USA)
- EndNote X9 (Clarivate Analytics; Philadelphia, USA)
- FlowJo™ v10.6.2 (FlowJo, LLC; Ashland, USA)
- GraphPad PRISM 8 (GraphPad; La Jolla, USA)
- Magellan™ (Tecan; Männedorf, Swizerland)
- Microsoft Office 365 (Microsoft; Redmond, USA)

2.2 Methods

2.2.1 Standard procedures

Cell culture

All cells were cultured in their appropriate medium (Table 8) in a humidified atmosphere at 5% CO_2 and 37°C. For passaging, adherent cells were washed once with phosphate buffered saline (PBS), trypsinized and replated at the appropriate density in fresh medium. Cells in suspension – unless described differently – were mixed by pipetting, the appropriate amount was discarded and replaced with fresh medium. Mycoplasma-PCR was performed regularly.

Table 8: Cell culture conditions

Cell lines	**Cell type & use**	**Culture medium**
AGE	Duck retina cell line (for TCID50 assay)	DMEM F12 + 10% FBS + 1% P/S
HepG2_core	Human hepatoblastoma cell line with intracellular expression of Hepatitis B core antigen (tumor model)	DMEM + 10% FBS, 1% P/S, 1% L-Gln, 1% NEAA, 1% SodPyr
RD114_6K	Retrovirus producer cell line with stable expression of HepB-Core-specific TCR (for transduction of human T-cells)	DMEM + 10% FBS, 1% P/S, 1% L-Gln, 1% NEAA, 1% SodPyr
Primary cells		
moDCs	Human monocyte derived dendritic cells freshly generated from healthy donors	RPMI + 1,5% human serum
T cells	Human T-cells freshly generated from healthy donors	RPMI + 10% FBS, 1% P/S, 1% L-Gln, 1% NEAA, 1% SodPyr, 1% HEPES, 16,64µg/ml Gentamicin

For freezing, cells were adjusted to a density – depending on the cell type – of 5 x 10^6/ml or 1 x 10^7/ml in full medium containing 10% dimethylsulfoxide and frozen at -80°C with -1°C/min cooling rate in a cryo freezing container with isopropanol. For recultivation, frozen vials were rapidly thawed at 37°C, prediluted in medium, washed once and resuspended in the appropriate medium for cell culture.

Cell counting was performed using the LunaFL cell counter, diluting 10µl of the cell suspension 1:1 with trypan blue.

Virus growth curves and cytotoxicity

All experiments that include viruses were performed under biosafety level 2 conditions (S2).

For all experiments with VSV-NDV, a variant of this virus equipped with a green fluorescent protein (GFP) was used to allow observation of virus replication under a fluorescence microscope. To investigate the infectibility of a cell line with VSV-NDV-GFP, virus growth curves were performed. Cells were plated one day prior to the infection to reach a confluency of approximately 70% to 90% by the time of infection. They were then infected at two different multiplicities of infection (MOIs) – MOI 1

and 0.01 – in PBS containing Ca^{2+} and Mg^{2+}. After incubation at 37°C for 1h (within this time the virus would enter the cell), the cells were washed three times with PBS to remove the remaining virus. Now they were cultured in their appropriate medium. At 0, 16, 24, 48 and 72 hours post infection (p.i.), microscopic images of the infection process were taken, as well as samples of the supernatant to determine the virus titer and the tumor cell cytotoxicity.

Tissue culture infectious dose 50-assay

To quantify the virus titre in a sample, the tissue culture infectious $dose_{50}$ ($TCID_{50}$) assay was performed. It describes the dilution of virus per ml at which 50% of culture cells are infected.

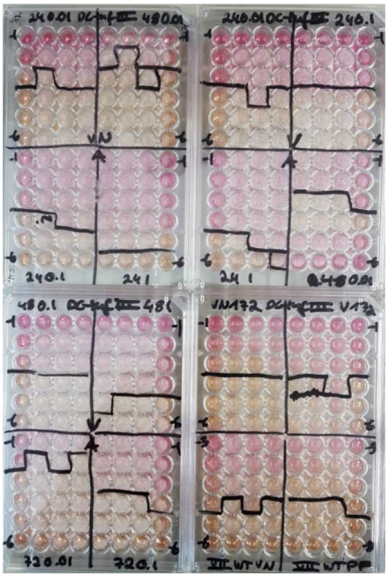

Figure 10: TCID50 plates after analysis

AGE cells were seeded in a flat-bottom 96-well plate in 100µl/well of their appropriate medium one day prior to performing the assay so that the density would reach approximately 70% the next day. On the day of the assay, serial dilutions of each virus sample were prepared in AGE medium and 100 µl of each dilution were added to four wells of the cells.

After an incubation period of 72 hours, the cytopathic effect (CPE) was observed under the microscope, marked on the plate (Figure 10) and the concentration of infectious viral particles in the sample was calculated using the Spearman and Karber algorithm.

LDH-cytotoxicity-assay

The lactate dehydrogenase (LDH) is expressed in the cytoplasm of all cells and therefore released as soon as the integrity of the cell membrane is disturbed, serving as a surrogate parameter for quantifying cell death. Its half-life in the supernatant is approximately 9 hours. For the investigation of the cytotoxic potential of a virus or T cells, LDH was measured in the supernatant taken from treated cells at different time points, using the CytoTox 96® Non-Radioactive Cytotoxicity Assay (Promega) according to the manufacturer's instructions. Using an enzymatic reaction, the red product Formazan is generated – proportional to the amount of LDH in the sample – and measured photometrically. All values are then depicted as percent of the maximum cytotoxicity, which is measured at each time point via the incubation of untreated control cells with a cell lysis buffer.

Flow cytometry

Staining was performed in a round bottom 96-well plate. All centrifugation steps were performed at a speed of 450g for 2 minutes at room temperature. The cells were washed once with PBS. After that, 50µl/well of the staining solution – consisting of antibodies and dyes diluted in PBS – were added,

mixed thoroughly, and incubated for 30 minutes at 4°C in the dark. Afterwards the cells were washed 3 times with 200µl/well of PBS and resuspended in 180µl/well of PBS for analysis. Cells were analysed with the Beckman Coulter CytoFLEX S flow cytometer, using the CytExpert Software, both kindly provided by our collaborators from AG Prof. Dr. Ulrike Protzer.

2.2.2 Generation and processing of primary human immune cells

Generation of peripheral blood mononuclear cells from human blood

After written informed consent, a peripheral blood sample was taken from a healthy donor (aged between 20 and 50) into a Heparin-coated syringe within the regulations of Ethikantrag 318/19 S-SR (approved by the Ethikkommission of the Technical University of Munich). The blood sample was diluted 1:1 in PBS. In a 50ml centrifuge tube, 30ml of diluted blood were carefully layered on 12.5ml of separating solution. The tube was centrifuged at 1000g for 30 minutes at room temperature (RT) with slow acceleration and deceleration to separate the blood components. The PBMC-layer (Figure 11) was then collected into a 50ml centrifuge tube and washed 2 times with PBS (900g/10mins/RT).

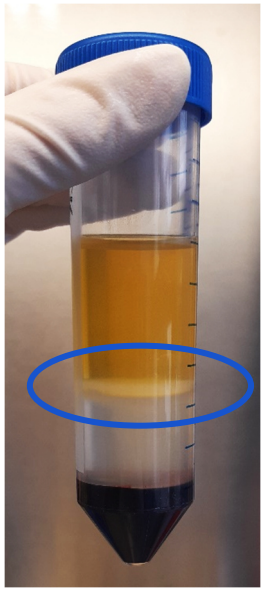

Figure 11: PBMC-layer after centrifugation

Magnetic selection of CD14+ monocytes for the generation of moDCs

To achieve a pure population of monocytes for the generation of moDCs, a negative magnetic selection of CD14+ PBMCs was performed using the MojoSort™ Human Pan Monocyte Isolation Kit (BioLegend).

The freshly obtained PBMCs were filtered through a 100µm cell strainer and adjusted to a concentration of 10^8 cells/ml in cell separation buffer (5X PBS + 2.5% BSA + 10mM EDTA). Fc-receptor blocking solution was added (5µl/ml) and incubated for 10 minutes at room temperature (RT). Then the appropriate amount of the biotin-antibody cocktail, followed by streptavidin nanobeads was added and incubated on ice for 15 minutes, respectively. After washing and resuspension of the now labelled cells in cell separation buffer (10^8/5ml), the suspension was rinsed through a magnetic column, using the MidiMACS™ Starting Kit (Miltenyi Biotec).

To initially determine the dilution of antibodies and beads that leads to the highest purity and yield, the antibody cocktail was diluted 1:2, 1:4, 1:6, 1:8 and 1:10 in separation buffer, while the ratio of antibodies to beads was always 2:1. Purity and yield were assessed via flow cytometry, using a CD3 (APC-Cy7) and CD14 (PE-Cy7) staining for the obtained monocytes and a CD14 (PE-Cy7) staining for the labelled fraction.

Generation of human moDCs from peripheral blood mononuclear cells

The protocol for the generation of human moDCs, as well as for the activation cocktail described under 2.2.3, was kindly provided by our collaborators from AG Prof. Dr. Marion Subklewe. The freshly isolated

and magnetically sorted CD14+ PBMCs were adjusted to a concentration of $1.3x10^6$ cells/ml in RPMI with 1.5% human serum and cultured in a non-adherent plate (6-well: 3ml/well or 24-well: 1.3 ml/well). On the day of isolation and every second following day, 580 U/ml of IL-4 and 800 U/ml of GM-CSF were added.

Generation and transduction of human T-cells with a Hepatitis B core protein-specific T-cell receptor

The transduction protocol and the TCR-specific retrovirus producer cell line RD114 were kindly provided by our collaborators from AG Prof. Dr. Ulrike Protzer. PBMCs were generated as described above and stimulated in a non-adherent 24-well plate coated with anti-CD3- and anti-CD28-antibodies (coating: 5µg/ml anti-CD3-antibody and 0.05µg/ml anti-CD28-antibody in PBS) at a concentration of 10^6/1.5ml in T cell-medium (Table 8) including 300 U/ml IL-2. In the meantime, the TCR-specific retrovirus producer cells, RD-114, were cultured in a 6-well plate in T cell medium to a confluency of 90% on the day of transduction. Transduction was performed two times (day 2 and 3 post PBMC-stimulation) in the following manner in a 24-well non-tissue plate: 500µl of filtered supernatant (SN) from the RD-114 cells – containing the TCR-specific retrovirus – were added to a retronectin-coated well, the plate was then centrifuged (2000g/2h/32°C). Now the stimulated T cells were added to the well coated with retrovirus at a concentration of $5\text{-}8x10^5$/0.5ml in T cell-medium supplemented with 180U/ml IL-2. After a short centrifugation step (1000g/10mins/32°C), the plate was incubated at 37°C for one day. After transduction, T cells were cultured at a density of $2.5x10^5$/ml in T cell-medium incl. 180U/ml IL-2 and adjusted to this concentration every third day until culture was ended 14 days after PBMC-isolation. Transduction rate was determined via flow cytometry as described above.

The cytotoxic effect of the TCR-transduced T cells on their target tumor cells (HepG2_Core) was tested in a T cell/tumor cell co-culture. HepG2_Core cells were plated one day prior to the co-culture to reach a confluency of approximately 80 to 90%, and TCR-transduced T cells were added at different ratios (5:1, 1:1 and 1:5 T-cells vs. tumor cells). Mock-transduced T cells served as a control. Microscopic images were taken after 16, 24, 48 and 72 hours.

2.2.3 Key experiment: Stimulation of moDCs with VSV-NDV-lysed HepG2 cells

The main objective of this project was to investigate the potential of our therapeutic idea (see 1.6), using an *in vitro*-cell culture system. This model system consists of the HCC tumor cell line HepG2 and immune cells from a healthy volunteer (Figure 12). To create the "therapeutic agent", HepG2 cells were infected with VSV-NDV-GFP, and on the next day the oncolysate created was used to stimulate moDCs. The degree of activation of these stimulated moDCs was assessed via flow cytometry and in a cytokine array, whereas their effect was investigated in a functional readout as follows: The stimulated moDCs were co-cultured with T cells from the same donor, and after one to five days, T cell activation was on the one hand investigated via cytokine measurement in the supernatant and flow cytometry,

whereas on the other hand the functional readout was continued in a co-culture of the stimulated T-cells with HepG2 cells. The latter was performed to observe whether the effect the whole process is aiming for – the death of tumor cells, mediated by cytotoxic T cell responses induced by DCs – could really be achieved.

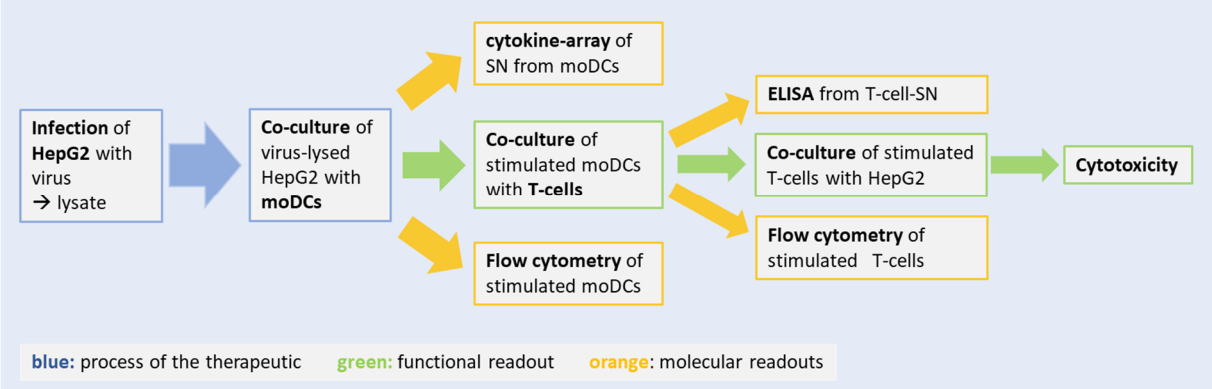

Figure 12: Workflow of the key experiment

Creating the oncolysate: Infection of HepG2 cells with VSV-NDV variants

HepG2 cells were seeded in a 96-well plate in their appropriate culture medium so that they would reach a confluency of 90% on the day of infection. On that day, the medium was replaced by 100µl of DC-medium and the cells were infected at MOI 0.1, 0.01 and 0.001 with VSV-NDV-GFP. Some control wells were left uninfected.

Stimulation of moDCs with viral oncolysate

24h p.i., the oncolysate was mixed thoroughly, a specific amount of oncolysate (25 – 100µl) was harvested and co-cultured in a non-tissue 96-well plate for 24h with 200,000 moDCs per well in a total volume of 200µl.

This experiment was performed with

I. Naïve moDCs (treated with 580 U/ml IL-4 and 800 U/ml GM-CSF every second day) → "imDCs"
II. Activated moDCs → "coDCs"
    a. treated with 580 U/ml IL-4 and 800 U/ml GM-CSF every second day
    b. treated with the following activation cocktail one day prior to the experiment:
        i. 1100U/ml TNFα
        ii. 2000U/ml IL-1β
        iii. 5000U/ml IFN-γ
        iv. 250ng/ml PGE_2
        v. 1µg/ml R848 (=Resiquimod → TLR7/8 agonist)

Untreated DCs served as a negative control (NC), whereas moDCs treated with the activation cocktail were used as a positive control (PC). To investigate the effect of the single components of the oncolysate on the DCs, imDCs were separately co-cultured with UV-inactivated tumor cells and UV-inactivated virus, respectively.

Since it might be beneficial for clinical translation not to have live virus in the vaccine, the experiment was first performed using oncolysate containing live virus in comparison to oncolysate in which the virus had been inactivated with UV-light before harvesting the oncolysate in order to compare the effects on DC activation.

After 24h, the moDCs were stained with fluorophore-conjugated antibodies as described above for the following cell surface markers (fluorophore in brackets) and analysed via flow cytometry:

- lineage markers: CD14 (FITC), CD83 (PerCP-Cy5.5)
- activation markers: CD86 (PE), MHC-I (BV421), MHC-II (BV 605), PD-L1 (APC)

After gating on the CD14-/CD83+ moDC population, the mean fluorescence intensity (MFI) of the activation markers was quantified and – with regards to interindividual differences in the maximum activation – related to the MFI of the positive control (cocktail-stimulated moDCs = coDCs) of the respective marker. Therefore, activation is depicted as "activation in percent of the positive control".

At the same time (after 24h), a sample of the SN was taken and a broad screening for the following cytokines potentially secreted by the DCs during co-culture was performed using the BioLegend LEGENDplex™ Multi-Analyte Flow Assay Kit according to the manufacturer's instructions:

- IFN-α and IFN-β: anti-viral activity, paracrine DC-activation, CTL-activation
- IFN-γ: induces Th1-response
- IL-4: induces Th2-response
- IL-6: promotes inflammation in general and B-cell-maturation
- IL-10: autocrine, blocks DC-maturation
- IL-12: induces Th1-response, NK-cell-killing and CTLs
- IL-15: induces NK-cell-proliferation, promotes CTL-maintenance
- TGF-β: induces Th17-cells and Tregs
- TNF-α: autocrine for DC survival

In brief, this assay follows the principles of a sandwich immunoassay: Capture beads – they differ in size and fluorescence intensity – are equipped with antibodies for a specific analyte. Upon incubation with a sample, the target analyte binds to these antibodies. The "sandwich" is now completed with the binding of a biotinylated detection antibody. The addition of streptavidin-phycoerythrin, which binds to the detection antibody, leads to a fluorescent signal proportional to the analytes bound on the capture beads.

Co-culture of stimulated moDCs with T-cells

As a functional readout, moDCs were incubated with T-cells in a 96-well round bottom plate for five days in a 1:10 moDC:T-cell ratio in 100µl of RPMI. T cell activation was assessed as follows:

After 24 hours of co-culture, the T cells were stained with the following fluorophore-conjugated antibodies and analysed via flow cytometry:

- lineage markers: CD3 (APC-Cy7), CD4 (PacBlue), CD8 (PE), VioBlue (viability dye)
- activation markers: CD44 (PerCP-Cy5.5), CD69 (APC)

After 120 hours of co-culture, samples of the SN were taken and IFN-γ-ELISA was performed using the BioLegend Human IFN-γ ELISA MAX™ Standard Set according to the manufacturer's instructions.

Co-culture of stimulated T-cells with HepG2 cells

To now close the loop of the functional readout, the cytotoxic effect of these DC-stimulated T cells on their target tumor cells was tested. They were co-cultured in a 1:5 effector:target ratio with HepG2_Core tumor cells plated in a 96-well flat bottom plate in 200µl of RPMI. After 48 hours, a sample of the SN was taken to assess tumor cell death, using the LDH cytotoxicity assay as described above.

3. Results

3.1 Viral oncolysis of HepG2_Core human hepatoblastoma cells

HepG2_Core cells were infected with VSV-NDV-GFP at MOI 1 and 0.01, and microscopy pictures and samples of the supernatant for the LDH cytotoxicity assay as well as for the TCID50 assay were taken as described above.

3.1.1 Microscopy

As an example, microscopy pictures of HepG2_Core infected with VSV-NDV-GFP at MOI 0.01 are depicted here (Figure 13). Already 16 hours p.i., several syncytia – giant multinuclear "cell" aggregates that represent a preliminary stage of cell death and form upon infection with VSV-NDV due to its fusogenic properties – are visible, and a slight fluorescence signal reflecting virus replication can be observed. After 24 hours, most cells are pulled into syncytia which emit a fluorescent signal. This signal is substantially diminished after 48 hours – which reflects progressing cell death –, some small syncytia and cell clumps are still attached to the bottom of the well and several dark aggregates of dead cell particles are floating in the supernatant. Nearly all cell clumps are floating after 72 hours while no cell in its physiological shape can be found anymore.

Infection with VSV-NDV-GFP at MOI 1 leads to the same result but a lot faster (pictures not shown here). 16h p.i., most cells already lost their normal phenotype, reducing the confluence on the well

bottom to approximately 40%: some are pulled into syncytia, whereas others are just rounding. This reflects that at MOI 1 there is one infectious particle per cell and theoretically no virus spread is necessary for the infection of all cells. A fluorescent signal is emitted by nearly all cells. After 24 hours, the fluorescence signal is clearly reduced, and some cell clumps are floating in the medium. This trend continues until at 48 hours, when no cell in its physiological phenotype is present anymore.

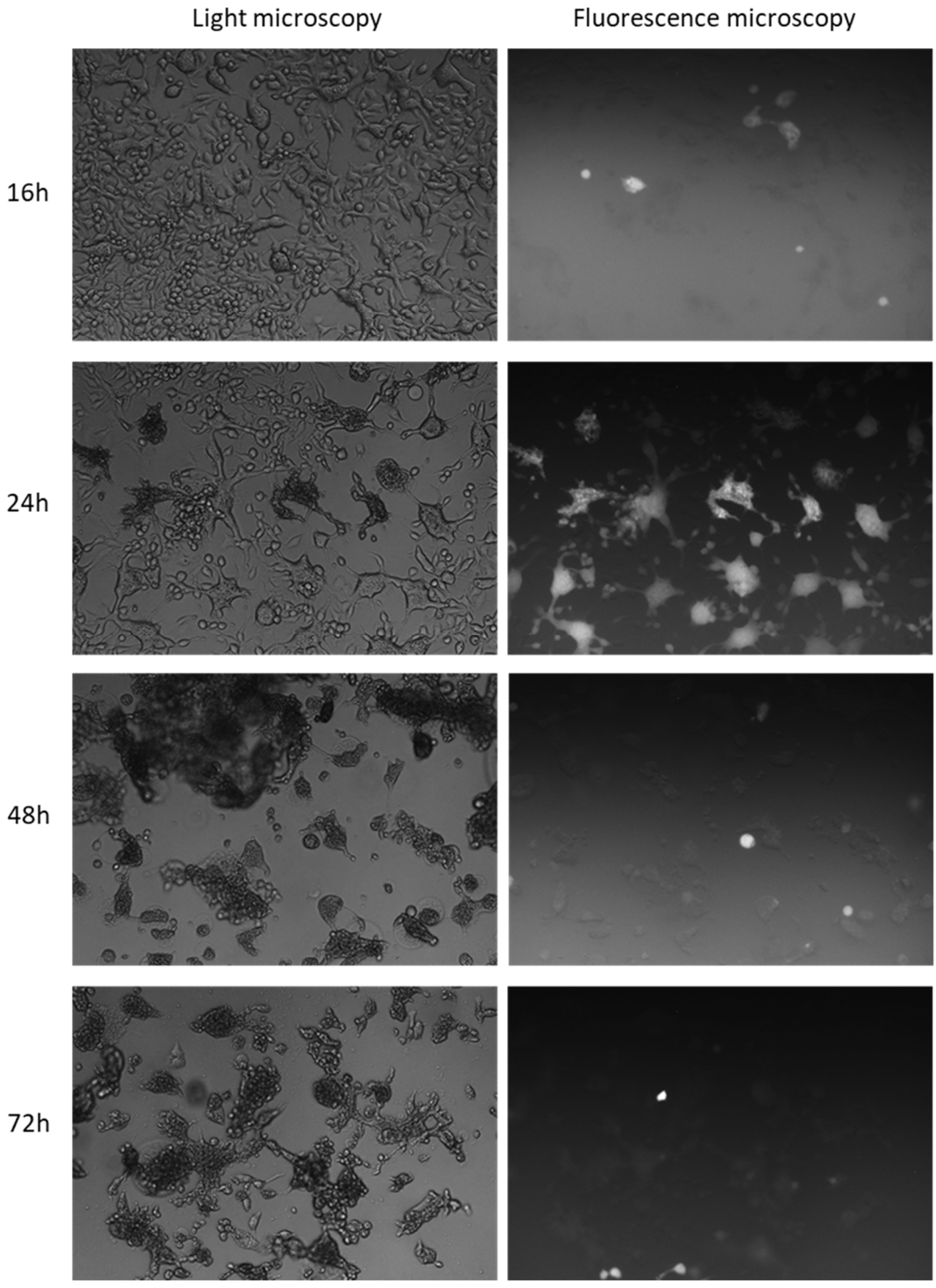

Figure 13: HepG2_Core cells infected with VSV-NDV-GFP at MOI 0.01 die completely
HepG2_Core cells were infected with VSV-NDV-GFP at MOI 0.01, tumor cell death and virus replication were observed with light and fluorescence microscopy, respectively, at 16, 24, 48 and 72 hours p.i. Representative images are shown here.

3.1.2 Virus replication and tumor cell cytotoxicity

After infection of HepG2_Core cells with VSV-NDV-GFP at an MOI of 0.01, the virus titer (Figure 14A) rises to a maximum of $9.75*10^5$/ml at 48 hours, the most rapid increase being between 0 and 16 hours. At 72 hours, a decrease of the titer to $2.89*10^5$/ml is measured. This corresponds to microscopy that shows a replication maximum at 24 hours and large amounts of dead cells from 48 hours onwards. Most likely, the virus produced around the 24h timepoint is stable in the SN until the 48h measurement, but due to a lack of viable cells that can produce new viral particles from 48 hours onwards the titer then starts to drop. Also reflecting the microscopic image, infection with MOI 1 already leads to the maximum titer of $1.18*10^6$/ml after 24h, followed by a decrease down to $1.34*10^4$/ml by 72h p.i.

A peak in cytotoxicity (Figure 14B) after infection of HepG2_Core cells with VSV-NDV-GFP at MOI 1 is reached 48 hours p.i., whereas at MOI 0.01 there is a steady increase until the final 72h measurement. These findings correspond to the microscopic images showing a complete cell death 48h p.i. with VSV-NDV-GFP at MOI 1 and 72h p.i. at MOI 0.01, as well as to the virus titers, since the maximum cytotoxicity is usually reached after the peak of the virus titer.

There are clear trends in cytotoxicity that also correspond to microscopy, but the absolute values of cytotoxicity in percent of the maximum LDH release do not fit to the principle of the assay. Ideally, the lysis buffer induces complete death of all cells, leading to the maximum release of LDH all samples are related to. Therefore, no sample should show a cytotoxicity higher than 100%, despite the data shown here. Since a CPE can always be observed microscopically upon treatment with lysis buffer, the HepG2_Core cells plated in collagen-coated wells perhaps do not become as leaky upon treatment with the lysis buffer as upon virus infection. Here, the assay is performed only to underline infectibility of HepG2_Core and absolute values are secondary in comparison to the general trends.

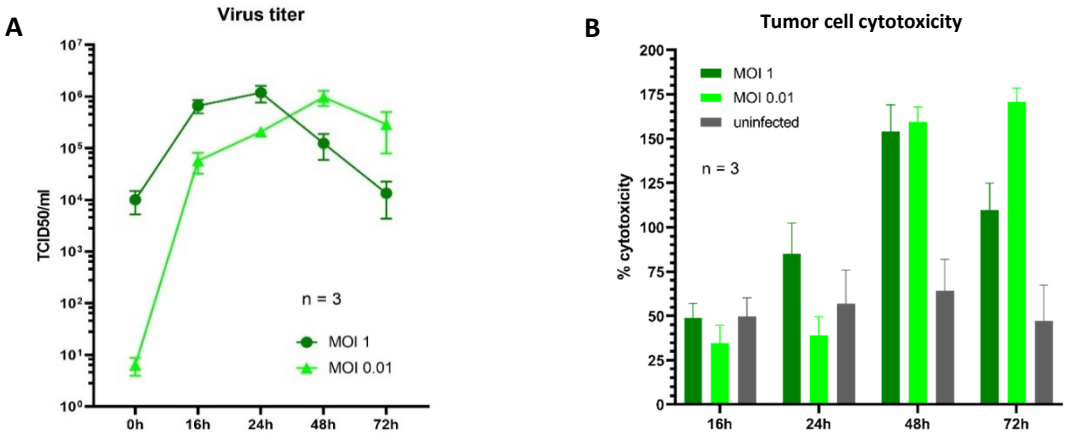

Figure 14: VSV-NDV-GFP replicates efficiently in HepG2_Core cells and induces cell death
HepG2_Core cells were infected with VSV-NDV-GFP with MOIs 1 and 0.01, the virus titer **(A)** measured by TCID50, and the cytotoxicity **(B)** measured by LDH assay, were observed over time. Cells were infected in triplicate and experiments were performed three times; results are plotted as mean ± SEM.

3.2 Generation and processing of primary human immune cells

3.2.1 Monocyte-derived dendritic cells

Magnetic isolation of CD14+ PBMCs: Determining the appropriate amount of antibodies and beads

In order to investigate purity and yield of the CD14+ monocyte isolation, freshly isolated PBMCs were labelled with different dilutions of isolation antibodies (1:2, 1:4, 1:6, 1:8 and 1:10) as described above and subsequently incubated with the corresponding amount of magnetic beads, keeping the ratio of antibodies to beads at 2:1. After passing all test preparations through the magnetic column, the expression of CD3 and CD14 was quantified in the unlabelled fraction (the obtained "CD14+ monocyte population") via flow cytometry to determine the purity of the population, whereas in the labelled fraction (the "CD14- cells" retained in the column) CD14 was quantified as well to test how many CD14+ monocytes are "lost" in the magnetic column (yield).

As it is depicted in the bar chart in Figure 15, the portion of the lymphocyte population within all cells rises from 14.5% at a dilution of the antibody cocktail of 1:2 towards 26.2% at a dilution of 1:8 while the portion of the monocyte population is reduced correspondingly. Therefore, the purity is higher the more antibody is used.

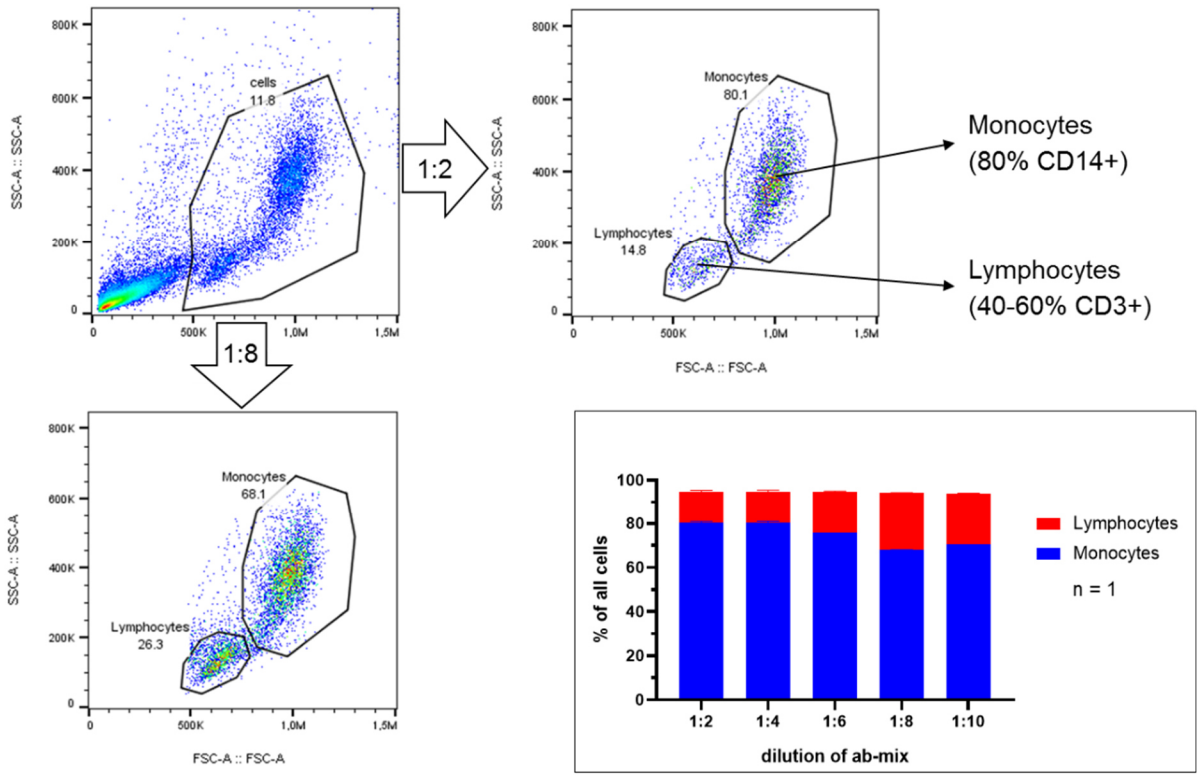

Figure 15: The purity of the monocyte population increases with a higher concentration of the isolation antibody-mix
Freshly isolated PBMCs were labelled with a 1:2, 1:4, 1:6, 1:8 and 1:10 dilution of the isolation antibodies for magnetic selection, magnetic beads were added in a 1:2 bead:antibody ratio. After magnetic selection, the obtained cells were analysed via flow cytometry for the expression of CD3 and CD14. The experiment was performed with three technical replicates, the mean ± SD is shown.

When investigating the yield by measuring the percentage of CD14+ cells lost in the labelled fraction, a small population of CD14+ cells can be seen in the dot plot (Figure 16). Its portion from all cells correlates with the amount of antibody used: When the antibody is diluted 1:2 only, 12.7% of all cells are CD14+, whereas it is rapidly diminished to 5.7% at a dilution of 1:4 and to 2.6% at an antibody dilution of 1:10. In line with these findings a 1:5 dilution has been used in the following experiments in order to achieve a satisfactory purity in line with a sufficient yield. Nevertheless, it should always be considered that approximately 20% of all separated cells are lymphocytes that – in culture with other potentially stimulating and cytokine secreting immune cells – could always proliferate and secrete a vast set of cytokines.

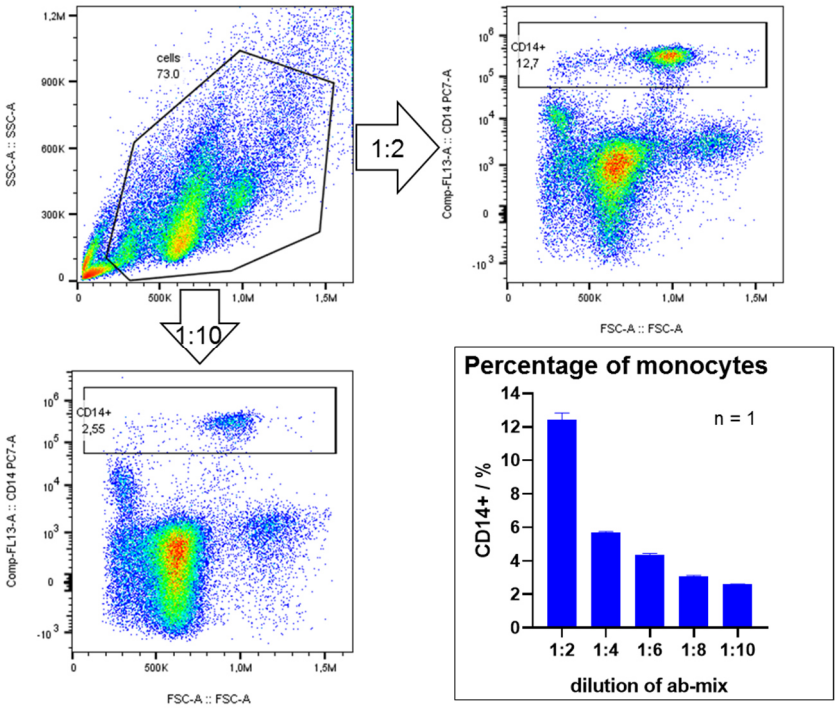

Figure 16: The yield of monocytes decreases with a higher concentration of the isolation antibody-mix
Freshly isolated PBMCs were labelled with a 1:2, 1:4, 1:6, 1:8 and 1:10 dilution of the isolation antibodies for magnetic selection, magnetic beads were added in a 1:2 bead:antibody ratio. After magnetic selection, the magnetic column was removed from the magnet, the retained cells were collected and analysed via flow cytometry for the expression of CD14. The experiment was performed with three technical replicates, the mean ± SD is shown.

Investigation of the moDC population over time

To determine the optimal time-point for harvesting the monocyte-derived dendritic cells concerning purity and yield, as well as to observe the solidity of the moDC population over time, moDCs were generated as described above. On day 2, 3, 4, 5 and 6 post isolation, a well was harvested and the CD14-/CD83+ moDC population was quantified. While on day 3, less than 10% of all immune cells were moDCs (Figure 17), this population was drastically increased to approximately 30% on day 4 and remained on this level until day 7. These findings lead to the conclusion that day 4 is the optimal time point for harvesting the cells because first the population has already reached its maximum and second remains stable for at least three more days, which is important for downstream experiments.

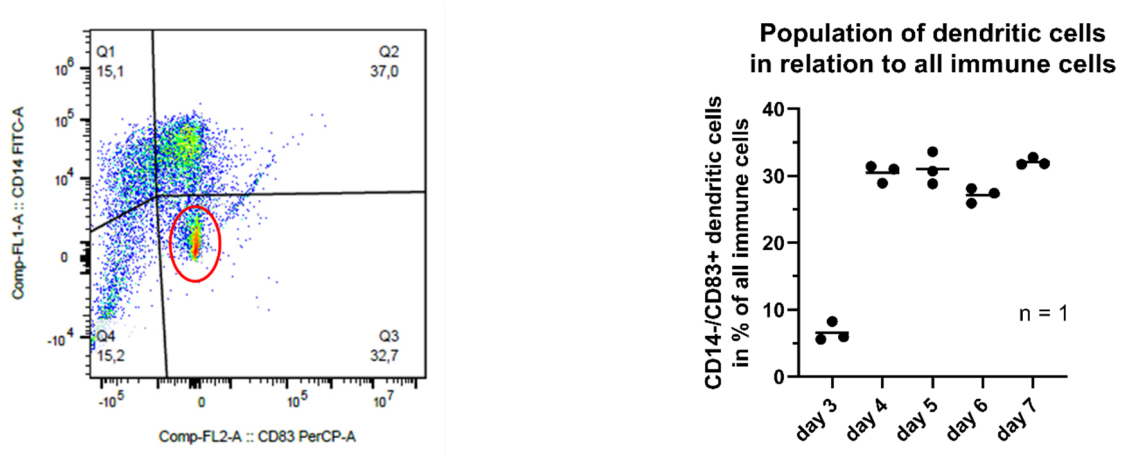

Figure 17: The moDC population remains stable from day 4 to day 7

The moDCs were generated as described above. On day 2, 3, 4, 5 and 6 post-isolation, the CD14-/CD83+ moDC population was quantified via flow cytometry. The experiment was performed with three technical replicates, the mean with individual values is shown.

3.2.2 T-cell transduction with a Hepatitis B Core protein-specific TCR

T cells from freshly obtained PBMCs were stimulated and transduced twice with a Hepatitis B core protein-specific TCR as described above. Four days after the second transduction, transduction rate was assessed via flow cytometry. In a relatively pure population of CD4+ and CD8+ T cells, both subsets show a transduction rate of on average 40% in the CD4+ T cells and 48% in the CD8+ T cells. In the mock-transduced population no TCR-positive cells were detected (Figure 18).

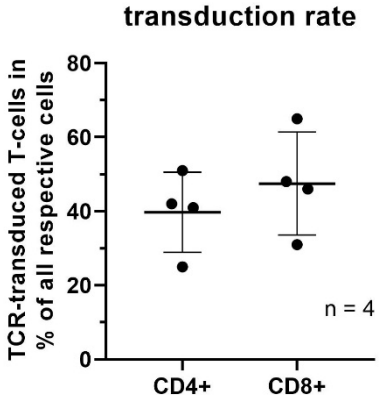

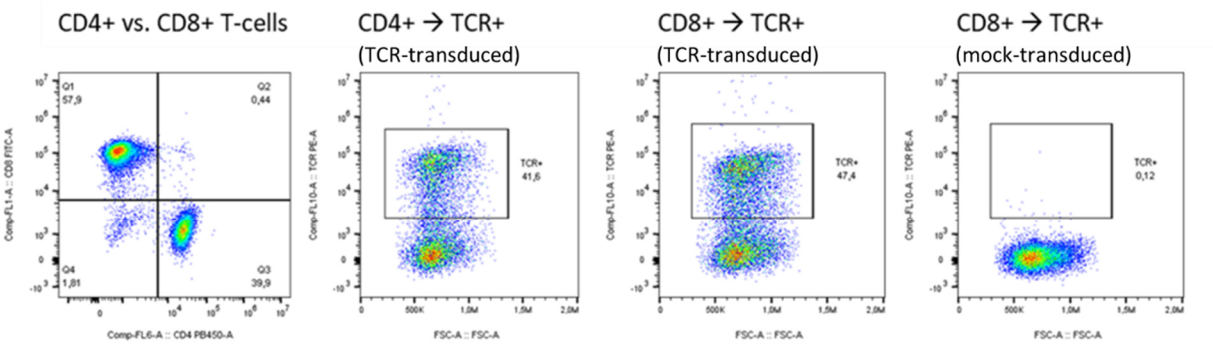

Figure 18: T cell transduction leads to a transduction rate between 40% and 48%

T cells from freshly obtained PBMCs were stimulated with anti-CD3 and anti-CD28 antibodies and transduced twice with a TCR specific for the Hepatitis B Core protein, four days after the second transduction the transduction rate was assessed in the CD3+/CD4+ and CD3+/CD8+ population via flow cytometry, mock-transduced CD3+/CD8+ T cells served as a negative control. Cells were transduced in triplicates and experiments were performed 4 times; the mean ± SEM is shown.

Functionality of the transduced T-cells

For testing the functionality of the TCR-transduced T cells on their target tumor cells (HepG2_Core), TCR-transduced T cells were co-cultured in a 5:1, 1:1 and 1:5 ratio with their target tumor cells, mock-transduced T cells in a 5:1 T cell:tumor cell ratio served as a negative control. The cytotoxic effect of the T cells on the tumor cells was observed microscopically at multiple time points until 72 hours.

The microscopy pictures show a clear cytotoxic effect of the TCR-transduced T cells on the HepG2_Core tumor cells (Figure 19) at a 5:1 ratio already after 16 hours; only very few tumor cells are still attached to the bottom of the well. After 24 hours, no adherent tumor cells are visible anymore whereas the number of T cells even seems to be increased, which is decreased again after 48 and 72 hours. At a lower T cell:tumor cell ratio of 1:1, the cytotoxic effect can be observed from 24 hours onwards, when the confluency of the tumor cell layer is reduced to approximately 50%, whereas after 48 hours it is further reduced to 30% and dark cell clumps are floating in the supernatant. After 72 hours only very few tumor cells are still attached and in their physiological shape.

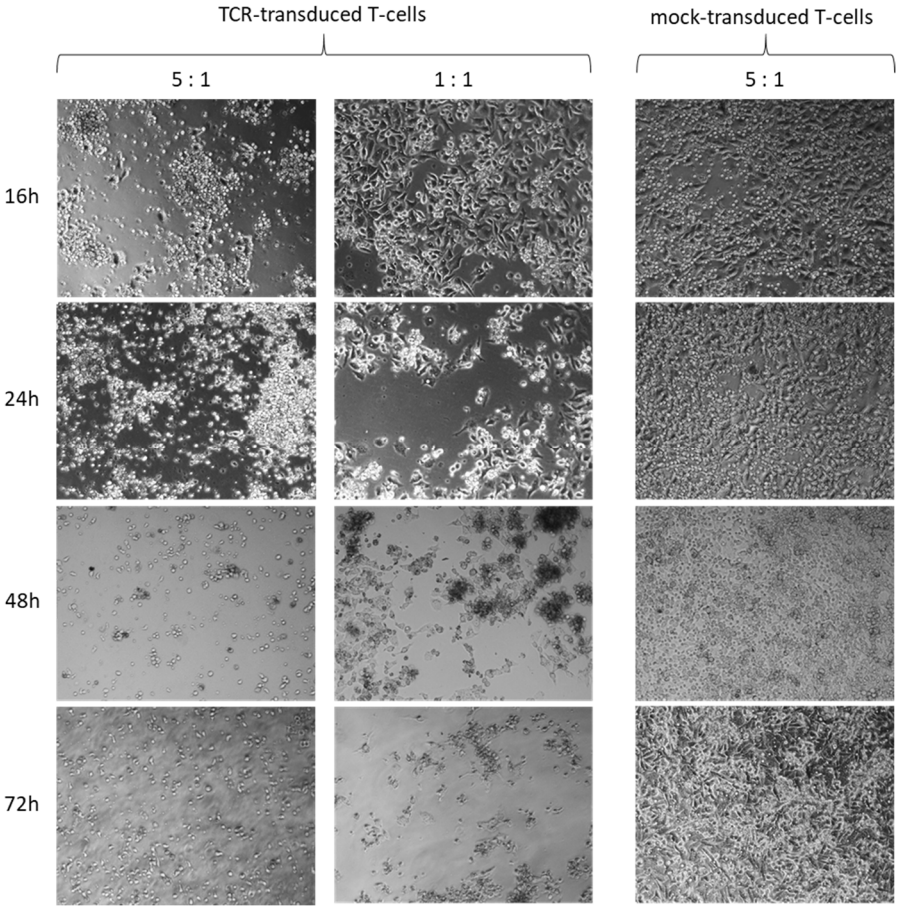

Figure 19: TCR-transduced T-cells show an efficient tumor cell killing
TCR-transduced T-cells were co-cultured with their target tumor cells HepG2_Core at a ratio of 5:1 and 1:1, mock-transduced T-cells served as a control. The co-culture was observed microscopically at 16, 24, 48 and 72 hours post-co-culture. Cells were co-cultured in triplicate; experiments were performed 3 times. Representative images are shown here.

This cytotoxicity does not occur in the control wells with mock-transduced T-cells. In contrast, even in the highest T-cell:tumor cell ratio of 5:1, the tumor cells – as far as they can be evaluated underneath the dense layer of T-cells – seem to proliferate since the confluency of the cell layer is increasing from approximately 90% to a beginning overgrowth.

3.3 Key experiment: Stimulation of moDCs with VSV-NDV-lysed HepG2 cells

HepG2 cells were infected with VSV-NDV-GFP at different MOIs to create an oncolysate, and 24 hours p.i. the oncolysate was co-cultured with monocyte-derived dendritic cells. These stimulated moDCs – the model therapeutic agent – were then investigated in functional as well as molecular readouts.

3.3.1 Finding the optimal conditions of the viral oncolysate for the stimulation of moDCs

Stimulation of moDCs with a viral oncolysate containing live VSV-NDV

HepG2 were infected with VSV-NDV-GFP as described above at MOI 0.001, 0.01 and 0.1. 24 hours p.i., 100µl of the oncolysate were co-cultured with immature as well as cocktail-treated moDCs. Freeze-thaw-lysed HepG2 served to determine the effect of a simple cell lysate on moDCs. The moDCs were observed microscopically and analysed via flow cytometry one day later.

Already under the microscope, differences between untreated moDCs and those treated with viral oncolysate were visible. Whereas in the untreated sample the cells show their physiological small, round and light phenotype, they are forming dark cell aggregates in the virus-treated conditions.

In flow cytometry, there are clear differences in the distribution of cell populations in the FSC/SSC dot plot (Figure 20). In the samples with untreated imDCs, there is a clear monocyte population (which also includes the moDCs) visible, representing 26% of all cells and debris[3]. Upon treatment of imDCs with oncolysate VN 0.001, a significant reduction of the monocyte population down to 4% can be observed in line with a significant increase of cell debris from 9% to 32%. Partially, the portion of cell debris can of course be attributed to the oncolysate itself. The freeze/thaw control, in which the same amount of tumor cells as in the virus-treated conditions has been used, however consists of only 11% cell debris whilst the monocyte population isn't altered significantly. This also holds true for MOI 0.01 and 0.1, but contradictory to the expectation that with a higher viral load (at a higher MOI) the cell population would be further reduced, trends lead into the opposite direction. Maybe a lower viral load first leads to DC tolerance resulting in no secretion of anti-viral cytokines but later on the virus still harms the cell, whereas upon a higher viral load the DCs sense the danger immediately and act against it. Possibly the replication also still continues after co-culture at lower MOIs in the tumor cells that are still viable, leading to a sudden release of many virions, whereas at higher MOIs the tumor cells are already dead, and no replication is possible anymore.

[3] Although a flow cytometry analysis usually consists of the gating for the cell population to exclude the debris, the cell debris was included here because of the specific interest in the debris caused by visible differences in the morphology of the populations in the dot plot. This gating strategy allows a quantification of the differences.

These findings also translate to the coDC-conditions. Interestingly, here the monocyte populations are larger than in the imDC-conditions, e.g., in the control of pure monocytes they represent 40% of all cells after pre-treatment with the activation cocktail but only 27% without pre-treatment.

Taking together microscopy, morphology of the dot plots and relations of populations, it has to be assumed that live VSV-NDV-GFP impairs monocyte integrity under *in vitro*-conditions. These findings favour the idea of using UV-inactivated oncolysate for DC stimulation.

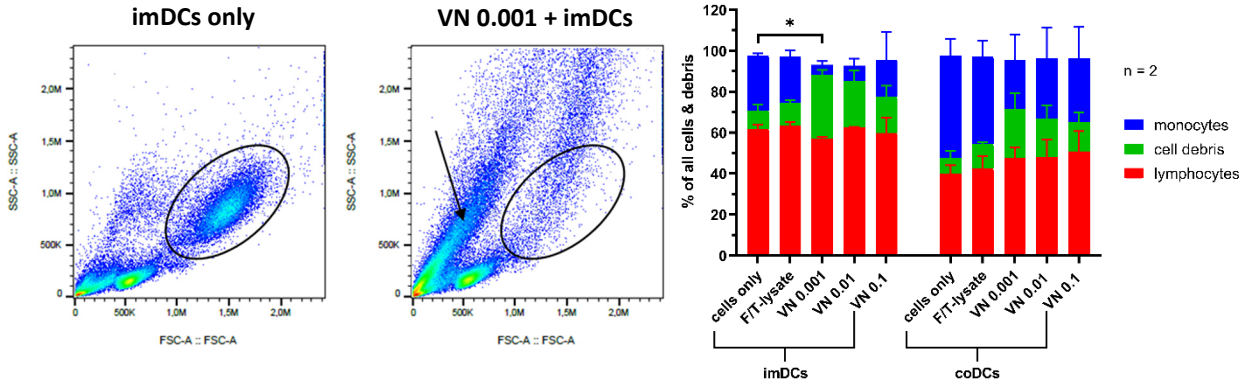

Figure 20: Live VSV-NDV-GFP reduces the monocyte population
HepG2_Core cells were infected with VSV-NDV-GFP at MOI 0.001, 0.01 and 0.1. 24 hours p.i., the oncolysate was co-cultured with imDCs and coDCs, respectively. ImDCs and coDCs alone as well as their co-culture with freeze/thaw lysed HepG2 served as controls. After 24 hours of co-culture, the cells were analysed via flow cytometry and the distribution of populations was quantified. Co-culture was performed in triplicates, experiments were performed twice (* $p < 0.05$).

Note: At this stage of experiments the magnetic selection for monocytes for the generation of moDCs has not been performed yet. The large lymphocyte populations detected in this experiment led to the introduction of the selection.

Stimulation of moDCs with UV-inactivated viral oncolysate

As a next step, HepG2 were infected with VSV-NDV-GFP as described above at MOI 0.001 and 0.01. 24 hours p.i., the oncolysate was treated with UV-light to inactivate the virus and then co-cultured with imDCs. To further optimize the DC vaccine, different amounts of oncolysate (25µl and 75µl) were used. Untreated coDCs served as a positive, untreated imDCs as a negative control. The moDCs were observed microscopically and the distribution of populations as well as the upregulation of activation markers in the CD14-/CD83+ moDC population were analysed via flow cytometry 24 hours later.

> For simplicity, as an abbreviation for the "UV-inactivated viral oncolysate 24 hours after the infection of HepG2_Core cells with VSV-NDV-GFP at – e.g. – MOI 0.001" the term "VN 0.001" is used from now on.

In light microscopy, no phenotypical differences in DC morphology were detectable between different conditions. Upon comparison of flow cytometry results (Figure 21), the distribution of populations in the FSC/SSC dot plot still differs a little between treated and untreated samples. The monocyte population in the sample stimulated with 75µl of VN 0.001 lysate isn't as clearly defined as in the untreated control and slightly shifted upwards but still clearly visible, for the corresponding 25µl-sample these trends also hold true but to a lower extent. In later experiments, the trend that the population shifts a little could also be observed in conditions where DCs were activated with the cytokine cocktail only without being treated with oncolysate, indicating that a slight shift might also reflect activation (data not shown here). Together with the microscopic image, it can therefore be concluded that UV-inactivation of the viral oncolysate favours the integrity of the monocyte population and should therefore be pursued.

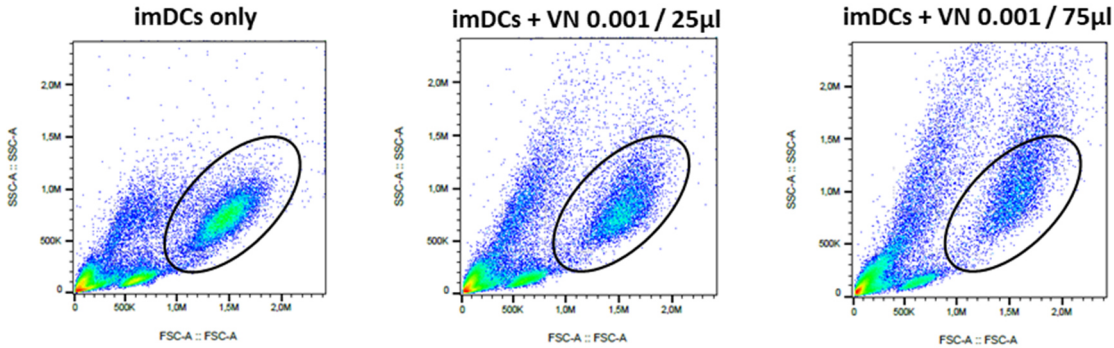

Figure 21: Treatment with UV-inactivated oncolysate does not impair the integrity of the monocyte population
HepG2_Core cells were infected with VSV-NDV-GFP at MOI 0.001, 0.01 and 0.1. 24 hours p.i., the virus was inactivated by a 15-minute treatment of the oncolysate with UV-light, and the oncolysate was co-cultured with imDCs. After 24 hours of co-culture, the cells were analysed via flow cytometry and the distribution of populations was observed. Co-culture was performed in triplicates, experiments were performed twice.

The activation markers CD86, PD-L1 and MHC-II all show an increase upon treatment with viral oncolysate in all conditions (VN 0.001/0.01, 25/75µl) (Figure 22). As described above, to support interexperimental comparability, the PC is used as a baseline of "100% activation". E.g., PD-L1 is significantly upregulated from an MFI of 30% in the NC up to 70% upon treatment with 75µl of VN 0.001. MHC-II even surpasses the PC with MFIs up to 124% of the PC. Tendencies indicate that after infection of HepG2 at the higher MOI of 0.01, DC activation is stronger. Comparing the merged data from both replicates to the single experiments and taking into account that the two experiments were performed with blood from different healthy donors, the data is suggestive of attributing the high interexperimental variability to general interindividual differences in the strength of upregulation of activation markers upon treatment with oncolysate. While some trends are the same in both replicates, e.g., that PD-L1 is slightly higher at VN 0.01 than at VN 0.001, this marker varies between approximately 60% and 70% in replicate one but even increases up to 130% in replicate two.

Since significant difference in DC activation could neither be detected between using 25 or 75µl of oncolysate nor between using VN 0.001 nor VN 0.01 and considering that a monocyte population was visible in all conditions, for feasibility 50µl of VN 0.01 were used in all subsequent experiments.

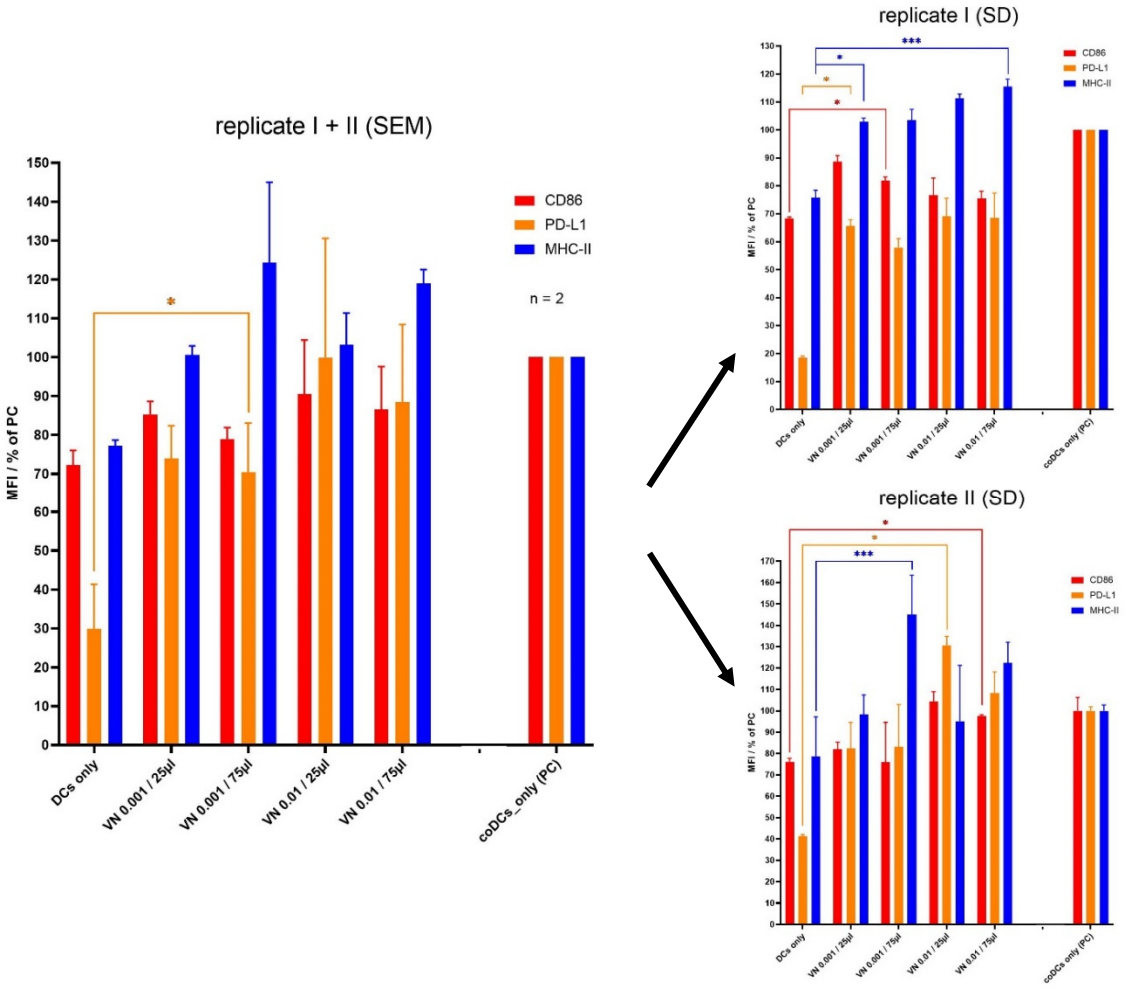

Figure 22: MoDCs stimulated with VSV-NDV-lysed HepG2_Core show high inter-individual differences in activation
HepG2_Core cells were infected with VSV-NDV-GFP at MOI 0.001, 0.01 and 0.1. 24 hours p.i., the virus was inactivated by a 15-minute treatment of the oncolysate with UV-light, and the oncolysate was co-cultured with moDCs. After 24 hours of co-culture, the cells were analysed via flow cytometry for the expression of the activation markers CD86, PD-L1 and MHC-II in the CD83+/CD14- moDC population. Co-culture was performed in triplicates, experiments were performed twice. Means ± SEM of both experiments are shown on the left, means ± SD of the single experiments on the right (* $p < 0.05$, *** $p < 0.001$).

3.3.2 Activation of moDCs by VSV-NDV-lysed HepG2

In order to now evaluate the degree of activation of the moDCs induced by the viral oncolysate, as in the previous experiment, imDCs were co-cultured with 50µl of UV-inactivated, virus-lysed HepG2 after an infection at MOI 0.001, 0.01 and 0.1; coDCs were co-cultured with virus-lysed HepG2 after an infection at MOI 0.01. A sample of untreated coDCs served as positive, untreated imDCs as negative control. To get a clearer picture of the effect of lysed tumor cells alone as well as virus alone on the moDCs, UV-inactivated HepG2 as well as UV-inactivated VSV-NDV-GFP (to the amount that is present in the oncolysate by the time of DC co-culture) were separately co-cultured with imDCs.

Flow cytometry of stimulated moDCs

After 24 hours, again the mean fluorescence intensity of the activation markers was determined via flow cytometry in the CD83+/CD14- moDC population, defining the PC as a baseline of "100% activation". For reasons of clarity, the results of the various conditions of the same set of experiments are depicted in different figures.

In comparison to untreated imDCs, all activation markers tend to be upregulated upon treatment of imDCs with viral oncolysate (Figure 23). E.g., in VN 0.01 there is a significant upregulation of PD-L1 from 15% to 18%, in line with MHC-II being significantly increased from 91% to 115%, even surpassing the positive control. Due to the fact that experiments were performed with primary immune cells from different healthy donors that show interindividual differences in the upregulation of activation markers upon treatment with viral oncolysate, further statements about statistical significance are limited. Although – as already demonstrated in the previous experiment – there are again significant differences within individual experiments (data not shown here). Nevertheless, the upregulation of CD86, PD-L1, MHC-I and -II represents an activation of imDCs upon treatment with viral oncolysate, that now need to be investigated further for their functionality as a therapeutic DC vaccine.

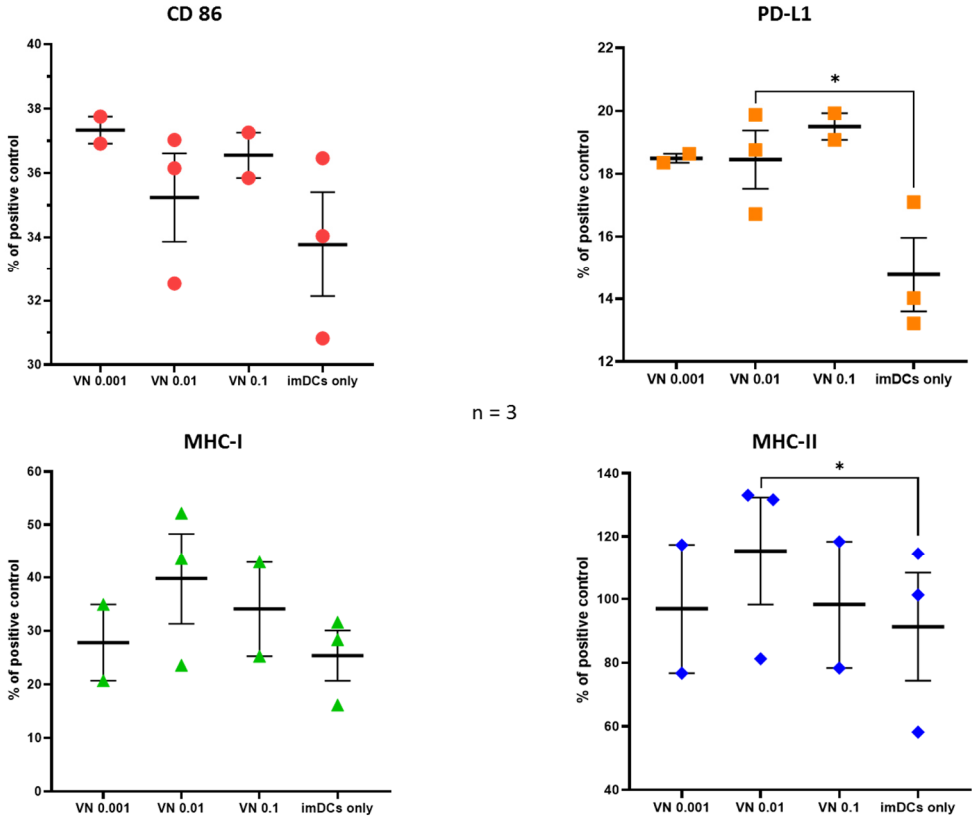

Figure 23: VSV-NDV-lysed HepG2 activate imDCs
HepG2_Core cells were infected with VSV-NDV-GFP at MOI 0.001, 0.01 and 0.1. 24 hours p.i., the virus was inactivated by a 15-minute treatment of the oncolysate with UV-light, and the oncolysate was co-cultured with imDCs; imDCs only served as a negative control. After 24 hours of co-culture, the cells were analysed via flow cytometry for the expression of the activation markers CD86, PD-L1, MHC-I and MHC-II in the CD83+/CD14- moDC population. Co-culture was performed in triplicates, experiments were performed 3 times. Means ± SEM are shown (* $p < 0.05$).

Also, moDCs that had already been pre-treated with the activation cocktail (=coDCs), show a distinct upregulation of all activation markers upon co-culture with VN 0.01. A significant upregulation of CD86 of 9% from the defined baseline (PC = 100%) to 109% can be detected (Figure 24), which is an even stronger upregulation than in the imDCs upon VN 0.01 treatment (1.5%, compare to Figure 23). The upregulation of PD-L1 in VN 0.01 is stronger in coDCs (19%) than in the imDCs (3%) as well, whilst MHC-I and MHC-II are upregulated to a similar extent in imDCs and coDCs. It now remains to be tested if those cocktail-pretreated coDCs, that are not only strongly activated as described previously (Subklewe et al., 2014) but via the treatment with viral oncolysate activated to an even higher degree and in addition potentially loaded with tumor antigens, also lead to a strong anti-tumor immune response, possibly more effectively than the oncolysate-treated imDCs.

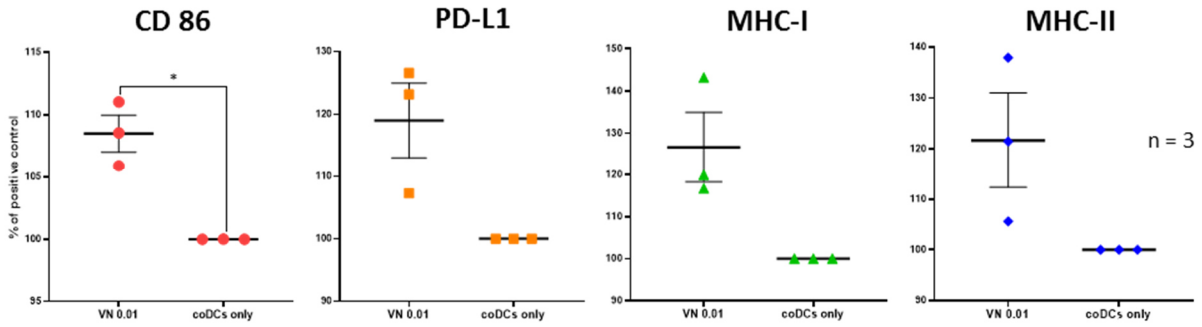

Figure 24: VSV-NDV-lysed HepG2 increase the degree of activation of coDCs
HepG2_Core cells were infected with VSV-NDV-GFP at MOI 0.01, on the same day the moDCs were treated with the activation cocktail. After 24h, the virus was inactivated by a 15-minute treatment of the oncolysate with UV-light, and the oncolysate was co-cultured with the coDCs; coDCs only served as a control. After 24 hours of co-culture, the cells were analysed via flow cytometry for the expression of the activation markers CD86, PD-L1, MHC-I and MHC-II in the CD83+/CD14- coDC population. Co-culture was performed in triplicates, experiments were performed 3 times. Means ± SEM are shown (* $p < 0.05$).

The separate treatments of imDCs with UV-inactivated HepG2 and UV-inactivated VSV-NDV-GFP were performed as controls (Figure 25). Upon treatment with UV-inactivated HepG2, CD86 and PD-L1 tend to be slightly upregulated, whereas MHC-I and MHC-II show a decent downregulation. The imDCs treated with UV-inactivated virus alone tend to lead to an upregulation of all activation markers, even significant for CD86. This suggests that the activation induced by the treatment with the whole viral oncolysate is partially mediated by the effect of the inactivated virus particles – that contain PAMPs – alone, supporting our hypothesis that the viral particles would serve as an adjuvant which would then further be enhanced by the immunogenic cell death of the tumor cells. At this point, the functional readout is necessary to get a clearer picture of the potential of the therapeutic approach since DCs activated by virus particles alone would of course not be able to induce a tumor-specific immune response.

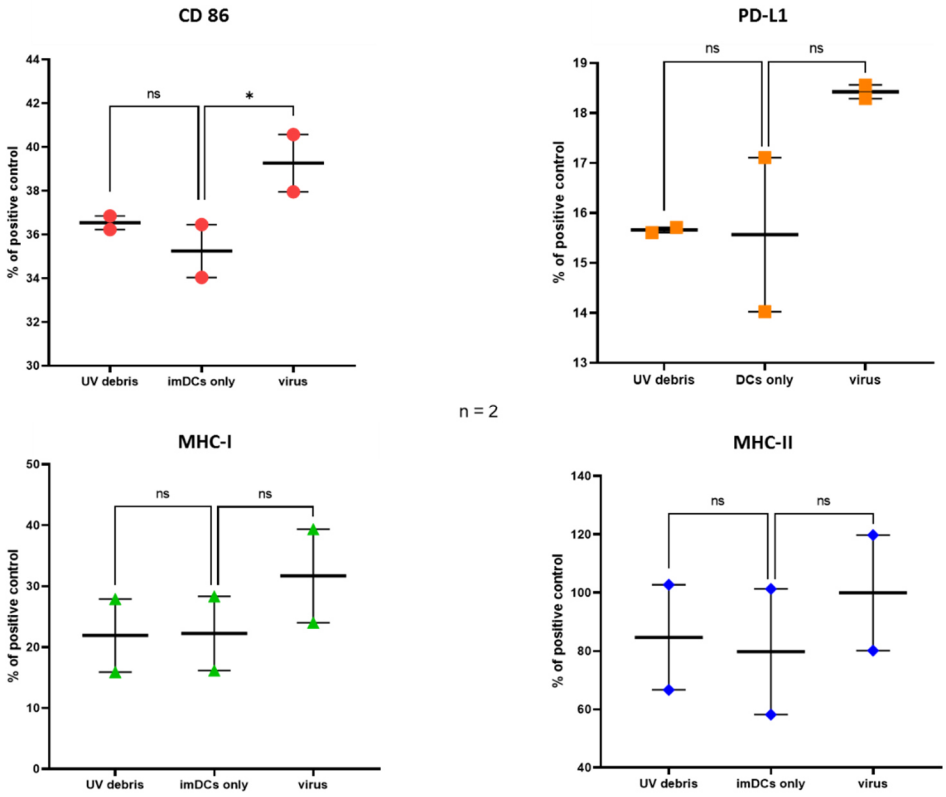

Figure 25: UV-inactivated virus alone leads to a slight activation of imDCs, UV-lysed cell debris doesn't
ImDCs were co-cultured with UV-lysed HepG2_Core cells or UV-inactivated VSV-NDV alone, imDCs only served as a control. After 24 hours of co-culture, the cells were analysed via flow cytometry for the expression of the activation markers CD86, PD-L1, MHC-I and MHC-II in the CD83+/CD14- imDC population. Co-culture was performed in triplicates, experiments were performed twice. Means ± SEM are shown (* $p < 0.05$, ns = not significant).

Cytokine array from supernatant of stimulated moDCs

After 24 hours of co-culture of moDCs with viral oncolysate, a sample of the supernatant was taken, and a broad screening for the cytokines secreted by the DCs was performed, using the LEGENDplex™ Multi-Analyte Flow Assay Kit.

As already described in the flow cytometry data, there is a high interexperimental variability due to interindividual differences. In unstimulated imDCs, only low levels of cytokines could be detected for most analytes (Figure 26). For example, 34 pg/ml of TNF-α – the autocrine secretion supports DC survival – were measured in the supernatant of imDCs, whereas 317 pg/ml could be detected in the coDC condition. This also translates to the stimulatory cytokines IFN-γ (2 pg/ml vs. 445 pg/ml), IL-6 (6 pg/ml vs. 4425 pg/ml) and IL-12 (1 pg/ml vs. 420 pg/ml). This is different in IL-4, where the secretion is already on a high level in the imDCs and not clearly altered in coDCs (2160 pg/ml vs. 2162 pg/ml), as well as in IL-15, whose secretion stays on a low level (12 pg/ml vs. 13 pg/ml). The latter can also be observed in IL-10 (1 pg/ml vs. 2 pg/ml) and TGF-β1 (both 3 pg/ml), but those two cytokines have to be seen in another light due to their immunosuppressive properties. Measurements of IFN-α and IFN-β

mostly led to results below the detection limit and are therefore not depicted here. The analytes measured in the imDC VN 0.01 conditions didn't show reproducible results and are therefore not shown here.

In this context it is even more interesting that there tends to be an increase in the secretion of all analytes by coDCs upon stimulation with VN 0.01. E.g., IL-6 secretion reaches a significantly higher concentration of 5408 pg/ml upon VN 0.01 co-culture compared to 4425 pg/ml in coDCs only. In most analytes the increase isn't particularly high, for example the significant increase in IL-12 secretion from 420 pg/ml to 462 pg/ml, but taking into consideration that there has already been the strong increase described above induced by the activation cocktail, with the additional increase the limits of cytokine production by the moDCs might be reached.

These findings again show a broad increase in the DC's stimulatory activity upon treatment with VSV-NDV-lysed tumor cells, which underlines the potential of the therapeutic approach.

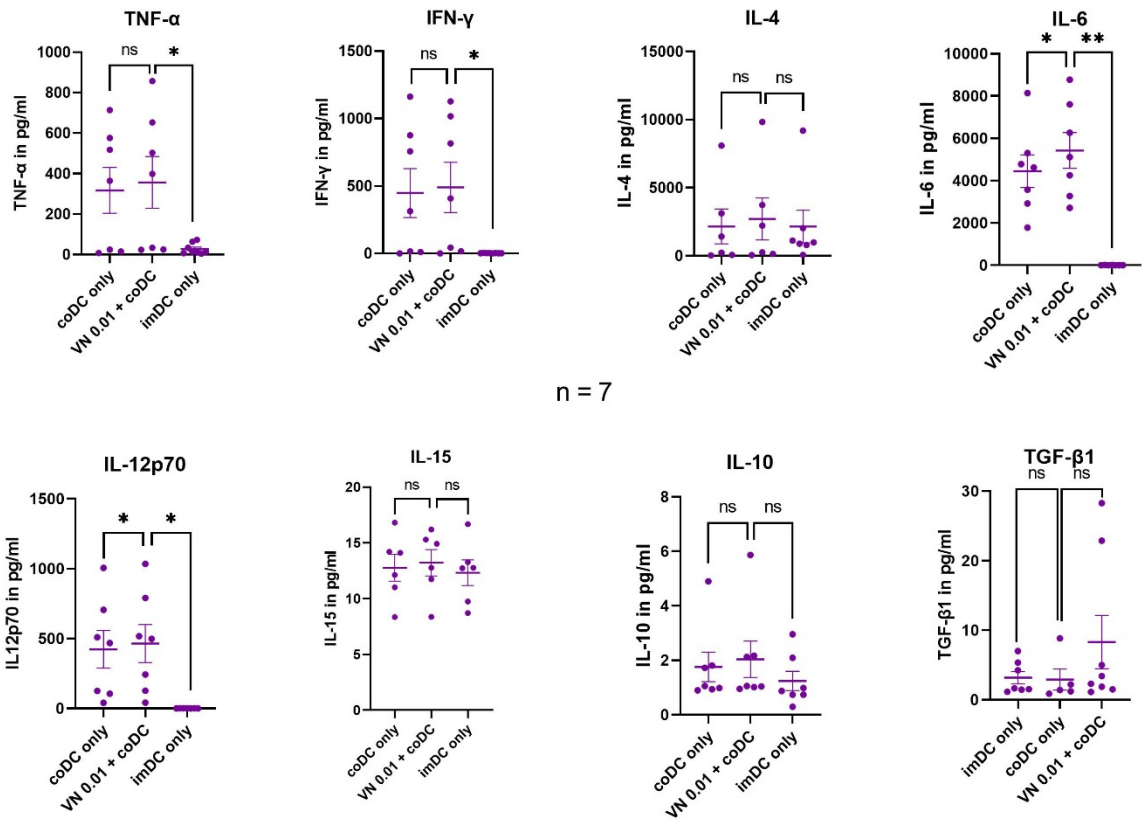

Figure 26: Co-culture with the viral oncolysate increases the secretion of cytokines by coDCs
HepG2_Core cells were infected with VSV-NDV-GFP at MOI 0.01, on the same day the moDCs were treated with the activation cocktail. After 24h, the virus was inactivated by a 15-minute treatment of the oncolysate with UV-light, and the oncolysate was co-cultured with the coDCs; coDCs only and imDCs only served as controls. After 24 hours of co-culture, a sample of the supernatant was taken and screened for TNF-α, IFN-α/-β/-γ, IL-4, -6, -10, -12p70, -15 and TGF-β1, using the LEGENDplex™ Multi-Analyte Flow Assay Kit. Cells were co-cultured in triplicates and experiments were performed 7 times. Means ± SEM are shown (* $p < 0.05$).

3.3.3 Functional readout: Co-culture of stimulated moDCs with T cells

To overcome the limitations of a cell culture model with a limited number of T cells per well and therefore also a limited set of TCRs for a potential interaction with antigens presented by DCs, the core protein of Hepatitis B-virus – a real tumor antigen – was included into every step of the functional readout as a model antigen. HepG2 cells transduced with a cytoplasmic core protein (HepG2_Core) were used to show that the virus breaks up the cell, the core is released and taken up, processed, and presented by the moDCs. Furthermore, T cells were transduced with a core-specific TCR for showing the state of T cell activation after stimulation with their specific antigen presented by a DC. This model antigen assay was kindly provided by our collaborators from AG Protzer.

The moDCs stimulated as described above were now co-cultured with T cells for 24 to 120 hours in a 1:10 ratio. A co-culture of HepG2_Core cells with TCR-transduced T cells served as positive control and its results again served as a baseline, whereas untransduced T cells alone are the negative control.

Flow cytometry of stimulated T cells

As a first step, the co-cultured T cells were analysed for activation via flow cytometry. After gating on CD3+ and CD8+ T cells – in which we are particularly interested due to their cytotoxic effect on tumor cells –, the mean fluorescence intensity of the activation markers CD44 and CD69 was measured. Whilst the positive control showed a clear upregulation of the activation markers, there were no obvious differences in the other conditions (data not shown here). There might be a more distinct trend with a larger number of replicates and further optimization of the protocol, but due to a limited number of cells from the healthy donor, this experiment wasn't pursued any further in favour of the final functional readout.

Analysis of IFN-γ secretion in supernatant of stimulated T cells

After 120 hours of DC/T cell co-culture, the concentration of IFN-γ in the supernatant was measured by ELISA (Figure 27). Although the maximum IFN-γ levels in the positive controls are in the same range (2998 pg/ml – 3522 pg/ml), the secretion of IFN-γ upon treatment with the same condition again varies a lot between experiments, leading to a lack of statistical significance and difficulties in the interpretation of the data.

Nevertheless, there is a clear trend that in conditions involving coDCs, T cells secrete more IFN-γ. E.g., TCR-transduced T cells stimulated with VN 0.01-treated imDCs reach IFN-γ levels of 9% of the PC, whereas TCR-transduced T cells stimulated with VN 0.01-treated coDCs secrete 65% of IFN-γ. This also translates to the untransduced T cells, with IFN-γ levels of 36% in imDCs only and 83% in coDCs only.

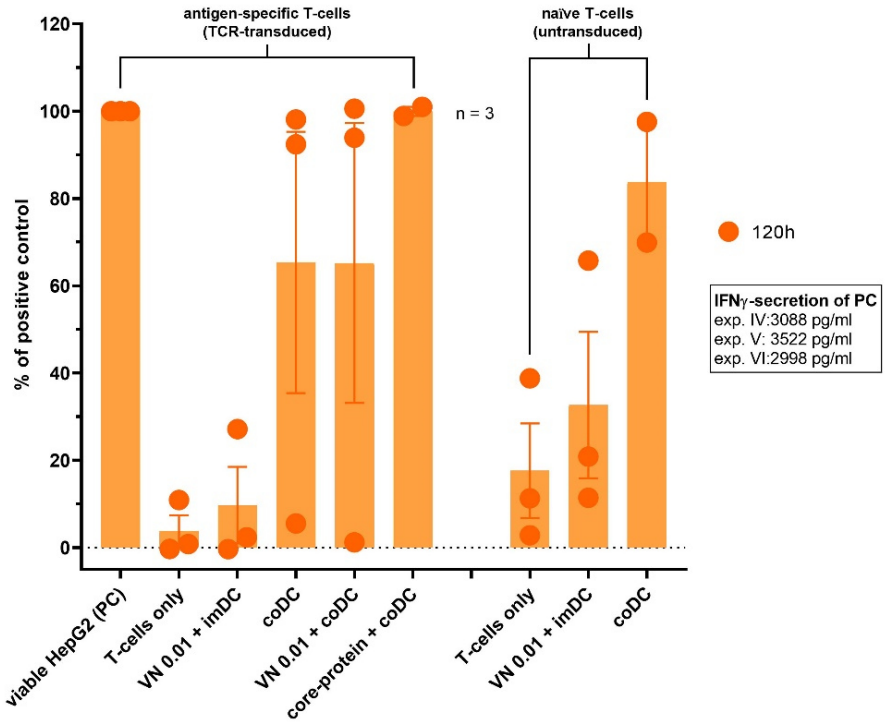

Figure 27: T cells secrete more IFN-γ upon stimulation with coDCs than with imDCs
TCR-transduced as well as untransduced T cells were co-cultured with VN 0.01-treated imDCs and coDCs. Co-culture of TCR-transduced T cells with HepG2_Core cells and core-protein stimulated coDCs served as PCs, T cells only as NC. After 120 hours of DC/T cell co-culture, IFN-γ secretion was measured by ELISA as a surrogate parameter for T cell activation. Cells were co-cultured in triplicates, and experiments were performed 3 times. Means ± SEM are shown (* $p < 0.05$).

Co-culture of stimulated T cells with HepG2: LDH-cytotoxicity assay

To close the loop of the functional readout starting with the stimulation of moDCs with virus-lysed HepG2_Core tumor cells, followed by a co-culture of those stimulated moDCs with T cells for 120 hours, the T cells were finally tested for their cytotoxic effect on the target tumor cells. After a 48-hour co-culture of the T cells with HepG2 tumor cells freshly plated the day before, tumor cell death is measured via LDH assay as described above.

TCR-transduced T cells alone served as a negative control and showed a baseline cytotoxicity of 28% of the tumor cells plus T cells (Figure 28). TCR-transduced T cells stimulated with HepG2_Core tumor cells – that had shown the highest values of T cell activation in the previous T cell readouts – again served as a positive control, inducing a cytotoxicity of 34%. Interestingly, the cytotoxicity induced by TCR-transduced T cells activated by oncolysate-stimulated imDCs reaches levels up to 58%. Also, TCR-transduced T cells stimulated with coDCs alone induce a cytotoxicity of 55%, which is slightly higher than the same setup but with additional oncolysate-stimulation of the coDCs. All conditions involving untransduced T cells lead to an unspecific cytotoxicity of 29%.

This data suggests that the high secretion of IFN-γ – measured previously in coDC-stimulated naïve as well as antigen-specific T-cells – does not automatically lead to a stronger cell killing activity. Of course, the specificity of the TCR is crucial, which is also represented in this data by the large differences between TCR-transduced and untransduced T-cells that have otherwise been stimulated in the same manner. Apart from that, the much higher secretion of IFN-γ by coDC-stimulated TCR-transduced T-cells in comparison to imDC-stimulated ones does not go in line with the induction of more tumor cell death.

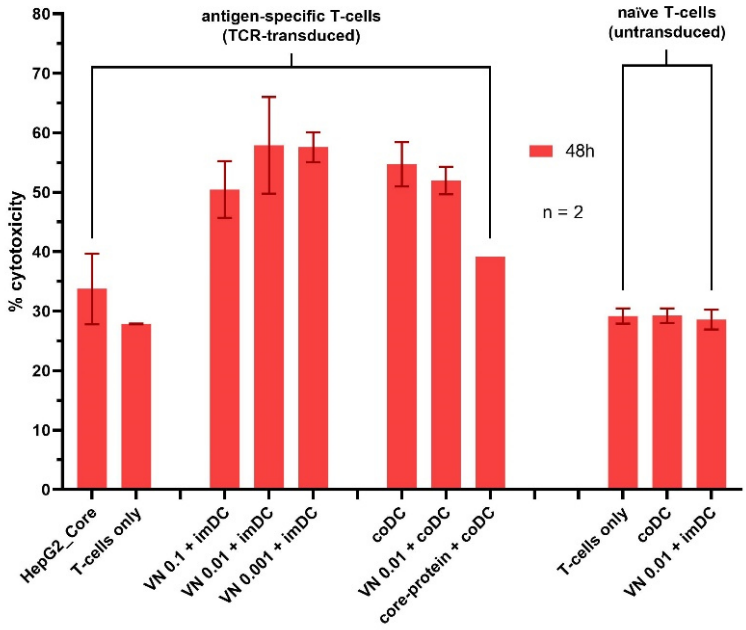

Figure 28: Oncolysate-treated imDCs induce tumor cell killing by TCR-transduced T cells
TCR-transduced as well as untransduced T cells, previously co-cultured with VN 0.001, VN 0.01 and VN 0.1-treated imDCs and coDCs for 120 hours, were co-cultured with fresh HepG2_Core tumor cells for 48 hours and cytotoxicity was measured via LDH assay. Co-culture of TCR-transduced T cells with HepG2_Core cells served as positive control, T cells alone as negative control. Cells were co-cultured in triplicates, and experiments were performed twice. Means ± SEM are shown (* $p < 0.05$).

4. Discussion and Outlook

Hepatocellular carcinoma is a very frequent cancer entity, but there is a lack of curative therapies for later stages of the disease (Figure 1, Figure 2) and therefore a strong need for new therapeutic approaches. In the evolving field of cancer immunotherapies, the liver plays a unique role due to the high tolerance of its immune system (Altomonte & Ebert, 2014). We therefore hypothesized, that by reversing the immunosuppressive environment of the HCC – but potentially also other cancer entities since most of them develop mechanisms to escape immune surveillance – with the stimulation of a broad and individualized anti-tumor immune response, not only the tumor but also distant and unknown metastases could be controlled.

Dendritic cells are the immune system's allrounder. They initiate innate as well as adaptive immune responses, they stimulate immediate reactions as well as long-term immunologic memory (Murphy & Weaver, 2017) and are therefore crucial in the induction of a broad immune response. So-called dendritic cell vaccines are tested in various pre-clinical experiments and clinical trials, in which DCs are stimulated to act against tumor-associated antigens (Filley & Dey, 2017).

A crucial point for the effectiveness of these DC-vaccines is the state of DC activation. Only sufficiently activated DCs are able to induce immune activation; otherwise, they promote immune tolerance. The immunogenic oncolytic virus, VSV-NDV, not only specifically infects tumor cells, but furthermore kills them via an immunogenic cell death (Abdullahi et al., 2018). In this type of cell death, various mediators are released by the dying cell in a defined temporal sequence that specifically lead to the attraction and activation of dendritic cells that will subsequently take up and present the dying cell's antigens (Kroemer et al., 2013).

Hypothesis and aim of the project

Based on this concept, we developed the hypothesis that an effective immunotherapeutic approach could be developed, whereby VSV-NDV-mediated tumor oncolysates generated from *ex vivo* infection of patient tumor material could be used to activate DCs and load them with the autologous library of tumor antigens (Figure 8) in order to generate a potent individualized DC vaccine, capable of mediating a broad and long-lasting adaptive immune response.

The aim of this project was to establish the proof-of-concept of this therapeutic approach *in vitro* in a human cell culture model system. As a first step, the infectibility of the model HCC cell line with VSV-NDV was assessed and the conditions of the oncolysate were optimized. After the stimulation of the DCs with the oncolysate, their state of activation was analysed via flow cytometry and cytokine measurements, whereas their functionality was assessed in a T cell co-culture.

Optimization of the viral oncolysate

Taking together microscopy, cytotoxicity and virus growth curves of HepG2_Core cell line infections with VSV-NDV (Figure 13, Figure 14), it can be concluded that the cells are very susceptible to VSV-NDV infection. Already after 24 hours, the cells are lysed, representing the oncolysate necessary for downstream experiments.

Although it has been demonstrated previously (Abdullahi et al., 2018) that the administration of live VSV-NDV doesn't cause severe side effects in mice, it seems to have negative effects on human monocyte-derived dendritic cells under *in vitro* conditions (Figure 20). Taking into consideration the sensitivity of human moDCs in cell culture in general, the results observed could very well be attributed to those non-physiological conditions. The inactivation of live virus in the oncolysate prior to DC co-culture does not only protect the DCs in cell culture (Figure 21) but additionally facilitates potential clinical translation because no live virus will be present in the vaccine. Nevertheless, VSV-NDV can act out its beneficial functions for the vaccine before being inactivated: creating the tumor cell lysate, the DC-stimulating immunogenic cell death is induced, while the viral particles itself serve as an adjuvant, also after inactivation.

If the use of live virus – either for the vaccine itself or its combination with OV therapy – was desired later, the use of classical dendritic cells type I (cDC1) could be evaluated. While showing high cross-presentation capacities to CTLs, they are also more resistant to productive virus infection. This is likely due to their ability to produce type I IFN, which can attenuate virus replication (Silvin et al., 2017).

VSV-NDV-lysed tumor cells potently activate dendritic cells

When discussing the results of the DC activation experiments, several aspects concerning the experimental setup should always be considered: First, experiments have been performed with primary immune cells from different human donors, leading to high inter-experimental differences but similar trends (Figure 22). Furthermore, the moDC population used in the experiments is not pure but consists of many other lymphocytes (Figure 17). The role, if any, of these additional cell types in the outcome of the experiments remains to be determined. Moreover, it should be underlined that the activation cocktail used as a positive control consists of a broad range of activating cytokines and ligands (see 2.2.3) and has originally been developed and optimized to artificially activate moDCs to an extraordinary extent (Subklewe et al., 2014).

Throughout the different experiments the viral oncolysate demonstrates itself to be a potent activator of DCs, represented by the upregulation of activation markers on the DC's surface as well as the secretion of immune-stimulatory cytokines by the DCs. This not only holds true for activating immature moDCs (Figure 23), but even to a higher extent for the moDCs already activated with the cytokine

cocktail (Figure 24, Figure 26). This underlines the great potential of the approach: On the one, hand the addition of the viral oncolysate even increases the already very high degree of activation of the coDCs, but on the other hand, the oncolysate enables the DCs to induce the specific immune response against the tumor since it provides the broad range of TAAs.

It has been demonstrated in Figure 25 that also UV-inactivated VSV-NDV alone – not in the context of the viral oncolysate – tends to induce an increase in all DC activation markers. First, this indicates a mechanism of action in a "classical" OV therapy approach that is of increasing interest (Krabbe & Altomonte, 2018): Upon administration of an oncolytic virus, it not only infects and subsequently kills the tumor cells but also elicits an immune response, potentially against the tumor. But second, this finding also underlines the importance of testing the functionality of the oncolysate-activated DCs in their ability to induce an anti-tumor immune response in a functional readout. The upregulation of activation markers on the DC's surface or the release of cytokines upon stimulation with VSV-lysed tumor cells as demonstrated in Figure 23 and Figure 24 will most likely partially only reflect the DC's contact with the virus.

A closer look at the panel of cytokines secreted by stimulated moDCs (Figure 26) reveals that the major increase in cytokine secretion is induced by the addition of the cytokine cocktail to imDCs, but upon addition of the oncolysate the secretion of IL-6 and IL-12 by coDCs can be increased even more. The immunosuppressive cytokines IL-10 and TGF-β1 stay on a very low level. This is favourable because insufficiently activated DCs induce anergy against the presented antigens while fully activated DCs are necessary for the success of the vaccine approach (Filley & Dey, 2017). The increase in the secretion of the NK cell-activating cytokines – especially the strong increase in IL-12 – indicates that the vaccine approach might also favour NK cell-induced tumor cell killing. This could substantially support the effectiveness of the vaccine because high NK cell levels are associated with a reduced risk of cancer, which is of even higher importance when taking into consideration that the percentage of NK cells in the liver is a lot higher than in the peripheral blood (Imai et al., 2000).

Oncolysate-stimulated DCs mediate T cell-induced tumor cell death

The oncolysate's potential to stimulate DCs that subsequently activate T cells can't be fully evaluated with the data presented in this work, in part due to the extensive inter-individual differences that were encountered. In the IFN-γ-ELISA (Figure 27), unspecific activation of naïve T cells was measured, which could be attributed to the artificial *in vitro* conditions. The second trend visible in this data set is that coDCs, whether additionally cultured with oncolysate or not, induce the highest levels of IFN-γ. This suggests that for a strong T cell activation – using the secretion of IFN-γ as a surrogate parameter – a higher degree of activation of the stimulating DCs is necessary; however, this does not translate to the final functional readout, in which the ability of those T cells in tumor cell killing was assessed (Figure

28). Oncolysate-treated immature DCs lead to a stimulation of antigen-specific T cells that induced the highest levels of cytotoxicity in the target tumor cells, potentially slightly higher than the cytotoxicity induced by cocktail-stimulated DCs. In all previous readouts, coDCs had always reached the highest degrees of activation.

When comparing the cytotoxicity induced by T cells primed by coDCs with and without oncolysate-stimulation, no relevant differences could be detected. It could be hypothesized that the cytotoxic effect of the antigen-specific T cells was just mediated by unspecific DC stimulation. Even though this data cannot prove either hypothesis, it could be considered very unlikely that an unspecific stimulation by imDCs – that were proven to express lower levels of activation markers on the cell surface, to secrete lower amounts of cytokines and to induce lower levels of IFN-γ secretion by T cells – leads to the same cytotoxic activity as the one by coDCs. Much more likely they are presenting the antigen specific for the model TCR, stimulating the specific T cells to the same extent as the much more activated coDCs do in an unspecific manner. Concerning the lack of a difference between coDCs with and without oncolysate-stimulation, we are potentially reaching the maximum of T cell-cytotoxicity, whereas the oncolysate-treated DCs could have increased T cell-cytotoxicity even more. It should always be considered that those T cells have already been in the artificial experimental setting for two weeks by now and might already be functionally impaired.

Outlook

Altogether, there are still open questions concerning the effectiveness of oncolysate-treated DCs to induce an anti-tumor immune response. Further optimization of the functional T cell readout and performing this experiment in triplicates with cells from the same healthy donor might help by excluding the large inter-donor-variability. It would furthermore be interesting to investigate the DC's ability to activate NK cells since they also play an important role in tumor cell killing. Nevertheless, we can conclude that the higher expression of activation markers on the DC surface and the increase in cytokine secretion support the therapeutic approach.

To move one step further towards clinical translation, it will be interesting to perform these experiments with patient derived material – a sample of a patient's tumor cells with immune cells from the same patient's blood. It needs to be proven that the results achieved with blood from healthy donors in a nicely infectible cell line model system can also be validated in the context of patient-derived material.

For further investigation of the DC vaccine's effect, an *in vivo* model is necessary. Since this is very difficult in a human system, our research group is in parallel developing a model of the therapeutic approach in a murine system in order to then test the vaccine *in vivo*.

All in all, the results presented in this work provide a proof-of-concept for a highly translational oncolytic virus-based DC vaccine. Further studies will be needed to consolidate the data shown here and to clarify the details necessary for clinical translation.

5. List of Abbreviations

AFP	Alpha-fetoprotein
APC	Antigen presenting cell
ATP	Adenosine triphosphate
BCLC	Barcelona clinic liver cancer
CD	Cluster of differentiation
CPE	Cytopathic effect
CRT	Calreticulin
CTL	Cytotoxic T-cell
DAMP	Damage-associated molecular patter
DC	Dendritic cell
moDC	Monocyte-derived dendritic cell
imDC	immature (=naïve) monocyte-derived dendritic cell
coDC	cocktail-pre-treated (=activated) monocyte-derived dendritic cell
cDC	Classical dendritic cell
pDC	Plasmacytoid dendritic cell
EMA	European Medicines Agency
ER	Endoplasmic reticulum
FDA	Federal drug administration
F	Fusion
GFP	Green fluorescent protein
GM-CSF	Granulocyte-macrophage colony-stimulating factor
HBV	Hepatitis B virus
HCC	Hepatocellular Carcinoma
HCV	Hepatitis C virus
HLA	Human leucocyte antigen
HMGB1	High mobility group box 1-protein
HN	Hemagglutinin-neuraminidase
HSC	Hepatic stellate cell
i.d.	intradermal
i.l.	intralesional
i.n.	intranodal
i.v.	intravenous
ICD	Immunogenic cell death
IFN	Interferon
IL	Interleukin
KC	Kupffer cell
LC	Langerhans cell
LDH	Lactate dehydrogenase
LDL	Low density lipoprotein
LDLT	Living donor liver transplantation
LN	Lymph node
LSEC	Liver sinusoidal endothelial cell
LTx	Liver transplantation
MDSC	Myeloid derived suppressor cell
MHC	Major histocompatibility complex
MOI	Multiplicity of infection
NC	Negative control
NDV	Newcastle Disease Virus
NK	Natural killer
OS	Overall survival

OV	Oncolytic virus
p.i.	Post-infection
PAMP	Pathogen-associated molecular pattern
PBMC	peripheral blood mononuclear cell
PBS	Phosphate buffered saline
PC	Positive control
PFS	Progression-free survival
PRR	Pattern recognition receptor
RFA	Radiofrequency ablation
RNP	Ribonucleoprotein
RT	Room temperature
SD	Standard deviation
SEM	Standard error of the mean
SIRT	Selective internal radiotherapy
SN	Supernatant
TACE	Trans-arterial chemo embolization
$TCID_{50}$	Tissue culture infectious $dose_{50}$
TCR	T-cell receptor
TLR	Toll-like receptor
TME	Tumor microenvironment
Treg	T regulatory cell
VEGF	Vascular endothelial growth factor
VSV	Vesicular Stomatitis Virus

6. List of Figures and Tables

List of figures

List of tables

7. References

Abdullahi, S., Jakel, M., Behrend, S. J., Steiger, K., Topping, G., Krabbe, T., . . . Altomonte, J. (2018). A Novel Chimeric Oncolytic Virus Vector for Improved Safety and Efficacy as a Platform for the Treatment of Hepatocellular Carcinoma. *Journal of Virology, 92*(23). doi:10.1128/JVI.01386-18

Abou-Alfa, G. K., Meyer, T., Cheng, A. L., El-Khoueiry, A. B., Rimassa, L., Ryoo, B. Y., . . . Kelley, R. K. (2018). Cabozantinib in Patients with Advanced and Progressing Hepatocellular Carcinoma. *New England Journal of Medicine, 379*(1), 54-63. doi:10.1056/NEJMoa1717002

Altomonte, J., & Ebert, O. (2014). Sorting Out Pandora's Box: Discerning the Dynamic Roles of Liver Microenvironment in Oncolytic Virus Therapy for Hepatocellular Carcinoma. *Frontiers in Oncology, 4*, 85. doi:10.3389/fonc.2014.00085

Apetoh, L., Ghiringhelli, F., Tesniere, A., Obeid, M., Ortiz, C., Criollo, A., . . . Zitvogel, L. (2007). Toll-like receptor 4-dependent contribution of the immune system to anticancer chemotherapy and radiotherapy. *Nature Medicine, 13*(9), 1050-1059. doi:10.1038/nm1622

Avian Health: Virulent Newcastle Disease. (2019). Retrieved from https://www.cdfa.ca.gov/ahfss/Animal_Health/Newcastle_Disease_Info.html

Bachem, A., Guttler, S., Hartung, E., Ebstein, F., Schaefer, M., Tannert, A., . . . Kroczek, R. A. (2010). Superior antigen cross-presentation and XCR1 expression define human CD11c+CD141+ cells as homologues of mouse CD8+ dendritic cells. *Journal of Experimental Medicine, 207*(6), 1273-1281. doi:10.1084/jem.20100348

Banchereau, J., Thompson-Snipes, L., Zurawski, S., Blanck, J. P., Cao, Y., Clayton, S., . . . Klechevsky, E. (2012). The differential production of cytokines by human Langerhans cells and dermal CD14(+) DCs controls CTL priming. *Blood, 119*(24), 5742-5749. doi:10.1182/blood-2011-08-371245

Bao, M., & Liu, Y. J. (2013). Regulation of TLR7/9 signaling in plasmacytoid dendritic cells. *Protein Cell, 4*(1), 40-52. doi:10.1007/s13238-012-2104-8

Belkowski, L. S., & Sen, G. C. (1986). Inhibition of Vesicular Stomatitis Viral mRNA Synthesis by Interferons. *Journal of Virology, 61*(3), 653-660.

Bluming, A. Z., & Ziegler, J. L. (1971). Regression of Burkitt's lymphoma in association with measles infection. *The Lancet*, 105-106.

Bonifaz, L., Bonnyay, D., Mahnke, K., Rivera, M., Nussenzweig, M. C., & Steinman, R. M. (2002). Efficient targeting of protein antigen to the dendritic cell receptor DEC-205 in the steady state leads to antigen presentation on major histocompatibility complex class I products and peripheral CD8+ T cell tolerance. *Journal of Experimental Medicine, 196*(12), 1627-1638. doi:10.1084/jem.20021598

Breitbach, C. J., Arulanandam, R., De Silva, N., Thorne, S. H., Patt, R., Daneshmand, M., . . . Kirn, D. H. (2013). Oncolytic vaccinia virus disrupts tumor-associated vasculature in humans. *Cancer Research, 73*(4), 1265-1275. doi:10.1158/0008-5472.Can-12-2687

Breitbach, C. J., De Silva, N. S., Falls, T. J., Aladl, U., Evgin, L., Paterson, J., . . . Bell, J. C. (2011). Targeting tumor vasculature with an oncolytic virus. *Molecular Therapy, 19*(5), 886-894. doi:10.1038/mt.2011.26

Brown, V. R., & Bevins, S. N. (2017). A review of virulent Newcastle disease viruses in the United States and the role of wild birds in viral persistence and spread. *Veterinary Research, 48*(1), 68. doi:10.1186/s13567-017-0475-9

Bruix, J., Qin, S., Merle, P., Granito, A., Huang, Y. H., Bodoky, G., . . . Han, G. (2017). Regorafenib for patients with hepatocellular carcinoma who progressed on sorafenib treatment (RESORCE): a randomised, double-blind, placebo-controlled, phase 3 trial. *Lancet, 389*(10064), 56-66. doi:10.1016/s0140-6736(16)32453-9

Budhu, A., Forgues, M., Ye, Q. H., Jia, H. L., He, P., Zanetti, K. A., . . . Wang, X. W. (2006). Prediction of venous metastases, recurrence, and prognosis in hepatocellular carcinoma based on a unique

immune response signature of the liver microenvironment. *Cancer Cell, 10*(2), 99-111. doi:10.1016/j.ccr.2006.06.016

Cella, M., Jarrossay, D., Facchetti, F., Alebardi, O., Nakajima, H., Lanzavecchia, A., & Colonna, M. (1999). Plasmacytoid monocytes migrate to inflamed lymph nodes and produce large amounts of type I interferon. *Nature Medicine, 5*(8), 919-923. doi:10.1038/11360

Chaurasiya, S., Chen, N. G., & Warner, S. G. (2018). Oncolytic Virotherapy versus Cancer Stem Cells: A Review of Approaches and Mechanisms. *Cancers, 10*(4). doi:10.3390/cancers10040124

Chiappori, A. A., Williams, C. C., Gray, J. E., Tanvetyanon, T., Haura, E. B., Creelan, B. C., . . . Antonia, S. J. (2019). Randomized-controlled phase II trial of salvage chemotherapy after immunization with a TP53-transfected dendritic cell-based vaccine (Ad.p53-DC) in patients with recurrent small cell lung cancer. *Cancer Immunology, Immunotherapy, 68*(3), 517-527. doi:10.1007/s00262-018-2287-9

Collin, M., & Bigley, V. (2018). Human dendritic cell subsets: an update. *Immunology, 154*(1), 3-20. doi:10.1111/imm.12888

Cuadrado-Castano, S., Sanchez-Aparicio, M. T., Garcia-Sastre, A., & Villar, E. (2015). The therapeutic effect of death: Newcastle disease virus and its antitumor potential. *Virus Research, 209*, 56-66. doi:10.1016/j.virusres.2015.07.001

de Pace, N. (1912). Sulla scomparsa di un enorme cancre vegetante del collo dell' utero senza cura chirurgica. *Ginecologia, 9*, 82-89.

Dendreon - About us: Our history. (2018). Retrieved from https://www.dendreon.com/About-Us#OurHistory

Dhodapkar, M. V., Steinman, R. M., Krasovsky, J., Munz, C., & Bhardwaj, N. (2001). Antigen-specific inhibition of effector T cell function in humans after injection of immature dendritic cells. *Journal of Experimental Medicine, 193*(2), 233-238. doi:10.1084/jem.193.2.233

Diallo, J. S., Le Boeuf, F., Lai, F., Cox, J., Vaha-Koskela, M., Abdelbary, H., . . . Bell, J. C. (2010). A high-throughput pharmacoviral approach identifies novel oncolytic virus sensitizers. *Molecular Therapy, 18*(6), 1123-1129. doi:10.1038/mt.2010.67

Dudeck, A., Suender, C. A., Kostka, S. L., von Stebut, E., & Maurer, M. (2011). Mast cells promote Th1 and Th17 responses by modulating dendritic cell maturation and function. *European Journal of Immunology, 41*(7), 1883-1893. doi:10.1002/eji.201040994

Dudeck, J., Medyukhina, A., Frobel, J., Svensson, C. M., Kotrba, J., Gerlach, M., . . . Dudeck, A. (2017). Mast cells acquire MHCII from dendritic cells during skin inflammation. *Journal of Experimental Medicine, 214*(12), 3791-3811. doi:10.1084/jem.20160783

EASL. (2018). Clinical Practice Guidelines: Management of hepatocellular carcinoma. *Journal of Hepatology, 69*(1), 182-236. doi:10.1016/j.jhep.2018.03.019

Edele, F., Dudda, J. C., Bachtanian, E., Jakob, T., Pircher, H., & Martin, S. F. (2014). Efficiency of dendritic cell vaccination against B16 melanoma depends on the immunization route. *PloS One, 9*(8), e105266. doi:10.1371/journal.pone.0105266

El-Khoueiry, A. B., Sangro, B., Yau, T., Crocenzi, T. S., Kudo, M., Hsu, C., . . . Melero, I. (2017). Nivolumab in patients with advanced hepatocellular carcinoma (CheckMate 040): an open-label, non-comparative, phase 1/2 dose escalation and expansion trial. *Lancet, 389*(10088), 2492-2502. doi:10.1016/s0140-6736(17)31046-2

Eurotransplant. (2019). Annual report 2018.

Everts, B., & van der Poel, H. G. (2005). Replication-selective oncolytic viruses in the treatment of cancer. *Cancer Gene Therapy, 12*(2), 141-161. doi:10.1038/sj.cgt.7700771

FDA. (2019). FDA approves cabozantinib for hepatocellular carcinoma. Retrieved from https://www.fda.gov/drugs/fda-approves-cabozantinib-hepatocellular-carcinoma

Filley, A. C., & Dey, M. (2017). Dendritic cell based vaccination strategy: an evolving paradigm. *Journal of Neuro-Oncology, 133*(2), 223-235. doi:10.1007/s11060-017-2446-4

Finn, R. S., Qin, S., Ikeda, M., Galle, P. R., Ducreux, M., Kim, T. Y., . . . Cheng, A. L. (2020). Atezolizumab plus Bevacizumab in Unresectable Hepatocellular Carcinoma. *New England Journal of Medicine, 382*(20), 1894-1905. doi:10.1056/NEJMoa1915745

Ganguly, D., Chamilos, G., Lande, R., Gregorio, J., Meller, S., Facchinetti, V., . . . Gilliet, M. (2009). Self-RNA-antimicrobial peptide complexes activate human dendritic cells through TLR7 and TLR8. *Journal of Experimental Medicine, 206*(9), 1983-1994. doi:10.1084/jem.20090480

Garofalo, M., Villa, A., Rizzi, N., Kuryk, L., Mazzaferro, V., & Ciana, P. (2018). Systemic Administration and Targeted Delivery of Immunogenic Oncolytic Adenovirus Encapsulated in Extracellular Vesicles for Cancer Therapies. *Viruses, 10*(10). doi:10.3390/v10100558

Ghiringhelli, F., Apetoh, L., Tesniere, A., Aymeric, L., Ma, Y., Ortiz, C., . . . Zitvogel, L. (2009). Activation of the NLRP3 inflammasome in dendritic cells induces IL-1beta-dependent adaptive immunity against tumors. *Nature Medicine, 15*(10), 1170-1178. doi:10.1038/nm.2028

Gouttefangeas, C., & Rammensee, H. G. (2018). Personalized cancer vaccines: adjuvants are important, too. *Cancer Immunology, Immunotherapy, 67*(12), 1911-1918. doi:10.1007/s00262-018-2158-4

Graddis, T. J., McMahan, C. J., Tamman, J., Page, K. J., & Trager, J. B. (2011). Prostatic acid phosphatase expression in human tissues. *International Journal of Clinical and Experimental Pathology, 4*(3), 295-306.

Guilliams, M., & van de Laar, L. (2015). A Hitchhiker's Guide to Myeloid Cell Subsets: Practical Implementation of a Novel Mononuclear Phagocyte Classification System. *Frontiers in Immunology, 6*, 406. doi:10.3389/fimmu.2015.00406

Gulla, S. K., Rao, B. R., Moku, G., Jinka, S., Nimmu, N. V., Khalid, S., . . . Chaudhuri, A. (2019). In vivo targeting of DNA vaccines to dendritic cells using functionalized gold nanoparticles. *Biomater Sci, 7*(3), 773-788. doi:10.1039/c8bm01272e

Gunsar, F. (2017). Liver Transplantation for Hepatocellular Carcinoma Beyond the Milan Criteria. *Experimental and Clinical Transplantation, 15*(Suppl 2), 59-64. doi:10.6002/ect.TOND16.L16

Hochst, B., Schildberg, F. A., Sauerborn, P., Gabel, Y. A., Gevensleben, H., Goltz, D., . . . Diehl, L. (2013). Activated human hepatic stellate cells induce myeloid derived suppressor cells from peripheral blood monocytes in a CD44-dependent fashion. *Journal of Hepatology, 59*(3), 528-535. doi:10.1016/j.jhep.2013.04.033

Hsu, I. C., Metcalf, R. A., Sun, T., Welsh, J. A., Wang, N. J., & Harris, C. C. (1991). Mutational hotspot in the p53 gene in human hepatocellular carcinomas. *Nature, 350*(6317), 427-428. doi:10.1038/350427a0

Huang, Z., Krishnamurthy, S., Panda, A., & Samal, S. K. (2003). Newcastle disease virus V protein is associated with viral pathogenesis and functions as an alpha interferon antagonist. *Journal of Virology, 77*(16), 8676-8685. doi:10.1128/jvi.77.16.8676-8685.2003

Huber, A., Dammeijer, F., Aerts, J., & Vroman, H. (2018). Current State of Dendritic Cell-Based Immunotherapy: Opportunities for in vitro Antigen Loading of Different DC Subsets? *Frontiers in Immunology, 9*, 2804. doi:10.3389/fimmu.2018.02804

Ikeda, K., Ichikawa, T., Wakimoto, H., Silver, J. S., Deisboeck, T. S., Finkelstein, D., . . . Chiocca, E. A. (1999). Oncolytic virus therapy of multiple tumors in the brain requires suppression of innate and elicited antiviral responses. *Nature Medicine, 5*(8), 881-887. doi:10.1038/11320

Imai, K., Matsuyama, S., Miyake, S., Suga, K., & Nakachi, K. (2000). Natural cytotoxic activity of peripheral-blood lymphocytes and cancer incidence: an 11-year follow-up study of a general population. *Lancet, 356*(9244), 1795-1799. doi:10.1016/s0140-6736(00)03231-1

Kanitakis, J., Morelon, E., Petruzzo, P., Badet, L., & Dubernard, J. M. (2011). Self-renewal capacity of human epidermal Langerhans cells: observations made on a composite tissue allograft. *Experimental Dermatology, 20*(2), 145-146. doi:10.1111/j.1600-0625.2010.01146.x

Kantoff, P. W., Higano, C. S., Shore, N. D., Berger, E. R., Small, E. J., Penson, D. F., . . . Schellhammer, P. F. (2010). Sipuleucel-T immunotherapy for castration-resistant prostate cancer. *New England Journal of Medicine, 363*(5), 411-422. doi:10.1056/NEJMoa1001294

Karre, K., Ljunggren, H. G., Piontek, G., & Kiessling, R. (1986). Selective rejection of H-2-deficient lymphoma variants suggests alternative immune defence strategy. *Nature, 319*(6055), 675-678. doi:10.1038/319675a0

Kassel, R., Cruise, M. W., Iezzoni, J. C., Taylor, N. A., Pruett, T. L., & Hahn, Y. S. (2009). Chronically inflamed livers up-regulate expression of inhibitory B7 family members. *Hepatology, 50*(5), 1625-1637. doi:10.1002/hep.23173

Kim, J. H., Hu, Y., Yongqing, T., Kim, J., Hughes, V. A., Le Nours, J., . . . Winau, F. (2016). CD1a on Langerhans cells controls inflammatory skin disease. *Nature Immunology, 17*(10), 1159-1166. doi:10.1038/ni.3523

Kim, J. W., Kane, J. R., Panek, W. K., Young, J. S., Rashidi, A., Yu, D., . . . Lesniak, M. S. (2018). A Dendritic Cell-Targeted Adenoviral Vector Facilitates Adaptive Immune Response Against Human Glioma Antigen (CMV-IE) and Prolongs Survival in a Human Glioma Tumor Model. *Neurotherapeutics, 15*(4), 1127-1138. doi:10.1007/s13311-018-0650-3

Kim, Y., Clements, D. R., Sterea, A. M., Jang, H. W., Gujar, S. A., & Lee, P. W. (2015). Dendritic Cells in Oncolytic Virus-Based Anti-Cancer Therapy. *Viruses, 7*(12), 6506-6525. doi:10.3390/v7122953

Knolle, P., Schlaak, J., Uhrig, A., Kempf, P., Meyer zum Buschenfelde, K. H., & Gerken, G. (1995). Human Kupffer cells secrete IL-10 in response to lipopolysaccharide (LPS) challenge. *Journal of Hepatology, 22*(2), 226-229.

Knolle, P. A., Germann, T., Treichel, U., Uhrig, A., Schmitt, E., Hegenbarth, S., . . . Gerken, G. (1999). Endotoxin down-regulates T cell activation by antigen-presenting liver sinusoidal endothelial cells. *Journal of Immunology, 162*(3), 1401-1407.

Koks, C. A., De Vleeschouwer, S., Graf, N., & Van Gool, S. W. (2015). Immune Suppression during Oncolytic Virotherapy for High-Grade Glioma; Yes or No? *Journal of Cancer, 6*(3), 203-217. doi:10.7150/jca.10640

Koske, I., Rossler, A., Pipperger, L., Petersson, M., Barnstorf, I., Kimpel, J., . . . von Laer, D. (2019). Oncolytic virotherapy enhances the efficacy of a cancer vaccine by modulating the tumor microenvironment. *International Journal of Cancer*. doi:10.1002/ijc.32325

Krabbe, T., & Altomonte, J. (2018). Fusogenic Viruses in Oncolytic Immunotherapy. *Cancers, 10*(7). doi:10.3390/cancers10070216

Kroemer, G., Galluzzi, L., Kepp, O., & Zitvogel, L. (2013). Immunogenic cell death in cancer therapy. *Annual Review of Immunology, 31*, 51-72. doi:10.1146/annurev-immunol-032712-100008

Kudo, M., Finn, R. S., Qin, S., Han, K. H., Ikeda, K., Piscaglia, F., . . . Cheng, A. L. (2018). Lenvatinib versus sorafenib in first-line treatment of patients with unresectable hepatocellular carcinoma: a randomised phase 3 non-inferiority trial. *Lancet, 391*(10126), 1163-1173. doi:10.1016/s0140-6736(18)30207-1

Lande, R., Ganguly, D., Facchinetti, V., Frasca, L., Conrad, C., Gregorio, J., . . . Gilliet, M. (2011). Neutrophils activate plasmacytoid dendritic cells by releasing self-DNA-peptide complexes in systemic lupus erythematosus. *Science Translational Medicine, 3*(73), 73ra19. doi:10.1126/scitranslmed.3001180

Laoui, D., Keirsse, J., Morias, Y., Van Overmeire, E., Geeraerts, X., Elkrim, Y., . . . Van Ginderachter, J. A. (2016). The tumour microenvironment harbours ontogenically distinct dendritic cell populations with opposing effects on tumour immunity. *Nat Commun, 7*, 13720. doi:10.1038/ncomms13720

Lennert, K., & Remmele, W. (1958). Karyometric research on lymph node cells in man. I. Germinoblasts, lymphoblasts & lymphocytes. *Acta Haematologica, 19*(2), 99-113. doi:10.1159/000205419

Letchworth, G. J., Rodriguez, L. L., & Del C. Barrera, J. (1999). Vesicular stomatitis. *Veterinary Journal, 157*(3), 239-260. doi:10.1053/tvjl.1998.0303

Lichtenegger, F. S., Rothe, M., Schnorfeil, F. M., Deiser, K., Krupka, C., Augsberger, C., . . . Subklewe, M. (2018). Targeting LAG-3 and PD-1 to Enhance T Cell Activation by Antigen-Presenting Cells. *Frontiers in Immunology, 9*, 385. doi:10.3389/fimmu.2018.00385

Llovet, J. M., Ricci, S., Mazzaferro, V., Hilgard, P., Gane, E., Blanc, J. F., . . . Bruix, J. (2008). Sorafenib in advanced hepatocellular carcinoma. *New England Journal of Medicine, 359*(4), 378-390. doi:10.1056/NEJMoa0708857

Lorence, R. M., Katubig, B. B., Reichard, K. W., Reyes, H. M., Phuangsab, A., Sassetti, M. D., . . . Peeples, M. E. (1994). Complete regression of human fibrosarcoma xenografts after local Newcastle disease virus therapy. *Cancer Research, 54*(23), 6017-6021.

Lowenfeld, L., Mick, R., Datta, J., Xu, S., Fitzpatrick, E., Fisher, C. S., . . . Czerniecki, B. J. (2017). Dendritic Cell Vaccination Enhances Immune Responses and Induces Regression of HER2(pos) DCIS Independent of Route: Results of Randomized Selection Design Trial. *Clinical Cancer Research, 23*(12), 2961-2971. doi:10.1158/1078-0432.Ccr-16-1924

Lyles, D. S. (2000). Cytopathogenesis and Inhibition of Host Gene Expression by RNA Viruses. *Microbiology and Molecular Biology Reviews, 64*(4), 709-724.

Macedo, N., Miller, D. M., Haq, R., & Kaufman, H. L. (2020). Clinical landscape of oncolytic virus research in 2020. *J Immunother Cancer, 8*(2). doi:10.1136/jitc-2020-001486

Mahipal, A., Tella, S. H., Kommalapati, A., Lim, A., & Kim, R. (2019). Immunotherapy in Hepatocellular Carcinoma: Is There a Light at the End of the Tunnel? *Cancers, 11*(8). doi:10.3390/cancers11081078

Mansour, M., Palese, P., & Zamarin, D. (2011). Oncolytic specificity of Newcastle disease virus is mediated by selectivity for apoptosis-resistant cells. *Journal of Virology, 85*(12), 6015-6023. doi:10.1128/jvi.01537-10

Marchini, A., Scott, E. M., & Rommelaere, J. (2016). Overcoming Barriers in Oncolytic Virotherapy with HDAC Inhibitors and Immune Checkpoint Blockade. *Viruses, 8*(1). doi:10.3390/v8010009

Martinet, J., Dufeu-Duchesne, T., Bruder Costa, J., Larrat, S., Marlu, A., Leroy, V., . . . Aspord, C. (2012). Altered functions of plasmacytoid dendritic cells and reduced cytolytic activity of natural killer cells in patients with chronic HBV infection. *Gastroenterology, 143*(6), 1586-1596.e1588. doi:10.1053/j.gastro.2012.08.046

Melzer, M. K., Lopez-Martinez, A., & Altomonte, J. (2017). Oncolytic Vesicular Stomatitis Virus as a Viro-Immunotherapy: Defeating Cancer with a "Hammer" and "Anvil". *Biomedicines, 5*(1). doi:10.3390/biomedicines5010008

Melzer, M. K., Zeitlinger, L., Mall, S., Steiger, K., Schmid, R. M., Ebert, O., . . . Altomonte, J. (2019). Enhanced Safety and Efficacy of Oncolytic VSV Therapy by Combination with T Cell Receptor Transgenic T Cells as Carriers. *Mol Ther Oncolytics, 12*, 26-40. doi:10.1016/j.omto.2018.12.001

Merad, M., Sathe, P., Helft, J., Miller, J., & Mortha, A. (2013). The dendritic cell lineage: ontogeny and function of dendritic cells and their subsets in the steady state and the inflamed setting. *Annual Review of Immunology, 31*, 563-604. doi:10.1146/annurev-immunol-020711-074950

Mitchell, D. A., Batich, K. A., Gunn, M. D., Huang, M. N., Sanchez-Perez, L., Nair, S. K., . . . Sampson, J. H. (2015). Tetanus toxoid and CCL3 improve dendritic cell vaccines in mice and glioblastoma patients. *Nature, 519*(7543), 366-369. doi:10.1038/nature14320

Mullen, J. T., & Tanabe, K. K. (2002). Viral Oncolysis. *The Oncologist, 7*(2).

Murphy, K. M., & Weaver, C. (2017). *Janeway's immunobiology*. New York ; London: Garland Science.

Nadalin, S., Capobianco, I., Panaro, F., Di Francesco, F., Troisi, R., Sainz-Barriga, M., . . . Testa, G. (2016). Living donor liver transplantation in Europe. *Hepatobiliary Surg Nutr, 5*(2), 159-175. doi:10.3978/j.issn.2304-3881.2015.10.04

Nizzoli, G., Krietsch, J., Weick, A., Steinfelder, S., Facciotti, F., Gruarin, P., . . . Geginat, J. (2013). Human CD1c+ dendritic cells secrete high levels of IL-12 and potently prime cytotoxic T-cell responses. *Blood, 122*(6), 932-942. doi:10.1182/blood-2013-04-495424

The Nobel Prize in Physiology or Medicine 2011. (2019). Retrieved from https://www.nobelprize.org/prizes/medicine/2011/summary/

Otsuki, A., Patel, A., Kasai, K., Suzuki, M., Kurozumi, K., Antonio Chiocca, E., & Saeki, Y. (2008). Histone Deacetylase Inhibitors Augment Antitumor Efficacy of Herpes-based Oncolytic Viruses. *Molecular Therapy, 16*(9), 1546-1555. doi:10.1038/mt.2008.155

Palmer, D. H., Midgley, R. S., Mirza, N., Torr, E. E., Ahmed, F., Steele, J. C., . . . Adams, D. H. (2009). A phase II study of adoptive immunotherapy using dendritic cells pulsed with tumor lysate in patients with hepatocellular carcinoma. *Hepatology, 49*(1), 124-132. doi:10.1002/hep.22626

Pan, L., Shang, N., Shangguan, J., Figini, M., Xing, W., Wang, B., . . . Zhang, Z. (2019). Magnetic resonance imaging monitoring therapeutic response to dendritic cell vaccine in murine orthotopic pancreatic cancer models. *American Journal of Cancer Research, 9*(3), 562-573.

Panaretakis, T., Kepp, O., Brockmeier, U., Tesniere, A., Bjorklund, A. C., Chapman, D. C., . . . Kroemer, G. (2009). Mechanisms of pre-apoptotic calreticulin exposure in immunogenic cell death. *EMBO Journal, 28*(5), 578-590. doi:10.1038/emboj.2009.1

Pinato, D. J., North, B. V., & Sharma, R. (2012). A novel, externally validated inflammation-based prognostic algorithm in hepatocellular carcinoma: the prognostic nutritional index (PNI). *British Journal of Cancer, 106*(8), 1439-1445. doi:10.1038/bjc.2012.92

Pol, J., Kroemer, G., & Galluzzi, L. (2016). First oncolytic virus approved for melanoma immunotherapy. *Oncoimmunology, 5*(1), e1115641. doi:10.1080/2162402X.2015.1115641

Provenge - Withdrawal of the marketing authorisation in the European Union (2015). Retrieved from https://www.ema.europa.eu/en/documents/public-statement/public-statement-provenge-withdrawal-marketing-authorisation-european-union_en.pdf

PROVENGE (sipuleucel-T). (2019). Retrieved from https://www.fda.gov/vaccines-blood-biologics/cellular-gene-therapy-products/provenge-sipuleucel-t

Quiroz, E., Moreno, N., Peralta, P. H., & Tesh, R. B. (1988). A human case of encephalitis associated with vesicular stomatitis virus (Indiana serotype) infection. *American Journal of Tropical Medicine and Hygiene, 39*(3), 312-314. doi:10.4269/ajtmh.1988.39.312

Rajput, M. K. S., Kesharwani, S. S., Kumar, S., Muley, P., Narisetty, S., & Tummala, H. (2018). Dendritic Cell-Targeted Nanovaccine Delivery System Prepared with an Immune-Active Polymer. *ACS Appl Mater Interfaces, 10*(33), 27589-27602. doi:10.1021/acsami.8b02019

Russell, S. J., Peng, K. W., & Bell, J. C. (2012). Oncolytic virotherapy. *Nature Biotechnology, 30*(7), 658-670. doi:10.1038/nbt.2287

Sangiovanni, A., Prati, G. M., Fasani, P., Ronchi, G., Romeo, R., Manini, M., . . . Colombo, M. (2006). The natural history of compensated cirrhosis due to hepatitis C virus: A 17-year cohort study of 214 patients. *Hepatology, 43*(6), 1303-1310. doi:10.1002/hep.21176

Schirrmacher, V., Lorenzen, D., Van Gool, S. W., & Stuecker, W. (2017). A New Strategy of Cancer Immunotherapy Combining Hyperthermia/Oncolytic Virus Pretreatment with Specific Autologous Anti-Tumor Vaccination - A Review. *Austin Oncology Case Reports, 2*(1).

Shnyrova, A. V., Ayllon, J., Mikhalyov, II, Villar, E., Zimmerberg, J., & Frolov, V. A. (2007). Vesicle formation by self-assembly of membrane-bound matrix proteins into a fluidlike budding domain. *Journal of Cell Biology, 179*(4), 627-633. doi:10.1083/jcb.200705062

Siegal, F. P., Kadowaki, N., Shodell, M., Fitzgerald-Bocarsly, P. A., Shah, K., Ho, S., . . . Liu, Y. J. (1999). The nature of the principal type 1 interferon-producing cells in human blood. *Science, 284*(5421), 1835-1837. doi:10.1126/science.284.5421.1835

Silvin, A., Yu, C. I., Lahaye, X., Imperatore, F., Brault, J. B., Cardinaud, S., . . . Manel, N. (2017). Constitutive resistance to viral infection in human CD141(+) dendritic cells. *Sci Immunol, 2*(13). doi:10.1126/sciimmunol.aai8071

Simon, B., & Uslu, U. (2018). CAR-T cell therapy in melanoma: A future success story? *Experimental Dermatology, 27*(12), 1315-1321. doi:10.1111/exd.13792

Small, E. J., Fratesi, P., Reese, D. M., Strang, G., Laus, R., Peshwa, M. V., & Valone, F. H. (2000). Immunotherapy of hormone-refractory prostate cancer with antigen-loaded dendritic cells. *Journal of Clinical Oncology, 18*(23), 3894-3903. doi:10.1200/jco.2000.18.23.3894

Southam, C. M. (1960). Present status of oncolytic virus studies. *Transactions of the New York Academy of Sciences, 22*, 657-673.

Steinman, R. M., & Cohn, Z. A. (1973). Identification of a novel cell type in peripheral lymphoid organs of mice. I. Morphology, quantitation, tissue distribution. *Journal of Experimental Medicine, 137*(5), 1142-1162. doi:10.1084/jem.137.5.1142

Steinman, R. M., & Cohn, Z. A. (1974). Identification of a novel cell type in peripheral lymphoid organs of mice. II. Functional properties in vitro. *Journal of Experimental Medicine, 139*(2), 380-397. doi:10.1084/jem.139.2.380

Stojdl, D. F., Lichty, B., Knowles, S., Marius, R., Atkins, H., Sonenberg, N., & Bell, J. C. (2000). Exploiting tumor-specific defects in the interferon pathway with a previously unknown oncolytic virus. *Nature Medicine, 6*(7), 821-825.

Subklewe, M., Geiger, C., Lichtenegger, F. S., Javorovic, M., Kvalheim, G., Schendel, D. J., & Bigalke, I. (2014). New generation dendritic cell vaccine for immunotherapy of acute myeloid leukemia. *Cancer Immunology, Immunotherapy, 63*(10), 1093-1103. doi:10.1007/s00262-014-1600-5

Swiecki, M., & Colonna, M. (2015). The multifaceted biology of plasmacytoid dendritic cells. *Nature Reviews: Immunology, 15*(8), 471-485. doi:10.1038/nri3865

Tapper, E. B., Risech-Neyman, Y., & Sengupta, N. (2015). Psychoactive Medications Increase the Risk of Falls and Fall-related Injuries in Hospitalized Patients With Cirrhosis. *Clinical Gastroenterology and Hepatology, 13*(9), 1670-1675. doi:10.1016/j.cgh.2015.03.019

Taqi, A. M., Abdurrahman, M. B., Yakubu, A. M., & Fleming, A. F. (1981). Regression of Hodgkin's disease after measles. *The Lancet*, 1112.

Tel, J., Schreibelt, G., Sittig, S. P., Mathan, T. S., Buschow, S. I., Cruz, L. J., . . . de Vries, I. J. (2013). Human plasmacytoid dendritic cells efficiently cross-present exogenous Ags to CD8+ T cells despite lower Ag uptake than myeloid dendritic cell subsets. *Blood, 121*(3), 459-467. doi:10.1182/blood-2012-06-435644

Tomasicchio, M., Semple, L., Esmail, A., Meldau, R., Randall, P., Pooran, A., . . . Dheda, K. (2019). An autologous dendritic cell vaccine polarizes a Th-1 response which is tumoricidal to patient-derived breast cancer cells. *Cancer Immunology, Immunotherapy, 68*(1), 71-83. doi:10.1007/s00262-018-2238-5

Toro Bejarano, M., & Merchan, J. R. (2015). Targeting tumor vasculature through oncolytic virotherapy: recent advances. *Oncolytic Virother, 4*, 169-181. doi:10.2147/OV.S66045

Verweij, M. C., Horst, D., Griffin, B. D., Luteijn, R. D., Davison, A. J., Ressing, M. E., & Wiertz, E. J. (2015). Viral inhibition of the transporter associated with antigen processing (TAP): a striking example of functional convergent evolution. *PLoS Pathogens, 11*(4), e1004743. doi:10.1371/journal.ppat.1004743

Wang, F., Xiao, W., Elbahnasawy, M. A., Bao, X., Zheng, Q., Gong, L., . . . Song, X. (2018). Optimization of the Linker Length of Mannose-Cholesterol Conjugates for Enhanced mRNA Delivery to Dendritic Cells by Liposomes. *Frontiers in Pharmacology, 9*, 980. doi:10.3389/fphar.2018.00980

Wen, P. Y., Reardon, D. A., Armstrong, T. S., Phuphanich, S., Aiken, R. D., Landolfi, J. C., . . . Yu, J. S. (2019). A Randomized Double-Blind Placebo-Controlled Phase II Trial of Dendritic Cell Vaccine ICT-107 in Newly Diagnosed Patients with Glioblastoma. *Clinical Cancer Research, 25*(19), 5799-5807. doi:10.1158/1078-0432.Ccr-19-0261

WHO. (2018). Cancer Today - IARC. Retrieved from http://gco.iarc.fr/today/online-analysis-table?v=2018&mode=cancer&mode_population=continents&population=900&populations=900&key=asr&sex=0&cancer=39&type=1&statistic=5&prevalence=0&population_group=0&ages_group%5B%5D=0&ages_group%5B%5D=17&nb_items=5&group_cancer=1&include_nmsc=1&include_nmsc_other=1

Woltman, A. M., Op den Brouw, M. L., Biesta, P. J., Shi, C. C., & Janssen, H. L. (2011). Hepatitis B virus lacks immune activating capacity, but actively inhibits plasmacytoid dendritic cell function. *PloS One, 6*(1), e15324. doi:10.1371/journal.pone.0015324

Wongthida, P., Jengarn, J., Narkpuk, J., Koonyosying, P., Srisutthisamphan, K., Wanitchang, A., . . . Jongkaewwattana, A. (2016). In Vitro and In Vivo Attenuation of Vesicular Stomatitis Virus (VSV) by Phosphoprotein Deletion. *PloS One, 11*(6), e0157287. doi:10.1371/journal.pone.0157287

Yanagisawa, R., Koizumi, T., Koya, T., Sano, K., Koido, S., Nagai, K., . . . Shimodaira, S. (2018). WT1-pulsed Dendritic Cell Vaccine Combined with Chemotherapy for Resected Pancreatic Cancer in a Phase I Study. *Anticancer Research, 38*(4), 2217-2225. doi:10.21873/anticanres.12464

Yoshio, S., Kanto, T., Kuroda, S., Matsubara, T., Higashitani, K., Kakita, N., . . . Takehara, T. (2013). Human blood dendritic cell antigen 3 (BDCA3)(+) dendritic cells are a potent producer of

interferon-lambda in response to hepatitis C virus. *Hepatology, 57*(5), 1705-1715. doi:10.1002/hep.26182

Zabora, J., BrintzenhofeSzoc, K., Curbow, B., Hooker, C., & Piantadosi, S. (2001). The prevalence of psychological distress by cancer site. *Psycho-Oncology, 10*(1), 19-28.

Zhao, L., Niu, C., Shi, X., Xu, D., Li, M., Cui, J., . . . Jin, H. (2018). Dendritic cells loaded with the lysate of tumor cells infected with Newcastle Disease Virus trigger potent anti-tumor immunity by promoting the secretion of IFN-gamma and IL-2 from T cells. *Oncology Letters, 16*(1), 1180-1188. doi:10.3892/ol.2018.8785

Zhu, A. X., Kang, Y. K., Yen, C. J., Finn, R. S., Galle, P. R., Llovet, J. M., . . . Kudo, M. (2019). Ramucirumab after sorafenib in patients with advanced hepatocellular carcinoma and increased α-fetoprotein concentrations (REACH-2): a randomised, double-blind, placebo-controlled, phase 3 trial. *Lancet Oncology, 20*(2), 282-296. doi:10.1016/s1470-2045(18)30937-9

8. Acknowledgments

First of all, I would like to thank my group leader and Doktormutter PD Dr. Jennifer Altomonte. Dear Jennifer, you are not only a brilliant researcher but also a great supervisor and a real mentor. Your work with your students does not focus on your personal aims but on what is important for us students in a specific situation. Thank you for your optimism and empathy, for the chats during my Brotzeit, and for your inspiring ideas while discussing every detail of my data. Thank you very much for giving me the opportunity to start the DC project in your group!

Furthermore, I would like to thank Prof. Dr. Angela Krackhardt for the helpful discussions and encouraging ideas. The committee meeitings with you were always very fruitful!

I also want to thank Dr. Teresa Krabbe for introducing me into the lab world. Even though you had to start with me from the very beginning and I had so many stupid questions, you were always so patient and honestly friendly that you made me feel like a full lab member from the very first day. Dear Teresa, I wouldn't have had a chance without you, thank you so much!

I would furthermore like to thank all my lovely lab members for sharing good and bad times and for all the encouragement. A special thank you goes to Lorenz Hanesch and Cecilia Lozano Simón for continuing with the DC project – keep going!

Thanks to Gerulf Hänel from AG Subklewe and Alexandre Klopp and his collegues from AG Protzer for all their help with establishing the DC and T cell protocols.

Lastly, I would like to thank my family and friends. Dear Tobi, thank you for always encouraging me, dear Johi, thank you for your support in many different ways, dear mum, thank you for always believing in me. Without you three not only this work but my whole studies would have never been possible!